ANALYSIS AND SIMULATION OF MECHANICAL TRAINS DRIVEN BY VARIABLE FREQUENCY DRIVE SYSTEMS

A Thesis

by

XU HAN

Submitted to the Office of Graduate Studies of
Texas A&M University
in partial fulfillment of the requirements for the degree of

MASTER OF SCIENCE

December 2010

Major Subject: Mechanical Engineering

ANALYSIS AND SIMULATION OF MECHANICAL TRAINS DRIVEN BY VARIABLE FREQUENCY DRIVE SYSTEMS

A Thesis

by

XU HAN

Submitted to the Office of Graduate Studies of
Texas A&M University
in partial fulfillment of the requirements for the degree of

MASTER OF SCIENCE

Approved by:

Chair of Committee,	Alan B. Palazzolo
Committee Members,	Won-jong Kim
	Hamid A. Toliyat
Head of Department,	Dennis O'Neal

December 2010

Major Subject: Mechanical Engineering

ABSTRACT

Analysis and Simulation of Mechanical Trains Driven by
Variable Frequency Drive Systems. (December 2010)
Xu Han, B.S., Zhejiang University, P.R.China
Chair of Advisory Committee: Dr. Alan B. Palazzolo

Induction motors and Variable Frequency Drives (VFDs) are widely used in industry to drive machinery trains. However, some mechanical trains driven by VFD-motor systems have encountered torsional vibration problems. This vibration can induce large stresses on shafts and couplings, and reduce the lifetime of these mechanical parts. Long before the designed lifetime, the mechanical train may encounter failure. This thesis focuses on VFDs with voltage source rectifiers for squirrel-cage induction motors of open-loop Volts/Hertz and closed-loop Field Oriented Control (FOC).

First, the torsional vibration problems induced by VFDs are introduced. Then, the mathematical model for a squirrel-cage induction motor is given. Two common control methods used in VFD are discussed – open-loop Volts/Hertz and closed-loop FOC. SimPowerSystems and SimMechanics are used as the modeling software for electrical systems and mechanical systems respectively. Based on the models and software, two interface methods are provided for modeling the coupled system. A simple system is tested to verify the interface methods.

The study of open-loop Volts/Hertz control method is performed. The closed-form of electromagnetic torque sideband frequency due to Pulse Width Modulation is given. A torsional resonance case is illustrated. The effects of non-ideal power switches are studied, which shows little influence on the system response but which uses little energy consumption. A study of a non-ideal DC bus indicates that a DC

bus voltage ripple can also induce a big torsional vibration.

Next, the study of the closed-loop FOC control method is presented. Simulation for a complete VFD machinery train is performed. With the rectifier and DC bus dynamic braking, the system shows a better performance than the ideal-DC bus case. Lastly, a parametric study of the FOC controller is performed. The effects of primary parameters are discussed. The results indicate that some control parameters (i.e. speed ramps, proportional gain in speed PI controller) are also responsible for the mechanical torsional vibration.

DEDICATION

To my dear God and parents

ACKNOWLEDGMENTS

First I would like to acknowledge my advisor Dr. Palazzolo. He accepted me - a student without background on mechanical engineering - as his graduate student. He guided me into the field of mechanical engineering, and gave me the opportunity to lead a professional graduate research life. He is really nice and patient to students. His erudition on different fields of knowledge impressed me greatly. Under his guidance, I learned a lot about vibration and control systems, both theory and practice. Here I want to convey my sincere thank and respect to him.

Second I want to thank Dr. Toliyat and Dr. Kim. Dr. Toliyat's courses about motors are great and very useful for my research, especially the part about motor control systems. He extended my understanding of the background knowledge for my thesis. Dr. Kim's instructions of electromechanical systems strengthened my comprehension of coupled electrical and mechanical systems, which is the important base of my research.

Third I would like to say thank you to all my friends here. They brought me precious friendship and happiness in my life.

Finally, I really appreciate my dear parents, Ping Xiao and Qilin Han. Without their love and support, I cannot be who I am now.

TABLE OF CONTENTS

CHAPTER Page

I INTRODUCTION 1
A. Problem Statement 1
1. Novelty and Significance 2
2. Literature Review 5
3. Objectives 6

II SQUIRREL CAGE INDUCTION MOTOR AND VFDS 8
A. Squirrel-Cage Induction Motor 8
1. Principle for Squirrel Cage Induction Motor 8
2. Mathematical Model for Squirrel Cage Induction Motor . 9
B. Variable Frequency Drives 12
1. Open-Loop Volts/Hertz Control 12
2. Closed-Loop Field Oriented Control 13

III SYSTEM MODELING METHOD 18
A. Simulink Environment 18
B. SimPowerSystems for Electrical System Modeling 18
1. Overview 18
2. Main Blocks for Modeling 19
C. SimMechanics for Mechanical Systems 21
1. Overview 21
2. Main Components for Modeling 21
D. Interface Method Based on SimPowerSystems and SimMechanics 25
1. Method I - Extended Rotor with Zero Inertia 25
2. Method II - Two Rotor Model 26
E. Verification Cases 27
1. System Description 27
2. Model with SimPowerSystems Only 28
3. Model with Interface Method I 32
4. Model with Interface Method II 35

IV ANALYSIS OF OPEN-LOOP CONTROL – VOLTS/HERTZ . . . 42

CHAPTER Page

A. Analysis for Harmonic Sources 42
B. PWM Harmonic Identification 44
1. Carrier-Based PWM Generation 44
2. Three-Phase Inverter and PWM Sidebands 45
C. Motor-Compressor Machinery Train 48
1. Electric Induction Motor 48
2. Mechanical Components 49
D. Effects of Volts/Hertz Controller & PWM Sidebands 49
1. Assumptions 49
2. System Model in SimPowerSystems and SimMechanics . 51
3. Running at Nominal Frequency 53
4. Resonance 57
E. Effects of IGBT/Diodes with Non-Ideal Characteristics in Inverter 62
1. Assumptions 62
2. System Model in SimPowerSystems and SimMechanics . 63
3. Simulation with Non-Ideal IGBT/Diodes 63
F. Effects of Non-Ideal DC Bus Voltage 70
1. System Model 70
2. DC Bus Harmonic Frequency – Motor Operation Frequency 72
3. DC Bus Harmonic Frequency = Mechanical Torsional Natural Frequency 77
4. DC Bus Harmonic Frequency = 120 Hz 82

V ANALYSIS OF CLOSED-LOOP CONTROL-FOC 87

A. Analysis for Harmonic Sources 87
B. Motor-Gearbox-Compressor Machinery Train 89
1. Electric Induction Motor 89
2. Mechanical Components 89
C. FOC Controller with Ideal DC Bus Voltage and Ideal Switch in Inverter 90
1. Assumptions 90
2. System Model in SimPowerSystems and SimMechanics . 92
3. Simulation Results 92
D. Complete VFD Model with FOC 95
1. Motor-Gearbox-Compressor Machinery Train Model with FOC 95

CHAPTER Page

2. System Model in SimPowerSystems and SimMechanics . 100
3. Simulation Results 100
E. Parametric Study of the Controller 107
1. Speed Regulator 107
2. Flux Controller 129
3. FOC Controller 139

VI SUMMARY 149

A. Modeling for Machinery Train System with VFD 149
B. Study of Open-Loop Volts/Hertz Control 149
C. Study of Closed-Loop FOC Control 150
D. Future Work 153

REFERENCES 154

APPENDIX A VECTOR TRANSFORM 157

A. Transform between Three-Dimensional and Two-Dimensional Vectors 157
B. Park Transform 158
C. Clarke Transform 159

APPENDIX B PARAMETERS FOR SIMULATED SYSTEMS 160

A. Verification Case in Chapter III 160
1. 3 HP Motor 160
2. IGBT/Diode 160
3. PWM Generator 160
B. Motor-Compressor Train in Chapter IV 160
1. 150 HP Motor Parameters 160
2. IGBT/Diode Parameters 160
3. PWM Generator 160
C. Motor-Gearbox-Compressor Train in Chapter V 164
1. 200HP Motor Parameters 164
2. Converters and DC Bus 164

VITA 166

LIST OF FIGURES

FIGURE Page

1 General Structure of VFD System – Coupled Electrical System and Mechanical System 2

2 Coupling Failure Induced by VFD System 4

3 Motor Shaft Failure Induced by VFD System 4

4 Squirrel-Cage Induction Motor 8

5 Mechanical Model for Induction Motor Rotor 12

6 Basic Control Diagram for FOC with Speed Reference 15

7 IGBT/Diode Converter in SimPowerSystems 20

8 SimPowerSystems Block of Squirrel Cage Induction Motor 20

9 Field Oriented Control Drive in SimPowerSystems 22

10 Concentrated Mass in SimMechanics 23

11 Rotational Connections and Spring/Damper in SimMechanics 23

12 Gearbox in SimMechanics 24

13 Motion/Generalized Force Actuators in SimMechanics 24

14 Motion/Generalized Force Sensors in SimMechanics 25

15 Illustration for Method I – Extended Rotor with Zero Inertia 26

16 Illustration for Method II – Two-Rotor Model 27

17 Motor Control System for Interface Method Verification with Open-Loop Volts/Hertz Control 28

18 Mechanical System for Verification Case 29

FIGURE Page

19 Model with SimPowerSystems Only for Verification Case 30

20 Subsystem of Mechanical Load for Verification Case 30

21 Simulation Results for Model with SimPowerSystems Only 31

22 System Model with SimPowerSystems and SimMechanics with Interface Method I 33

23 Illustration for Interface Connections with Interface Method I 34

24 Angular Motion Vector Conversion 35

25 Simulation Results for Model with Interface Method I 36

26 System Model with SimPowerSystems and SimMechanics with Interface Method II 38

27 Illustration for Interface Connections with Interface Method II 39

28 Torque Vector Conversion 40

29 Simulation Results for Model with Interface Method II 41

30 Machinery Train Driven by VFD with Open-Loop Volts/Hertz Control 42

31 Carrier-Based PWM Signal Generation 44

32 Three-Phase IGBT/Diode Inverter 45

33 Compensated Pulses for Switch Q1 and Q4 in Three-Arm Inverter . . . 46

34 PWM Generation for Three-Phase Three-Arm Inverter 47

35 Motor-Compressor Machinery Train 48

36 Motor-Compressor Mechanical System 49

37 VFD Driven Motor-Compressor Train with Open-Loop Volts/Hertz Control; Assumptions: Ideal DC Bus Voltage and Ideal Inverter Switches 51

FIGURE Page

38 SimPowerSystems and SimMechanics Model for VFD Driven Motor-Compressor Train with Open-Loop Volts/Hertz Control; Assumptions: Ideal DC Bus Voltage and Ideal Power Switches for Inverter 52

39 Motor-Compressor Train with Volts/Hertz; Rotor Speed – Motor Operation Frequency 50 Hz; Assumptions: Ideal DC Bus Voltage and Ideal Switches 53

40 Motor-Compressor Train with Volts/Hertz; Relative Angular Displacement between Motor and Compressor – Motor Operation Frequency 50Hz; Assumptions: Ideal DC Bus Voltage and Ideal Switches 54

41 Motor-Compressor Train with Volts/Hertz; Electromagnetic Torque – Motor Operation Frequency 50 Hz; Assumptions: Ideal DC Bus Voltage and Ideal Switches 55

42 Motor-Compressor Train with Volts/Hertz; Shear Stress of Coupling – Motor Operation Frequency 50 Hz; Assumptions: Ideal DC Bus Voltage and Ideal Switches 56

43 Motor-Compressor Train with Volts/Hertz; Rotor Speed – Motor Operation Frequency 32 Hz; Assumptions: Ideal DC Bus Voltage and Ideal Switches 58

44 Motor-Compressor Train with Volts/Hertz; Relative Angular Displacement between Motor and Compressor – Motor Operation Frequency 32 Hz; Assumptions: Ideal DC Bus Voltage and Ideal Switches 59

45 Motor-Compressor Train with Volts/Hertz; Electromagnetic Torque – Motor Operation Frequency 32 Hz; Assumptions: Ideal DC Bus Voltage and Ideal Switches 60

46 Motor-Compressor Train with Volts/Hertz; Shear Stress of Coupling – Motor Operation Frequency 32 Hz; Assumptions: Ideal DC Bus Voltage and Ideal Switches 61

47 VFD Driven Motor-Compressor Train with Open-Loop Volts/Hertz Control; Assumptions: Ideal DC Bus Voltage 62

FIGURE Page

48 Non-Ideal Characteristic Model of Diode 63

49 Non-Ideal Characteristic Model of IGBT 64

50 SimPowerSystems and SimMechanics Model for Motor-Compressor Train with Open-Loop Volts/Hertz Control; IGBT/Diode Inverter Study 65

51 Motor-Compressor Train with Volts/Hertz; Rotor Speed – Motor Operation Frequency 50 Hz; IGBT/Diode Inverter Case Compared with Ideal Switch Case 66

52 Motor-Compressor Train with Volts/Hertz; Relative Angular Displacement between Motor and Compressor – Motor Operation Frequency 50 Hz; IGBT/Diode Inverter Case Compared with Ideal Switch Case 67

53 Motor-Compressor Train with Volts/Hertz; Electromagnetic Torque – Motor Operation Frequency 50 Hz; IGBT/Diode Inverter Case Compared with Ideal Switch Case 68

54 Motor-Compressor Train with Volts/Hertz; Shear Stress of Coupling – Motor Operation Frequency 50 Hz; IGBT/Diode Inverter Case Compared with Ideal Switch Case 69

55 SimPowerSystems and SimMechanics Model for Motor-Compressor Train with Open-Loop Volts/Hertz Control; DC Bus Harmonic Study . 71

56 Motor-Compressor Train with Volts/Hertz; Rotor Speed – Motor Operation Frequency 50 Hz; DC Bus Harmonic Frequency = Motor Operation Frequency 50 Hz 73

57 Motor-Compressor Train with Volts/Hertz; Relative Angular Displacement between Motor and Compressor – Motor Operation Frequency 50 Hz; DC Bus Harmonic Frequency = Motor Operation Frequency 50 Hz 74

58 Motor-Compressor Train with Volts/Hertz; Electromagnetic Torque – Motor Operation Frequency 50 Hz; DC Bus Harmonic Frequency = Motor Operation Frequency 50 Hz 75

FIGURE Page

59 Motor-Compressor Train with Volts/Hertz; Shear Stress of Coupling – Motor Operation Frequency 50 Hz; DC Bus Harmonic Frequency = Motor Operation Frequency 50 Hz 76

60 Motor-Compressor Train with Volts/Hertz; Rotor Speed – Motor Operation Frequency 50 Hz; DC Bus Harmonic Frequency = Mechanical Torsional Natural Frequency 20 Hz 78

61 Motor-Compressor Train with Volts/Hertz; Relative Angular Displacement between Motor and Compressor – Motor Operation Frequency 50 Hz; DC Bus Harmonic Frequency = Mechanical Torsional Natural Frequency 20 Hz 79

62 Motor-Compressor Train with Volts/Hertz; Electromagnetic Torque – Motor Operating Frequency 50 Hz; DC Bus Harmonic Frequency = Mechanical Torsional Natural Frequency 20 Hz 80

63 Motor-Compressor Train with Volts/Hertz; Shear Stress of Coupling – Motor Operation Frequency 50 Hz; DC Bus Harmonic Frequency = Mechanical Torsional Natural Frequency 20 Hz 81

64 Motor-Compressor Train with Volts/Hertz; Rotor Speed – Motor Operation Frequency 50 Hz; DC Bus Harmonic Frequency = 120 Hz 83

65 Motor-Compressor Train with Volts/Hertz; Relative Angular Displacement between Motor and Compressor – Motor Operationg Frequency 50 Hz; DC Bus Harmonic Frequency = 120 Hz 84

66 Motor-Compressor Train with Volts/Hertz; Electromagnetic Torque – Motor Operation Frequency 50 Hz; DC Bus Harmonic Frequency = 120 Hz 85

67 Motor-Compressor Train with Volts/Hertz; Shear Stress of Coupling – Motor Operating Frequency 50 Hz; DC Bus Harmonic Frequency = 120 Hz 86

68 Diagram for a Machinery Train Driven by Closed-Loop FOC Control VFD 87

FIGURE Page

69 Motor-Gearbox-Compressor Train 89

70 Motor-Gearbox-Compressor Mechanical System 90

71 VFD Driven Motor-Gearbox-Compressor Train with FOC; Assumptions: Ideal DC Bus Voltage and Ideal Inverter Power Switches . 92

72 SimPowerSystems and SimMechanics Model for VFD Driven Motor-Gearbox-Compressor Train with FOC; Assumptions: Ideal DC Bus Voltage and Ideal Inverter Power Switches 93

73 Motor-Gearbox-Compressor Train with FOC; Rotor Speed – Motor Target Speed 1750 rpm; Assumptions: Ideal DC Bus Voltage and Ideal Inverter Power Switches 96

74 Motor-Gearbox-Compressor Train with FOC; Relative Angular Displacement between Motor and Gear#1 – Motor Target Speed 1750 rpm; Assumptions: Ideal DC Bus Voltage and Ideal Inverter Power Switches 97

75 Motor-Gearbox-Compressor Train with FOC; Electromagnetic Torque – Motor Target Speed 1750 rpm; Assumptions: Ideal DC Bus Voltage and Ideal Inverter Power Switches 98

76 Motor-Gearbox-Compressor Train with FOC; Shear Stress of Coupling#1 – Motor Target Speed 1750 rpm; Assumptions: Ideal DC Bus Voltage and Ideal Inverter Power Switches 99

77 VFD Driven Motor-Gearbox-Compressor Machinery Train with FOC . 99

78 SimPowerSystems and SimMechanics Model for VFD Driven Motor-Gearbox-Compressor Machinery Train with FOC 101

79 Motor-Gearbox-Compressor Train with FOC; Rotor Speed – Motor Target Speed 1750 rpm; Complete VFD Case Compared with Ideal DC Bus/Switches Case 102

80 Motor-Gearbox-Compressor Train with FOC; Relative Angular Displacement between Motor and Gear#1 – Motor Target Speed 1750 rpm; Complete VFD Case Compared with Ideal DC Bus/Switches Case 103

FIGURE Page

81 Motor-Gearbox-Compressor Train with FOC; Electromagnetic Torque – Motor Target Speed 1750 rpm; Complete VFD Case Compared with Ideal DC Bus/Switches Case 104

82 Motor-Gearbox-Compressor Train with FOC; Shear Stress of Coupling#1 – Motor Target Speed 1750 rpm; Complete VFD Case Compared with Ideal DC Bus/Switches Case 105

83 Motor-Gearbox-Compressor Train with FOC; DC Bus Voltage – Motor Target Speed 1750 rpm; Complete VFD Case Compared with Ideal DC Bus/Switches Case 106

84 Motor-Gearbox-Compressor Train with FOC; Rotor Speed – Target Speed 1750 rpm; Speed PI Controller Study 110

85 Motor-Gearbox-Compressor Train with FOC; Relative Angular Displacement between Motor and Gear#1 – Motor Target Speed 1750 rpm; Speed PI Controller Study 111

86 Motor-Gearbox-Compressor Train with FOC; Electromagnetic Torque – Motor Target Speed 1750 rpm; Speed PI Controller Study . . 112

87 Motor-Gearbox-Compressor Train with FOC; Shear Stress of Coupling#1 – Motor Target Speed 1750 rpm; Speed PI Controller Study 113

88 Motor-Gearbox-Compressor Train with FOC; Relative Angular Displacement between Motor and Gear#1 – Motor Target Speed 1750 rpm; Speed P Controller Study – P = 300, 150 and 50 . . . 114

89 Motor-Gearbox-Compressor Train with FOC; Electromagnetic Torque – Motor Target Speed 1750 rpm; Speed P Controller Study – P = 300, 150 and 50 115

90 Motor-Gearbox-Compressor Train with FOC; Rotor Speed – Motor Target Speed 1750 rpm; Torque Output Limit = 12000 N·m and 20000 N·m 116

91 Motor-Gearbox-Compressor Train with FOC; Relative Angular Velocity between Motor and Gear#1 – Motor Target Speed 1750 rpm; Torque Output Limit = 12000 N·m and 20000 N·m 117

FIGURE Page

92 Motor-Gearbox-Compressor Train with FOC; Electromagnetic Torque – Motor Target Speed 1750 rpm; Torque Output Limit = 12000 N·m and 20000 N·m 118

93 Motor-Gearbox-Compressor Train with FOC; Shear Stress of Coupling#1 – Motor Target Speed 1750 rpm; Torque Output Limit = 12000 N·m and 20000 N·m 119

94 Motor-Gearbox-Compressor Train with FOC; Rotor Speed – Motor Target Speed 1750 rpm; Speed Ramps = 900 rpm/s and 1700 rpm/s 121

95 Motor-Gearbox-Compressor Train with FOC; Relative Angular Displacement between Motor and Gear#1– Motor Target Speed 1750 rpm; Speed Ramps = 900 rpm/s and 1700 rpm/s 122

96 Motor-Gearbox-Compressor Train with FOC; Electromagnetic Torque – Motor Target Speed 1750 rpm; Speed Ramps = 900 rpm/s and 1700 rpm/s 123

97 Motor-Gearbox-Compressor Train with FOC; Shear Stress of Coupling#1 – Motor Target Speed 1750 rpm; Speed Ramps = 900 rpm/s and 1700 rpm/s 124

98 Motor-Gearbox-Compressor Train with FOC; Rotor Speed – Motor Target Speed 1750 rpm; Torque Output Limit = 12000 N·m and 20000 N·m 125

99 Motor-Gearbox-Compressor Train with FOC; Relative Angular Velocity between Motor and Gear#1 – Motor Target Speed 1750 rpm; Torque Output Limit = 12000 N·m and 20000 N·m 126

100 Motor-Gearbox-Compressor Train with FOC; Electromagnetic Torque – Motor Target Speed 1750 rpm; Torque Output Limit = 12000 N·m and 20000 N·m 127

101 Motor-Gearbox-Compressor Train with FOC; Shear Stress of Coupling#1 – Motor Target Speed 1750 rpm; Torque Output Limit = 12000 N·m and 20000 N·m 128

FIGURE Page

102 Motor-Gearbox-Compressor Train with FOC; Rotor Speed – Motor Target Speed 1750 rpm; Flux PI Controller Study 130

103 Motor-Gearbox-Compressor Train with FOC; Relative Angular Displacement between Motor and Gear#1 – Motor Target Speed 1750 rpm; Flux PI Controller Study 131

104 Motor-Gearbox-Compressor Train with FOC; Electromagnetic Torque – Motor Target Speed 1750 rpm; Flux PI Controller Study . . . 132

105 Motor-Gearbox-Compressor Train with FOC; Shear Stress of Coupling#1 – Motor Target Speed 1750 rpm; Flux PI Controller Study 133

106 Motor-Gearbox-Compressor Train with FOC; Rotor Speed – Motor Target Speed 1750 rpm; Flux Output Limit = 1 Wb and 2 Wb . 135

107 Motor-Gearbox-Compressor Train with FOC; Relative Angular Displacement between Motor and Gear#1 – Motor Target Speed 1750 rpm; Flux Output Limit = 1 Wb and 2 Wb 136

108 Motor-Gearbox-Compressor Train with FOC; Electromagnetic Torque – Motor Target Speed 1750 rpm; Flux Output Limit = 1 Wb and 2 Wb 137

109 Motor-Gearbox-Compressor Train with FOC; Shear Stress of Coupling#1 – Motor Target Speed 1750 rpm; Flux Output Limit = 1 Wb and 2 Wb 138

110 Motor-Gearbox-Compressor Train with FOC; Rotor Speed – Motor Target Speed 1750 rpm; Current Hysteresis Band = 10 A and 30 A 140

111 Motor-Gearbox-Compressor Train with FOC; Relative Angular Displacement between Motor and Gear#1 – Motor Target Speed 1750 rpm; Current Hysteresis Band = 10 A and 30 A 141

112 Motor-Gearbox-Compressor Train with FOC; Electromagnetic Torque – Motor Target Speed 1750 rpm; Current Hysteresis Band = 10 A and 30 A 142

FIGURE Page

113 Motor-Gearbox-Compressor Train with FOC; Shear Stress of Coupling#1 – Motor Target Speed 1750 rpm; Current Hysteresis Band = 10 A and 30 A 143

114 Motor-Gearbox-Compressor Train with FOC; Rotor Speed – Motor Target Speed 1750 rpm; Maximum Switching Frequency = 5000 Hz and 20000 Hz 145

115 Motor-Gearbox-Compressor Train with FOC; Relative Angular Displacement between Motor and Gear#1 – Motor Target Speed 1750 rpm; Maximum Switching Frequency = 5000 Hz and 20000 Hz 146

116 Motor-Gearbox-Compressor Train with FOC; Electromagnetic Torque – Motor Target Speed 1750 rpm; Maximum Switching Frequency = 5000 Hz and 20000 Hz 147

117 Motor-Gearbox-Compressor Train with FOC; Shear Stress Coupling#1 – Motor Target Speed 1750 rpm; Maximum Switching Frequency = 5000 Hz and 20000 Hz 148

118 Three-Dimensional Frame a-b-c and Two-Dimensional Frame Q-D 157

119 a-b-c Frame and Stationary Q-D Frame 158

120 Stationary Q-D Frame and Synchronous Q-D Frame 159

LIST OF TABLES

TABLE		Page
I	3 HP Motor Nominal Parameters	29
II	Mechanical Parameters for Verification Case	29
III	150 HP Motor Nominal Parameters	50
IV	Mechanical Parameters for Motor-Compressor Train	50
V	Comparison of Oscillation for Motor-Compressor Train with Open-Loop Volts/Hertz Running at 50 Hz and 32 Hz	58
VI	IGBT/Diode Characteristics Setting	64
VII	Comparison of Oscillation with DC Bus Harmonic Frequency = Motor Operation Frequency 50 Hz for Motor-Compressor Train with Open-Loop Volts/Hertz	73
VIII	Comparison of Oscillation with DC Bus Harmonic Frequency = Torsional Natural Frequency 20 Hz for Motor-Compressor Train with Open-Loop Volts/Hertz	78
IX	Comparison of Oscillation with DC Bus Harmonic Frequency = 120 Hz for Motor-Compressor Train with Open-Loop Volts/Hertz	82
X	200HP Motor Nominal Parameters	90
XI	Mechanical Parameters for Motor-Gearbox-Compressor Train	91
XII	Controller Settings for FOC	94
XIII	Comparison of Oscillation for Motor-Compressor Train with Closed-Loop FOC; Complete VFD Case Compared with Ideal DC Bus/Switches Case	102
XIV	Comparison of Oscillation for Motor-Compressor Train with Closed-Loop FOC; Speed PI Controller Study	109

TABLE Page

XV Comparison of Oscillation for Motor-Compressor Train with Closed-Loop FOC; Speed Ramps = 900 rpm/s and 1700 rpm/s 120

XVI Comparison of Oscillation for Motor-Compressor Train with Closed-Loop FOC; Flux PI Controller Study 130

XVII Comparison of Oscillation for Motor-Compressor Train with Closed-Loop FOC; Flux Output Limit = 1 Wb and 2 Wb 134

XVIII Comparison of Oscillation for Motor-Compressor Train with Closed-Loop FOC; Current Hysteresis Band = 10 A and 30 A 139

XIX Comparison of Oscillation for Motor-Compressor Train with Closed-Loop FOC; Maximum Switching Frequency = 5000 Hz and 20000 Hz 144

XX 3 HP Motor Parameters 161

XXI IGBT/Diode Bridge Parameters for 3 HP Motor Train 161

XXII PWM Generator Settings for 3 HP Motor Train 162

XXIII 150 HP Motor Parameters 162

XXIV IGBT/Diode Bridge Parameters for 150 HP Motor Train 163

XXV PWM Generator Settings for 150 HP Motor Train 163

XXVI 200 HP Motor Parameters 164

XXVII Converters and DC Bus 165

CHAPTER I

INTRODUCTION

A. Problem Statement

Nowadays, in industry a lot of mechanical systems are driven by induction motors (asynchronous motors). For easy speed control in wide speed range and energy efficiency, most induction motors are controlled by Variable Frequency Drives (VFDs). VFDs are electrical drives using power electronics techniques. The induction motor and its VFD compose the electrical drive system. Thus for a complete motion train, the electrical and mechanical systems are coupled together.

However, in practice, some mechanical trains driven by VFD-motor systems have encountered torsional vibration problem. From the paper written by Feese (Engineering Dynamics Incorporated) and Maxfield (Tesoro Refining & Marketing Company)[1], these torsional vibration problems are identified as the result of using VFDs. This torsional vibration induced by VFDs can bring great damage to the mechanical train component, like failure of coupling or shaft.

This thesis will focus and analyze on the VFD system of voltage source and squirrel cage induction motor. Two VFD control methods will be studied and analyzed, including the open-loop Volts/Hertz control and the closed-loop Field Oriented Control (FOC). The complete machinery train system combining electrical and mechanical parts will be modeled and simulated. To achieve this object, a complete simulation method to model the electrical system and mechanical system together is developed.

This thesis follows the style of *Journal of Vibration and Acoustics, ASME.*

The coupled systems used for analysis have a general structure as shown in Fig. 1.

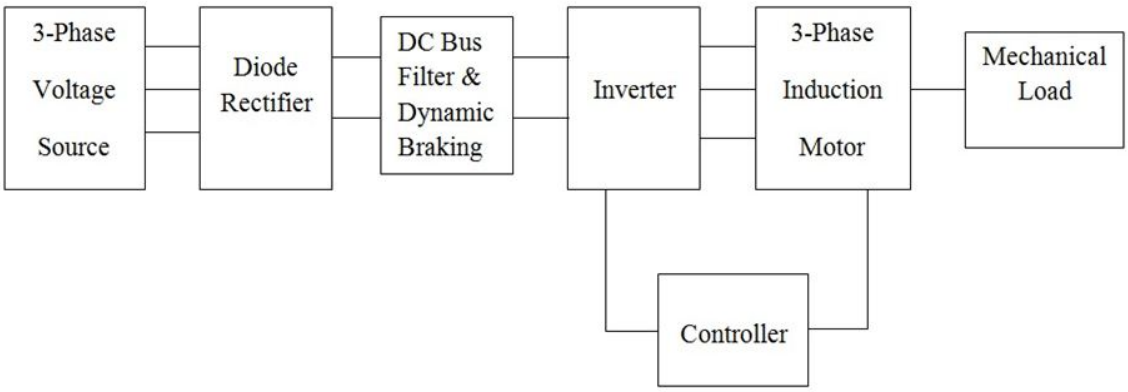

Fig. 1. General Structure of VFD System – Coupled Electrical System and Mechanical System

The system input is the three phase AC voltage source. Then, the three-phase voltage is rectified into two-phase DC voltage, smoothed and kept by filters and dynamic braking devices. This two-phase DC voltage is then inverted back to AC voltage by Pulse Width Modulation (PWM). This AC voltage contains controlled magnitude and frequency information, which feeds directly to the three-phase induction motor. The VFDs are used in this DC to AC inversion part, as shown in Fig. 1. The mechanical load is driven by the induction motor. The driven mechanical system may contain mechanical components like gear boxes, couplings, and compressors.

1. Novelty and Significance

Torsional vibration problem can bring great damage to mechanical components. The vibration can induce big stress on shafts and couplings, and reduce the lifetime of these mechanical parts. Far before the designed lifetime, the mechanical train may

encounter failures. Fig. 2 and Fig. 3 are coupling failure cases from industry practice [2] [3]. The mechanical trains in these cases are all driven by VFD motor systems.

Avoiding torsional vibration is very import in mechanical system design. In a pure mechanical system, designer can design and set the rotational natural frequency of the mechanical train far away from the potential excitation frequency [4].

However, for system driven by VFD induction motor system, the excitation frequency - which is always the harmonic frequency of the electromagnetic torque - is difficult to tell. Since the modulated electrical signal contains lots of harmonics, and their magnitude and frequency depend on the control method. On the other hand, when varying the motor speed, the harmonic frequency of electromagnetic torque varies. For example, during start up, the coupled system may be excited by time-varying harmonics.

Thus, due to the difficulty of determining the excitation frequency of electrical drives, designers are suggested to use estimate or experience values. For example, one can concern the harmonic frequency of electromagnetic torque as six times the motor operating frequency [4]. This method does not take all the possible exciting harmonics into consideration. From this point, it is very important to model and simulate the entire coupled electrical and mechanical system at the same time.

However, a search of the literature did not reveal prior coupling of electrical and mechanical systems to analyze VFD machinery trains for torsional vibration modeling. In this thesis, these two areas will be coupled together. The modeling tools are two toolboxes in Matlab - SimPowerSystems and SimMechanics. The first one is for modeling electrical system, while the later one is for mechanical system.

The simulation of coupled system can help to identify the operation points where the train suffers torsional vibration. Avoiding these operation points can protect mechanical components.

Fig. 2. Coupling Failure Induced by VFD System [2]

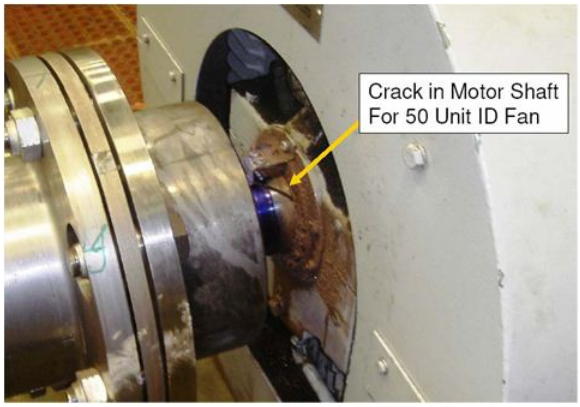

Fig. 3. Motor Shaft Failure Induced by VFD System [3]

2. Literature Review

Early in 1980s, the torsional vibration problem induced by VFD has been considered. Charles B. Mayer [5] discussed this kind of problem in the cement industry. His paper described the general conception of torsional vibration in mechanical trains. And a general VFD machinery train structure was given. The whole system was divided into four parts - electrical supply system, drive motors, mechanical system and load system. The excitation sources from each part were generally described. Then, several types of cement industry drives and potential resonant frequencies were discussed based on experience.

In 1988, David J. Sheppard [6] gave an outline of analysis and also provided a general conception about the performance effects of system components. In his paper, the concepts of torsional natural frequency, excitation and interface diagram were introduced. These discussions offered an analysis direction for VFD machinery trains.

As the induction motors and VFDs become widely used in the industry, the torsional vibration problem due to VFDs is greatly concerned. In the Turbomachinery Symposium, several torsional vibration failure problems of VFD machinery trains are discussed. In the 22nd Turbomachinery Symposium of 1993, J. C. Wachel and Fred R. Szenasi published a tutorial about rotating machinery torsional vibration analysis method [4]. This tutorial described the general procedures and methods of analysis for torsional vibration problems, including calculation of the torsional natural frequencies and mode shapes, development of interference diagram, definition of the coincidence of excitation frequencies, calculation of the dynamic torsional oscillations of all masses and the dynamic torsional stresses of all shafts, comparison with the specifications. Besides the mechanical component analysis, VFDs were detailed illustrated. The

unpredictable excitation frequencies were stated.

Harley Tripp, et al. [7] did a detailed analysis of a coupling failure case induced by VFD related torsional vibration. This analysis was based on a long term practice and measurement of a motor-gearbox-compressor system. Besides the measurement of the actual coupling stresses, the authors also used finite elements and fracture mechanics analysis methods to explain the failures. As stated in the paper, before the machinery train was installed, no excitation source near the first torsional natural frequency was predicted. But in the long term study, a torsional resonance just at the first torsional natural frequency was found, which was because of the use of VFD motor system.

The VFD-induction motor performance is also studied on the electrical side. In 2004, Kevin Lee and Thomas M. Jahns, et al. [8] considered the effect of VFD input voltage. They did a closed-form analysis of the performance of VFD under input voltage unbalance and sag conditions. Their simulation and experiments showed a torque pulsation in these non-ideal conditions. In 2006, they discussed the solution [9] for the unbalance input voltage and sag conditions.

3. Objectives

It is clear that the traditional method of analysis for a VFD machinery train may not predict the excitation frequencies due to VFD motor systems, which is very important in the design stage. This thesis will focus on the VFDs with voltage source rectifier and squirrel cage induction motors.

The main objective is to study and analyze the performances of two VFD control method - Volts/Hertz and FOC. This will provide a new, structured and systematic methodology for predicted torsional vibration in VFD machinery train.

To do this, a modeling method is required, which should be able to model and

simulate the entire coupled electrical and mechanical system. The main problem is to couple the electrical and mechanical fields. SimPowerSystems and SimMechanics are used in this study, for modeling electrical system and mechanical system respectively. An interface method in Matlab modeling and simulation environment should be provided to combine SimPowerSystems and SimMechanics tooboxes, which means the coupling of the electrical and mechanical fields. It should ensure the validation of the coupled model and the model in these two fields can be simulated at the same time. Several verification cases will be constructed and tested to check the combination of SimPowerSystems and SimMechanics. These cases will be detailed illustrated in the thesis. Then, a systematic study of the performance of VFD machinery trains will be studied. Both open-loop control (Volts/Hertz) and closed-loop control method (FOC) will be concerned.

CHAPTER II

SQUIRREL CAGE INDUCTION MOTOR AND VFDS

A. Squirrel-Cage Induction Motor

1. Principle for Squirrel Cage Induction Motor

The following figures show the basic structure of a squirrel cage induction motor. As noted in Fig. 4(a), the stator is located in the outside. The rotor is inside. The rotor is always supported by a bearing. Fig. 4(b) is a squirrel cage rotor. It is composed by bars of conductors and two end rings.

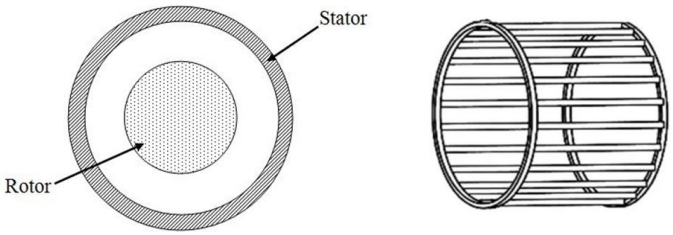

(a) Cross Section (b) Motor Rotor [10]

Fig. 4. Squirrel-Cage Induction Motor

The working principle of the induction motor is a pure electromagnetic induction procedure. The three-phase voltage source feeds the three-phase windings of stator. The resultant stator currents in stator produce a rotating magnetic field - Magneto-Motive Force (MMF). This results in a corresponding rotating flux in the air gap. When the rotor is at standstill, this rotating flux interacts with the conduction bars of rotor. Seen from the coordinate of the rotating flux, those rotor bars are cutting a standing magnetic field. Then currents are induced in the rotor conductors. Now,

there are flux rotating (moving) in the air gap and currents flowing in the standing conductors of rotor (which also connects the air gap). This results in magnetic force and produces torque to the rotor in the same direction of the rotating flux. The rotor starts to rotate.

As the rotor speed increases, the relative velocity between the rotating flux and rotor conductors decreases. But the rotor conductors are still cutting the magnetic field, since the speed of rotor conductors is still smaller than the rotating magnetic field. The resulting force and torque are still there to make the rotor rotate.

However, the rotor speed will never reach the velocity of rotating flux. In that case, there would be no speed difference between the magnetic field and the conductors. Then no current would be induced in the rotor, which means no force or torque generated.

2. Mathematical Model for Squirrel Cage Induction Motor

Because induction motor is a device converting electrical energy into mechanical energy, its mathematical description

a. Electrical Model

From the electrical side, an induction motor is modeled by resistances and inductances. A common model used is the two-phase Q-D model. This mathematical model is transformed from the original three-phase model of inductance motor. Please refer to the electrical machinery references [11]-[18] for the detail transformation procedure.

For a squirrel cage induction motor, the two-phase Q-D model[1] for a Q-D refer-

[1]All the resistances and inductances are based on the applied two-phase Q-D frame. All the rotor resistances and inductances are referred to the stator side (applied turn ratio transformation). Please refer to the references [11]–[18] for details.

ence frame with arbitrary rotational velocity ω is described as following

- For stator side

$$v_{qs} = r_s i_{qs} + \frac{d}{dt}\lambda_{qs} + \omega\lambda_{ds} \tag{2.1}$$

$$v_{ds} = r_s i_{ds} + \frac{d}{dt}\lambda_{ds} - \omega\lambda_{qs} \tag{2.2}$$

- For rotor side

$$0 = r_r{}' i'_{qr} + \frac{d}{dt}\lambda'_{qr} + (\omega - \omega_r)\lambda'_{dr} \tag{2.3}$$

$$0 = r_r{}' i'_{dr} + \frac{d}{dt}\lambda'_{dr} - (\omega - \omega_r)\lambda'_{qr} \tag{2.4}$$

- For flux

$$\lambda_{qs} = (L_{ls} + L_m)i_{qs} + L_m i'_{qr} \tag{2.5}$$

$$\lambda_{ds} = (L_{ls} + L_m)i_{ds} + L_m i'_{dr} \tag{2.6}$$

$$\lambda'_{qr} = (L_{lr} + L_m)i'_{qr} + L_m i_{qs} \tag{2.7}$$

$$\lambda'_{dr} = (L_{lr} + L_m)i'_{dr} + L_m i_{ds} \tag{2.8}$$

- For electromagnetic torque

$$T_e = \frac{3}{2}\frac{p}{2}(\lambda_{ds} i_{qs} - \lambda_{qs} i_{ds}) \tag{2.9}$$

where[2]

d/dt = time differentiation;

p = number of poles;

ω = rotating velocity of applied two-phase Q-D reference frame;

ω_r = rotating velocity of the motor rotor in electrical degree;

r_s = stator resistance;

[2]All terms are in SI units.

r'_r = rotor resistance;

L_m = mutual inductance;

L_{ls} = stator leakage inductance;

L'_{lr} = rotor leakage inductance;

i_{qs} = Q-axis component of stator current;

i_{ds} = D-axis component of stator current;

i'_{qr} = Q-axis component of rotor current;

i'_{dr} = D-axis component of rotor current;

λ_{qs} = Q-axis component of stator flux;

λ_{ds} = D-axis component of stator flux;

λ'_{qr} = Q-axis component of rotor flux;

λ'_{dr} = D-axis component of rotor flux;

v_{qs} = Q-axis component of stator voltage;

v_{ds} = D-axis component of stator voltage;

T_e = electromagnetic torque.

For induction motors fed by voltage source, the stator voltages for Q-axis v_{qs} and D-axis v_{ds} are both known. It can be transformed from the applied three-phase voltage source. This transformation between three-dimensional vector and two-dimensional vector is mentioned in Appendix A. It is also used for stator currents transform, which will be mentioned in the sections about VFDs.

b. Mechanical Model

The mechanical model is shown as below. And the model illustrated in Fig. 5.

$$\frac{d}{dt}\omega_m = \frac{1}{I}(T_e - T_m - b_m\omega_m) \tag{2.10}$$

$$\omega_m = \omega_r / \left(\frac{p}{2}\right) \tag{2.11}$$

where

ω_m = rotating velocity of the motor rotor in mechanical degree;

I = rotor inertia;

T_m = drag torque from rotor shaft (transmitted torque to mechanical load);

b_m = rotor friction (damping).

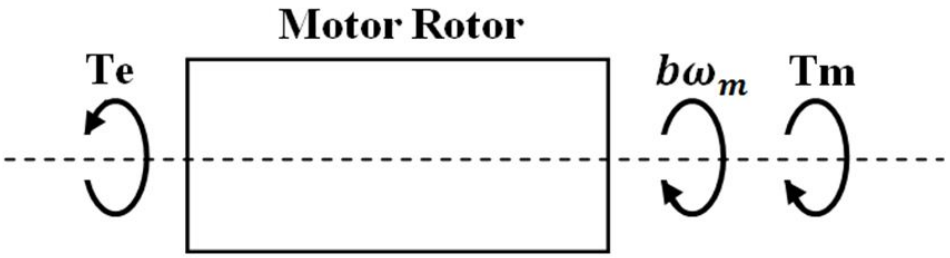

Fig. 5. Mechanical Model for Induction Motor Rotor

B. Variable Frequency Drives

1. Open-Loop Volts/Hertz Control

a. Description

Each induction motor has its nominal values, i.e. input three-phase voltage (RMS, phase-phase), frequency. Under the nominal condition, the fluxes in the air-gap and magnetizing materials are optimized. Thus it is the well designed operating condition for induction motors.

The goal of open-loop Volts/Hertz control is to maintain a constant ratio of the applied voltage and its frequency. This fixed ratio is equal to the ratio of nominal

voltage and frequency. This method is to maintain a good flux condition inside the motor, and make the best use of the magnetizing materials.

b. Implementation

In a machinery train system, the target mechanical speed of the motor is always given. From the target mechanical speed of the rotor, the electrical speed of rotor can be calculated by using Eq. (2.11). The corresponding operation frequency can be found from the following relationship for SI units.

$$f_e = \frac{\omega_r}{2\phi} \tag{2.12}$$

where f_e = electrical frequency of the input three-phase voltage.

The Volts/Hertz ratio is obtained from the nominal values of the motor. Then the applied voltage is calculated by multiplying the Volts/Hertz ratio and the electrical frequency. With Pulse Width Modulation (PWM) techniques and power electronics devices, it is easy to control the voltage supply with customized magnitude and frequency.

2. Closed-Loop Field Oriented Control

Field Oriented Control is a common VFD control method. It is a kind of closed-loop control with stator currents and rotor speed feedback. The basic idea is to find the rotor flux direction and choose the reference Q-D frame, such that it sets the Q-axis component of rotor flux to zero. This will simplify the motor model equations and make the motor easy to control.

a. Synchronous Q-D Reference Frame

The rotational velocity of the rotor flux in the air gap is the synchronous speed ω_e, which is calculated as the following equation.

$$\omega_e = 2\phi f_e \tag{2.13}$$

If the D-axis of the reference Q-D frame is always aligned with the rotor flux ($\lambda'_{qr} = 0$) and has the same speed as the rotor flux ($\omega = \omega_e$), than at steady state Eq. (2.1) – (2.9) will be simplified as the following. The superscript e indicates that all the variables are referred to the synchronous Q-D frame.

- For stator side

$$v^e_{qs} = r_s i^e_{qs} + \omega_e \lambda^e_{ds} \tag{2.14}$$

$$v^e_{ds} = r_s i_d s^e - \omega_e \lambda^e_{qs} \tag{2.15}$$

- For rotor side

$$0 = r'_r i'^e_{qr} + (\omega_e - \omega_r)\lambda'^e_{dr} \tag{2.16}$$

$$0 = i'^e_{dr} \tag{2.17}$$

- For flux

$$\lambda^e_{qs} = (L_{ls} + L_m) i^e_{qs} + L_m i'^e_{qr} \tag{2.18}$$

$$\lambda^e_{ds} = (L_{ls} + L_m) i^e_{ds} \tag{2.19}$$

$$\lambda'^e_{qr} = 0 \tag{2.20}$$

$$\lambda'^e_{dr} = L_m i^e_{ds} \tag{2.21}$$

- For electromagnetic torque

$$T_e = \frac{3}{2}\frac{p}{2}\frac{L_{ls} + L_m}{L_m}\lambda'^e_{dr} i^e_{qs} \tag{2.22}$$

This mathematic model described by Eq. (2.14) – (2.22) is much simpler than the original model. The electromagnetic torque (Eq. (2.22)) just depends on the rotor flux λ'_{dr} and the Q-axis component of stator current i_{qs}. And from Eq. (2.21) the rotor flux λ'_{dr} depends on the D-axis component of stator current i_{ds}. Thus, if the stator currents are well controlled, the output electromagnetic torque is controlled.

b. Description of FOC

Fig. 6 shows a basic control diagram for FOC with speed reference.

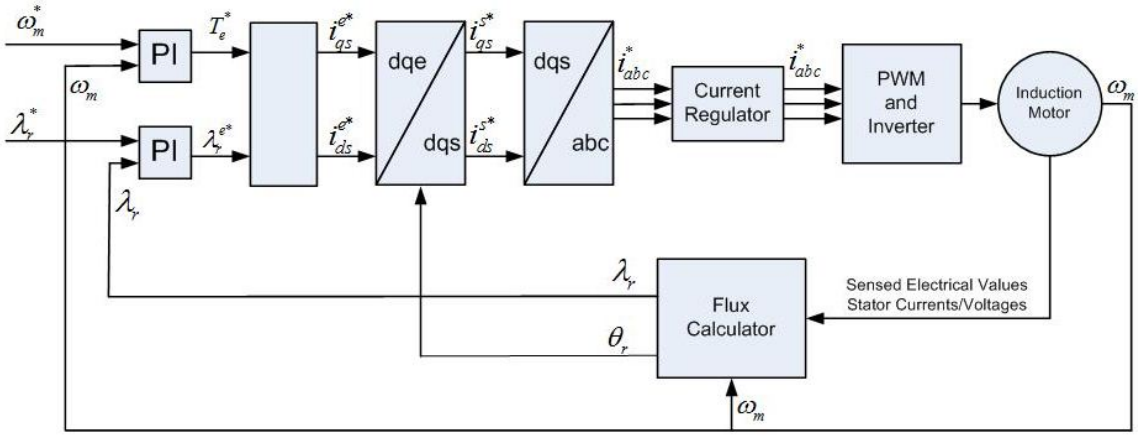

Fig. 6. Basic Control Diagram for FOC with Speed Reference

- Speed Regulation and Torque Reference

  The input to the controller is the reference rotor speed ω_m^* in mechanical degree, which is compared with the actual rotor speed ω_m. A PI controller is used. Its output is the reference electromagnetic torque T_e^*.

- Rotor Flux Reference

  Given the reference rotor flux value λ_r^* and it is just equal to the target D-axis component of rotor flux λ'_{dr}. It is compared with the actual rotor flux λ_r, which

is calculated by the flux calculator. A PI controller is used to regulate the target rotor flux value λ_r^{e*} in the synchronous Q-D frame.

- Reference Stator Currents in Synchronous Q-D Fram

  With reference electromagnetic torque T_e^* and reference rotor flux λ_r^{e*}, the corresponding reference stator current components in the synchronous Q-D frame i_{qs}^{e*} and i_{ds}^{e*} can be calculated by Eq. (2.21) and Eq. (2.22).

- Reference Stator Currents in Stationary Q-D Frame

  With the reference stator currents in the synchronous Q-D frame i_{qs}^{e*} and i_{ds}^{e*} and the rotor flux position θ_r, the reference stator currents in the stationary Q-D frame i_{qs}^{s*} and i_{ds}^{s*} can be obtained by performing the Clarke Transform, which is stated in Appendix A.

- Reference Three-Phase Stator Currents

  By using the Park Transform mentioned in Appendix A, the reference three-phase stator currents i_a^*, i_b^* and i_c^* can be calculated from the reference stator currents in the stationary Q-D frame i_{qs}^{s*} and i_{ds}^{s*}.

- Current Regulator, PWM and Inverter

  The current regulator regulates the reference three-phase stator currents within a hysteresis band width. And its outputs make the controller generate corresponding PWM signals, which controls the inverter switches. The inverter's outputs feed the induction motor.

- Flux Calculator

  The flux calculator is used to calculate the rotor flux λ_r and its position θ_r. These two values are obtained from the sensed electrical values, i.e. stator

currents/voltages. There are several methods to calculate the rotor flux and its position, depending on which electrical terms are selected to be sensed. Please refer to the reference [11]–[20] for details.

CHAPTER III

SYSTEM MODELING METHOD

A. Simulink Environment

Because the machinery train driven by VFDs s a coupled system, combining electrical field and mechanical field. To model this coupled system at the same time, modeling software with both electrical and mechanical modeling features is required. Matlab is a powerful software for engineering model and simulation. It provides modeling and simulating softwares for systems in specified engineering areas, i.e. electrical power system, mechanical system, electronic system, aerodynamic system, hydraulic power and control system. Best of all, all of these softwares for different specific areas can be combined and simulated together in Simulink environment in Matlab. This gives a way to model the machinery train driven by VFDs with coupled electrical and mechanical systems.

B. SimPowerSystems for Electrical System Modeling

1. Overview

SimPowerSystems is a software tool extending Simulink in Matlab. It can be mainly used to simulate two areas: power systems and electrical machinery with power electronics techniques. For the simulation of electrical machinery system, SimPowerSystems includes many useful blocks for power electronics and electrical machine drives. For basic power electronics, it has blocks for power switches, like MOSFETs and IGBTs. For electrical sources, it contains AC/DC voltage/current sources, both single phase and three phases, and also programmable sources which could contain harmon-

ics. For electrical machinery, SimPowerSystems does not only include single electrical machines (DC machines, synchronous machines, and induction machines), it also contains blocks of modern control drives for induction machines, like SVPWM drive, Field Oriented Control (FOC) drives, and Direct Torque Control (DTC) drives. Based on these blocks, electrical machinery control systems can be easily modeled with the build-on model or customized for specified requirements.

Models of SimPowerSystems are run in Simulink environment. That means blocks for electrical systems from SimPowerSystems can be interfaced freely with Simulink blocks, which provides flexible control blocks. These features help to build a customized induction motor control system.

Variable-step integration algorithms and fixed time-step trapezoidal integrations are available for SimPowerSystems models. Variable-step integration algorithms give highly accurate performance, while fixed time-step methods provides more efficiency.

2. Main Blocks for Modeling

The following sections discuss the SimPowerSystems models of the main components in the study of squirrel-cage induction motor and VFDs.

a. Converter with IGBT/Diodes

In this thesis, IGBT/Diode is used for rectifiers and inverters. Fig. 7 shows the power bridge composed of IGBT/Diodes. Fig. 7(a) is the bridge block in SimPowerSystems, while Fig. 7(b) is the electrical schematic. This three-arm converter can be used both as rectifier and inverter. Its mode depends on the side of the input voltage. If the input voltage is three-phase AC voltage, the bridge works as a rectifier. If the input is DC voltage, it is on inverter mode. The six IGBT/Diodes are controlled by PWM signals.

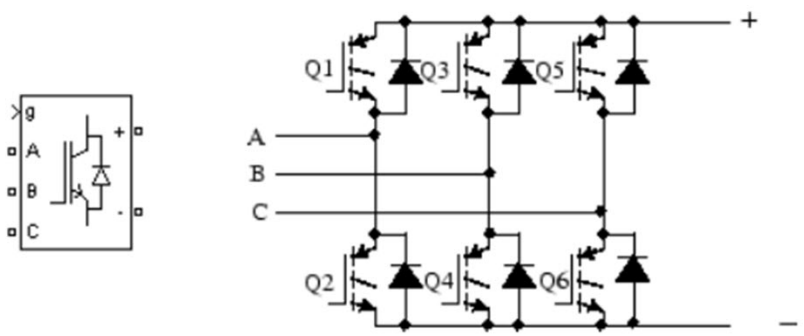

(a) Block Diagram (b) Electrical Schematic

Fig. 7. IGBT/Diode Converter in SimPowerSystems [22]

b. Induction Motor

Fig. 8 is the SimPowerSystems block for squirrel cage induction motor. The electrical input is three-phase voltage to terminals A, B and C. There is a torque signal input, which is the drag torque from mechanical load, of the transmitted torque from the motor to its mechanical load. The electrical and mechanical mathematical model for this block is identical the same as that mentioned in Chapter II. The output (terminal m) contains Simulink signals for currents, fluxes, voltages, electromagnetic torque, rotor angular velocity and angular displacement.

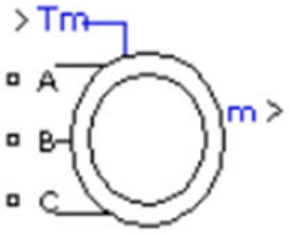

Fig. 8. SimPowerSystems Block of Squirrel Cage Induction Motor [22]

c. AC Electric Drive - FOC

Fig. 9 shows the integrated electric drive for Field Oriented Control (FOC). Fig. 9(a) is the block diagram. Fig. 9(b) is the electrical schematic. This drive block integrates the rectifier, DC chopper, inverter, induction motor, speed controller and field oriented controller. The input includes the target speed, mechanical drag torque and three-phase voltage. The output contains all the information for the motor and converter, including currents, voltages, flux, electromagnetic torque, rotor angular velocity and displacement. All the parameters for the controller can be customized.

C. SimMechanics for Mechanical Systems

1. Overview

SimMechanics extends Simulink, which can be used to model mechanical system by just connecting blocks. It contains blocks of bodies, joints, actuators, sensors and constrains. With these blocks, one can model a mechanical system with multiple degree of freedoms (Dofs), including translational and rotational motions, and set the coordinates of each body for visualization. In SimMechanics, both concentrated-mass and distributed-mass objects can be modeled and simulated. Forces and torques can be applied to a joint or a body via actuators, and the applied forces and torques can be Simulink signals. It also provides sensors to detect displacement, velocity, acceleration, transmitted force or torque (translational and rotational).

2. Main Components for Modeling

The following sections show the SimMechanics models of the main components for modeling a rotational mechanical train with one-degree of freedom.

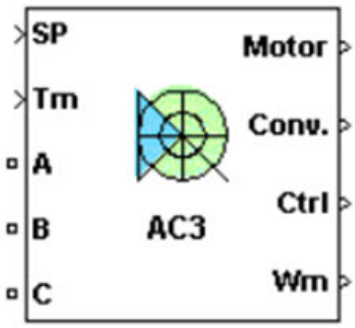

(a) Block Diagram

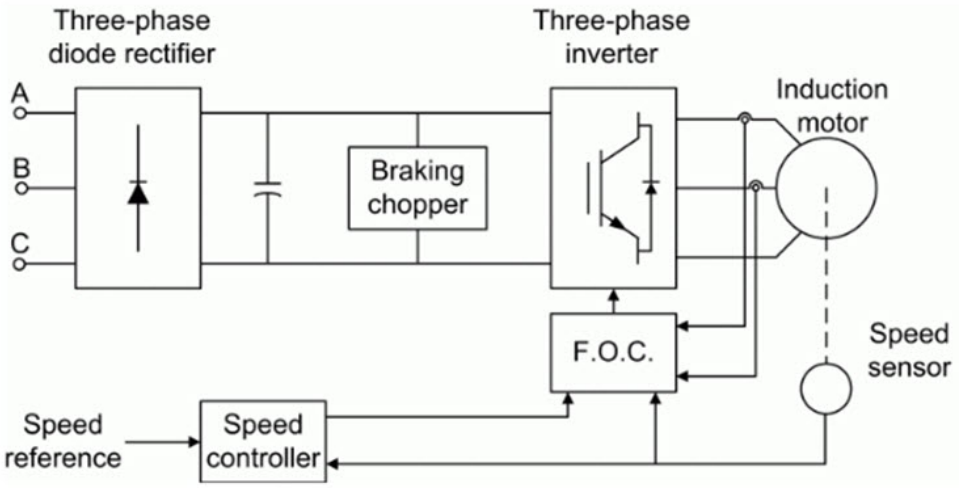

(b) Electrical Schematic

Fig. 9. Field Oriented Control Drive in SimPowerSystems [22]

a. Mass

The block for one concentrated mass is shown in Fig. 10. It is called "Body block". Its mass and inertia tensor can be customized.

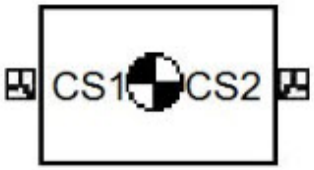

Fig. 10. Concentrated Mass in SimMechanics [22]

b. Connections with Spring and Damper

The following figure presents the blocks for rotational connections and rotational spring/damper. Fig. 11(a) is the rotational connection block called "Revolute joint". The axis of rotational motion can be customized. Fig. 11(b) is the block for adding stiffness and damping to a joint.

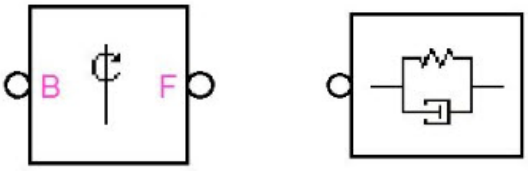

(a) Rotational Connection

(b) Spring/Damper

Fig. 11. Rotational Connections and Spring/Damper in SimMechanics [22]

c. Gear

Fig. 12 shows the block for gear box. The gear ratio is settable.

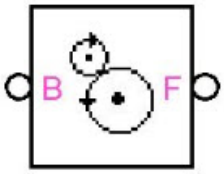

Fig. 12. Gearbox in SimMechanics [22]

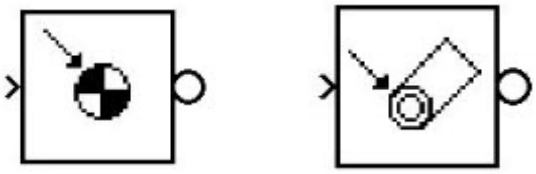

(a) Actuator for Mass

(b) Actuator for Connections

Fig. 13. Motion/Generalized Force Actuators in SimMechanics [22]

d. Actuators

Fig. 13 presents blocks for motion and generalized force (force or torque) actuators. Fig. 13(a) is used to apply motion or generalized force on a mass. A motion could be translational or rotational motion. The motion or generalized force should be defined in a three-dimension vector for x-y-z coordinate system. Fig. 13(b) is an actuator for joint connections.

e. Sensors

Fig. 14 shows sensors for motion, force and torque. Fig. 14(a) is used for mass objects. For detecting relative motion/force/torque of two masses connected by a joint, block in Fig. 14(b) should be used.

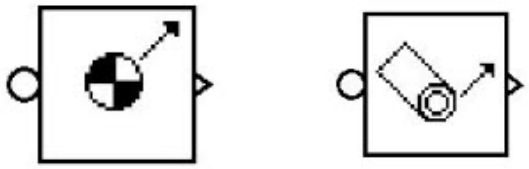

(a) Sensor for Mass

(b) Sensor for Connections

Fig. 14. Motion/Generalized Force Sensors in SimMechanics [22]

D. Interface Method Based on SimPowerSystems and SimMechanics

Since both SimPowerSystems and SimMechanics run in Simulink environment, they can be easily combined with Simulink signals as the interface media.

For a machinery train driven by VFDs, the electrical and mechanical components are influencing the performance of each other. The interface component between the electrical and mechanical systems is the motor rotor. It serves as an important component in both electrical side and mechanical side. In electrical system, the electromagnetic torque is developed from the motor. The motor rotor is forced to rotate and translate torque to other mechanical components. The interaction with other mechanical parts decides the rotational velocity of the motor rotor. Then the rotor velocity influences the electromagnetic field and control values, which influences the electromagnetic torque.

Based on the motor rotor acting in both sides, two interface methods are introduced.

1. Method I - Extended Rotor with Zero Inertia

Thus the motor rotor is the key component to interface the two simulation tools. Here two interface methods are provided. One is to model the rotor inside the electrical

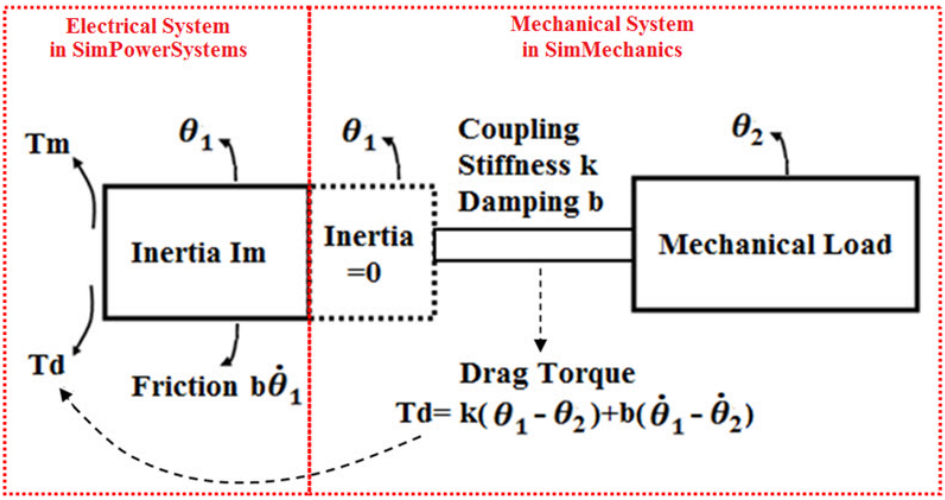

Fig. 15. Illustration for Method I – Extended Rotor with Zero Inertia

system (in SimPowerSystem blocks), and put a zero-inertia body in the mechanical system (in SimMechanics blocks) as an extension of the motor rotor. This method is illustrated in Fig. 15.

The main idea of this method is to copy the motion of the motor rotor in electrical system into the mechanical system. θ_1 is determined in SimPowerSystems and is used to evaluate the coupling torque. The coupling torque of the mechanical model becomes the load torque on the motor. The coupling torque is the input torque (drive torque) of the mechanical components.

2. Method II - Two Rotor Model

The other method is to model the entire mechanical system in SimMechanics – the rotor is modeled in SimMechanics. The motor rotor is copied from SimPowerSystems to SimMechanics, including the inertia and subjected torques. The load torque is obtained in SimMechanics and feedback to SimPowerSystems. The electromagnetic torque is obtained in SimPowerSystems and send to SimMechanics. This method is

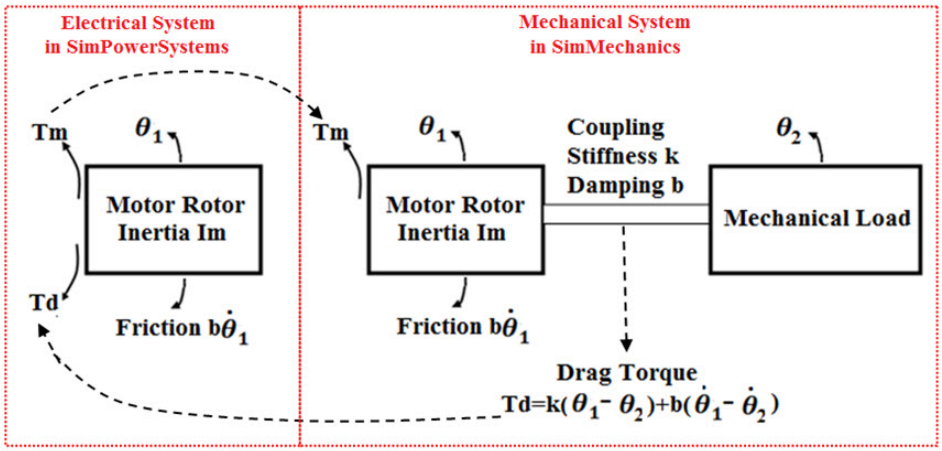

Fig. 16. Illustration for Method II – Two-Rotor Model

illustrated in Fig. ??fig:meth2).

E. Verification Cases

In order to verify the interface methods discussed above, a test case is performed. The verify approach is:

- Model one-inertia (motor rotor) system in SimPowerSystems only;
- Model the same one-inertia system with both SimPowerSystems and SimMechanics;
- Compare the simulation results.

If the two results are identically the same, this interface method is validated.

1. System Description

The test case is a simple motor control system using open-loop Volts/Hertz control method. The system is illustrated in Fig. 17.

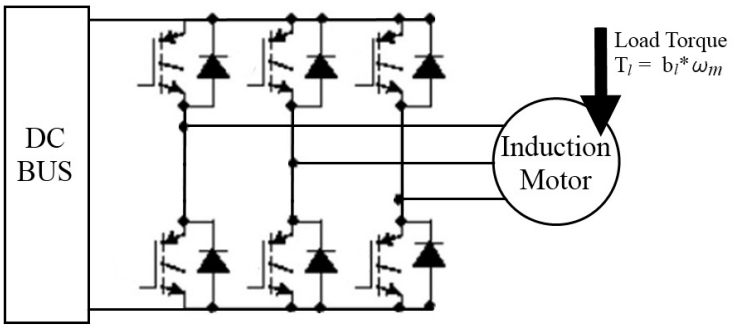

Fig. 17. Motor Control System for Interface Method Verification with Open-Loop Volts/Hertz Control

In the electrical side, a constant DC voltage is acting as the system input. It feeds a three-phase inverter directly, which is composed by six IGBT/Diode power switches. These switches are control by the PWM signals from the Volts/Hertz controller. The inverter output drives the squirrel cage induction motor.

The motor rotor is subject to a mechanical load torque, which is proportional to the velocity of the motor rotor, with the torque coefficient b_l. The motor is set to be operated at its nominal conditions.

The induction motor used here is a 3 HP squirrel cage motor. The detailed parameter settings for the motor, IGBT/Diodes and PWM generator are in Appendix B. Table I lists the nominal value for the motor.

The mechanical part for this system is shown in Fig. 18. The parameters for this mechanical train are listed in Table II.

2. Model with SimPowerSystems Only

Fig. 19 shows the system model build with SimPowerSystems only. No SimMechanics block is included.

The proposional mechanical load on the motor rotor is model as a math function

Table I. 3 HP Motor Nominal Parameters

Motor Nominal Parameters	
Rotor Type	Squirrel-Cage
Power	3 HP
Voltage (phase-phase RMS)	220 V
Frequency	60 Hz
Number of Poles	4

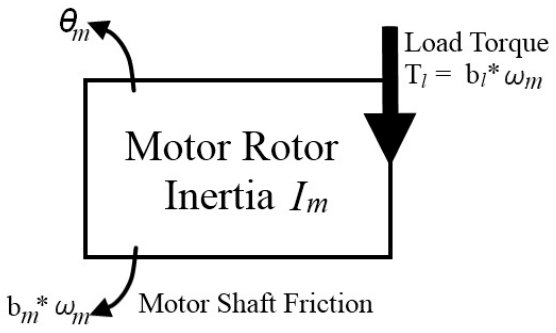

Fig. 18. Mechanical System for Verification Case

Table II. Mechanical Parameters for Verification Case

Mechanical Parameters	
Rotor Inertia I_m	$0.02\,\mathrm{kg{\cdot}m^2}$
Rotor Shaft Friction b_m	$0.005752\,\mathrm{N{\cdot}m/(rad/s)}$
Load Torque Coefficient b_l	$0.063\,\mathrm{N{\cdot}m/(rad/s)}$

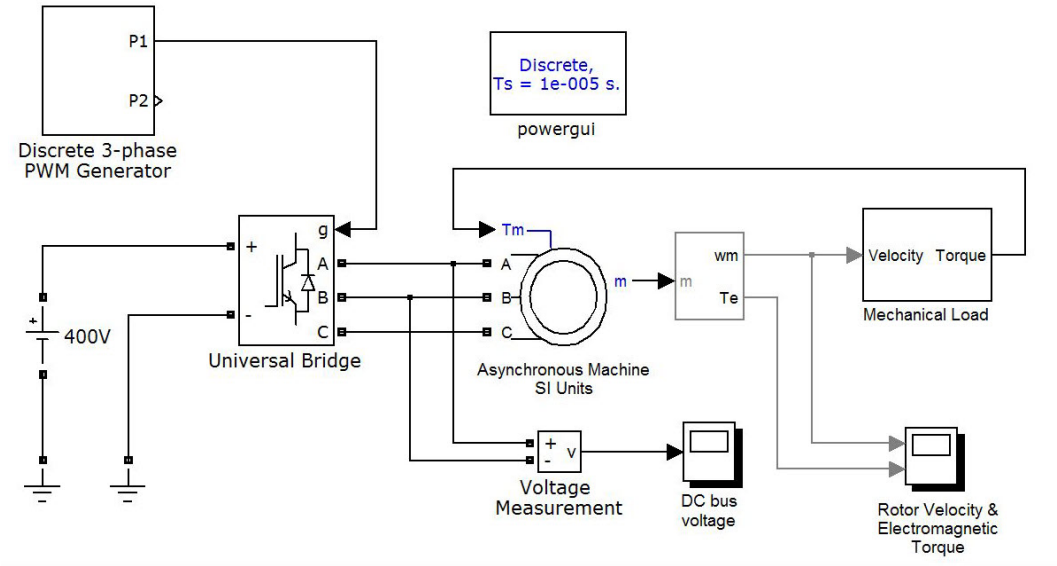

Fig. 19. Model with SimPowerSystems Only for Verification Case

applied to the rotor velocity. Sinulink blocks are used to implement the mechanical load as a subsystem. The blocksets are shown in Fig. 20. The Gain value is equal to the load torque coefficient b_l.

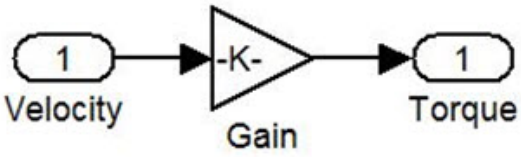

Fig. 20. Subsystem of Mechanical Load for Verification Case

The system is discretized with the sampling time ts as 1e-5 sec. The simulation time is set to be 5 sec. Fig. 21 shows the simulation results of the rotor velocity and the electromagnetic torque. The system reaches its steady state at around 0.5 sec.

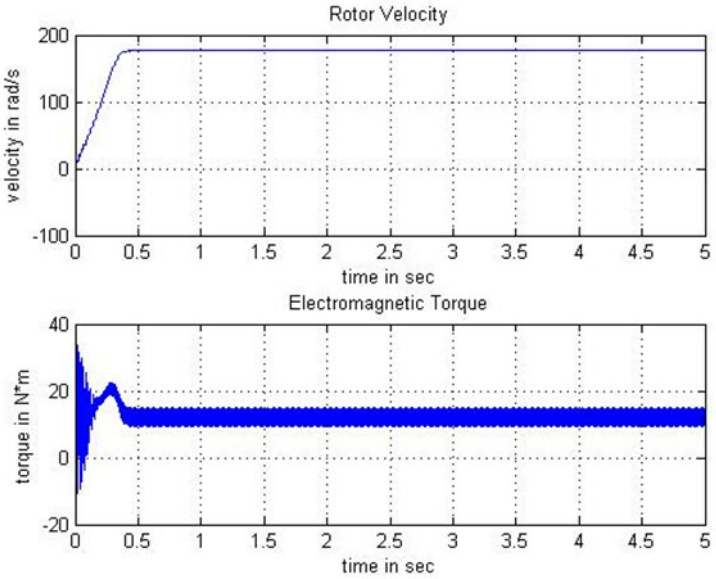

Fig. 21. Simulation Results for Model with SimPowerSystems Only. Upper: Rotor Velocity; Lower: Electromagnetic Torque

3. Model with Interface Method I

Fig. 22 is the model build with both SimPowerSystems and SimMechanis blocks. SimPowerSystems blocks are used for modeling the electrical system, while SimMechanics blocks are used for the mechanical part. The mechanical load torque is modeled as a shaft damping. The interface method used here is the first one – extended rotor with zero inertia.

Fig. 23 illustrates the interface connections. The blocks in left part are for electrical system. And the blocks in right are for mechanical system.

In the mechanical system, a extended rotor is modeled with setting its inertia to zero. This extended rotor is subject to a forced angular motion along its axis. The motion is the same as the motor rotor in angular displacement, angular velocity and angular accelaration (angular motion vector). This is implemented by using a motion actuator, as noted in Fig. 23. The angular motion vector is converted from the motor rotor velocity in electrical system, by using an integrator and a differentiator. The vector conversion subsystem is shown in Fig. 24.

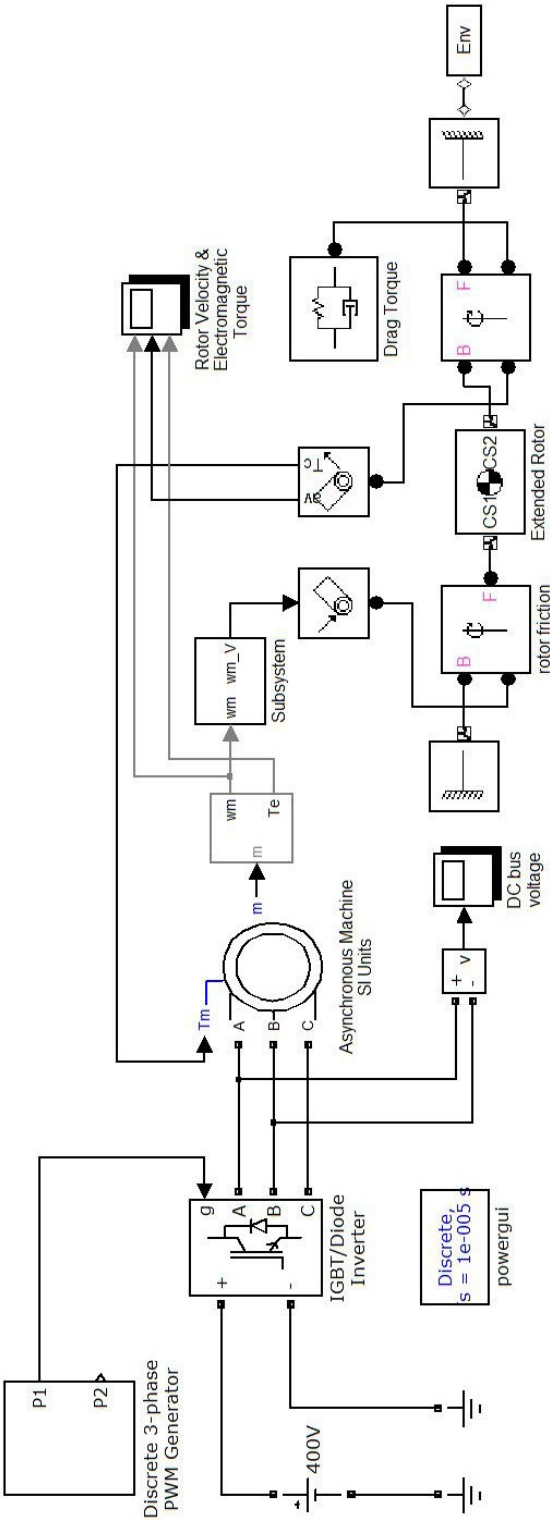

Fig. 22. System Model with SimPowerSystems and SimMechanics with Interface Method I. Extended Rotor with Zero Inertia

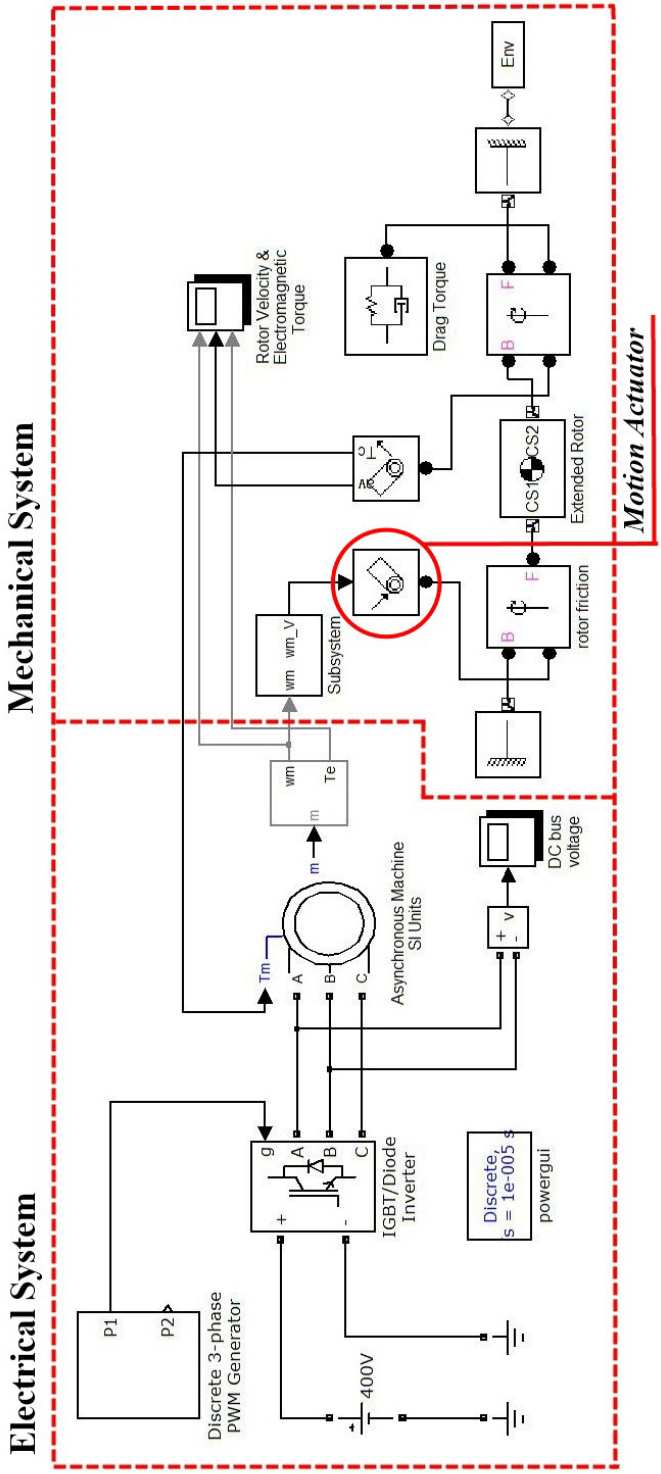

Fig. 23. Illustration for Interface Connections with Interface Method I. Extended Rotor with Zero Inertia

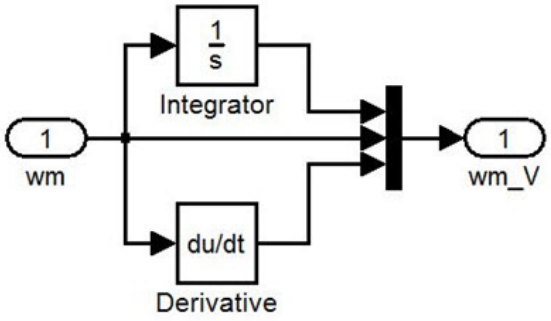

Fig. 24. Angular Motion Vector Conversion

The simulation condition is set to be the same as that for model with SimPowerSystems only. Fig. 25 shows the simulation results. Both the rotor velocity from the induction motor block and velocity of the extended rotor are shown. They are identically the same, which is as expected.

Compare Fig. 21 and Fig. 25, the two models give the same result for the rotor velocity and the electromagnetic torque. The interface method I – "extended rotor with zero inertia" has been verified.

4. Model with Interface Method II

Fig. 26 is the model build with both SimPowerSystems and SimMechanics, using the second interface method – two rotor model. The mechanical load is also model as a damping acting on the motor rotor.

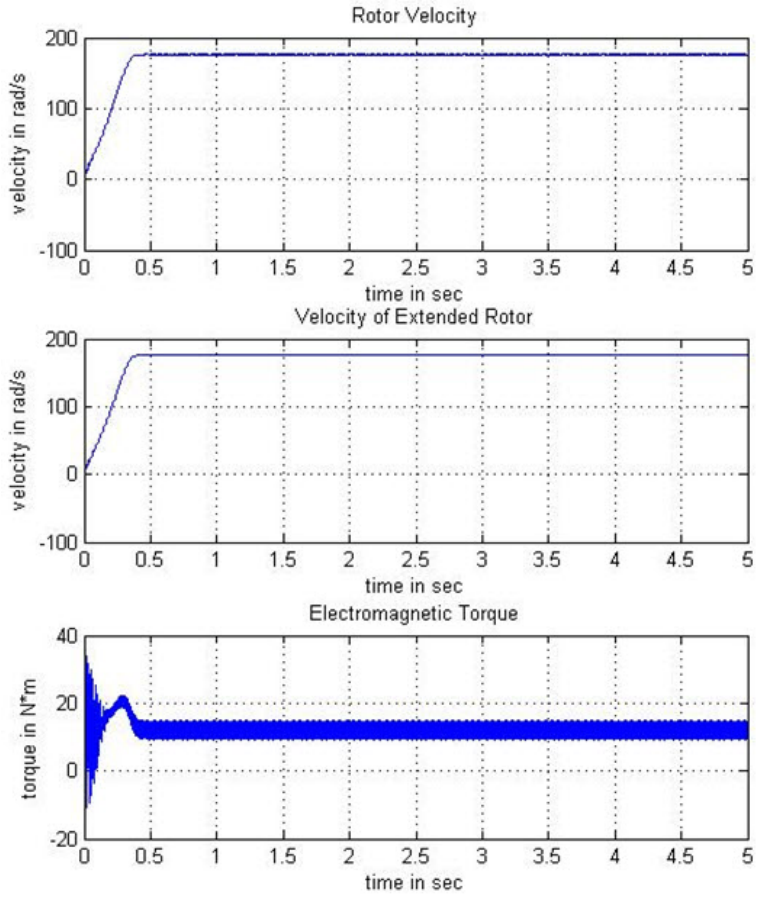

Fig. 25. Simulation Results for Model with Interface Method I.
Upper: Rotor Velocity from Induction Motor Block;
Middle: Velocity of Extended Rotor;
Lower: Electromagnetic Torque

The interface connection is illustrated in Fig. 27. The blocks are noted for electrical part and mechanical part.

In the mechanical system, a second rotor is modeled. This rotor is subject to the same conditions – one electromagnetic torque, one mechanical load torque and one rotor shaft friction. This makes sure the copied rotor in pure mechanical system has the same motion as the motor rotor in the electrical system. The mechanical load torque is also applied to the induction motor. The electromagnetic torque is applied to the second rotor by a actuator, which is circled in red in Fig. 27. The applied torque is converted from scalar to a three-dimension vector, due to the requirement of the joint actuator block. The vector conversion subsystem is shown in Fig. 28.

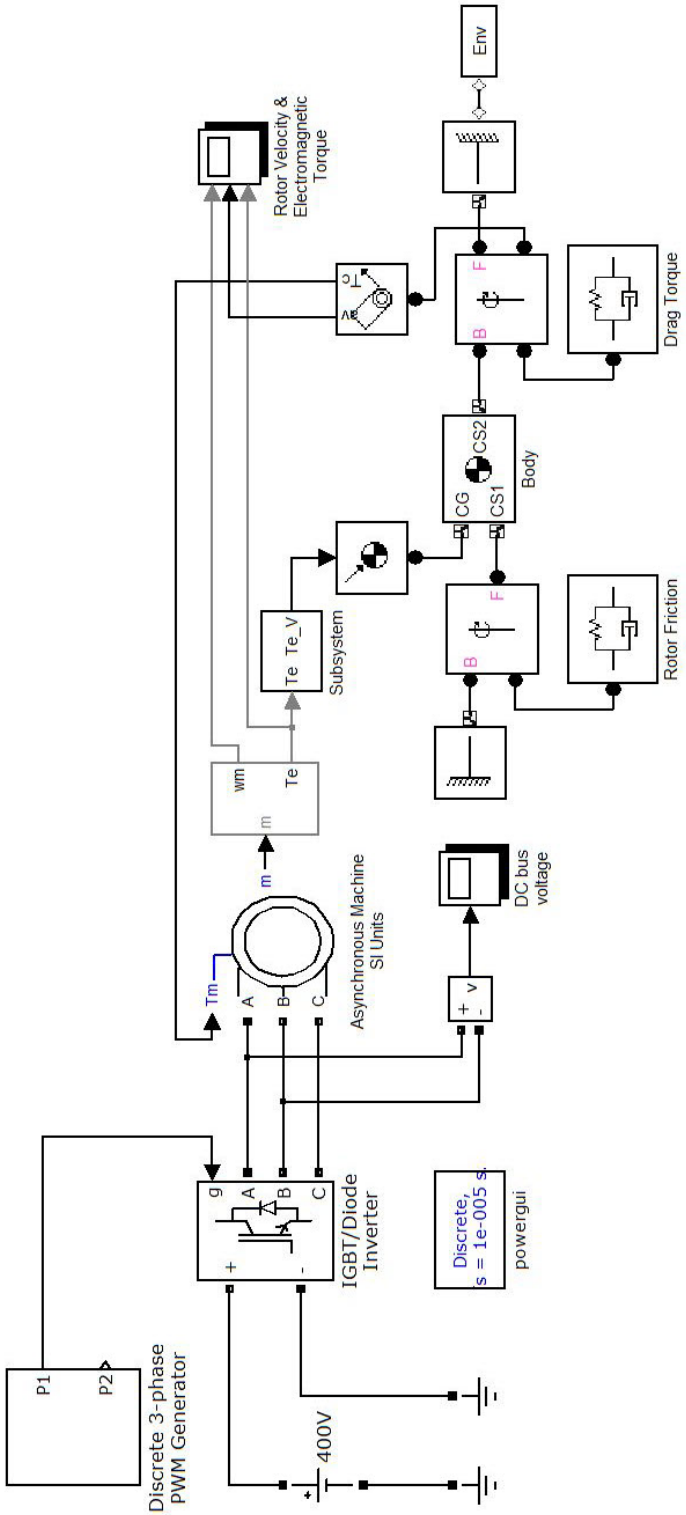

Fig. 26. System Model with SimPowerSystems and SimMechanics with Interface Method II. Two Rotor Model

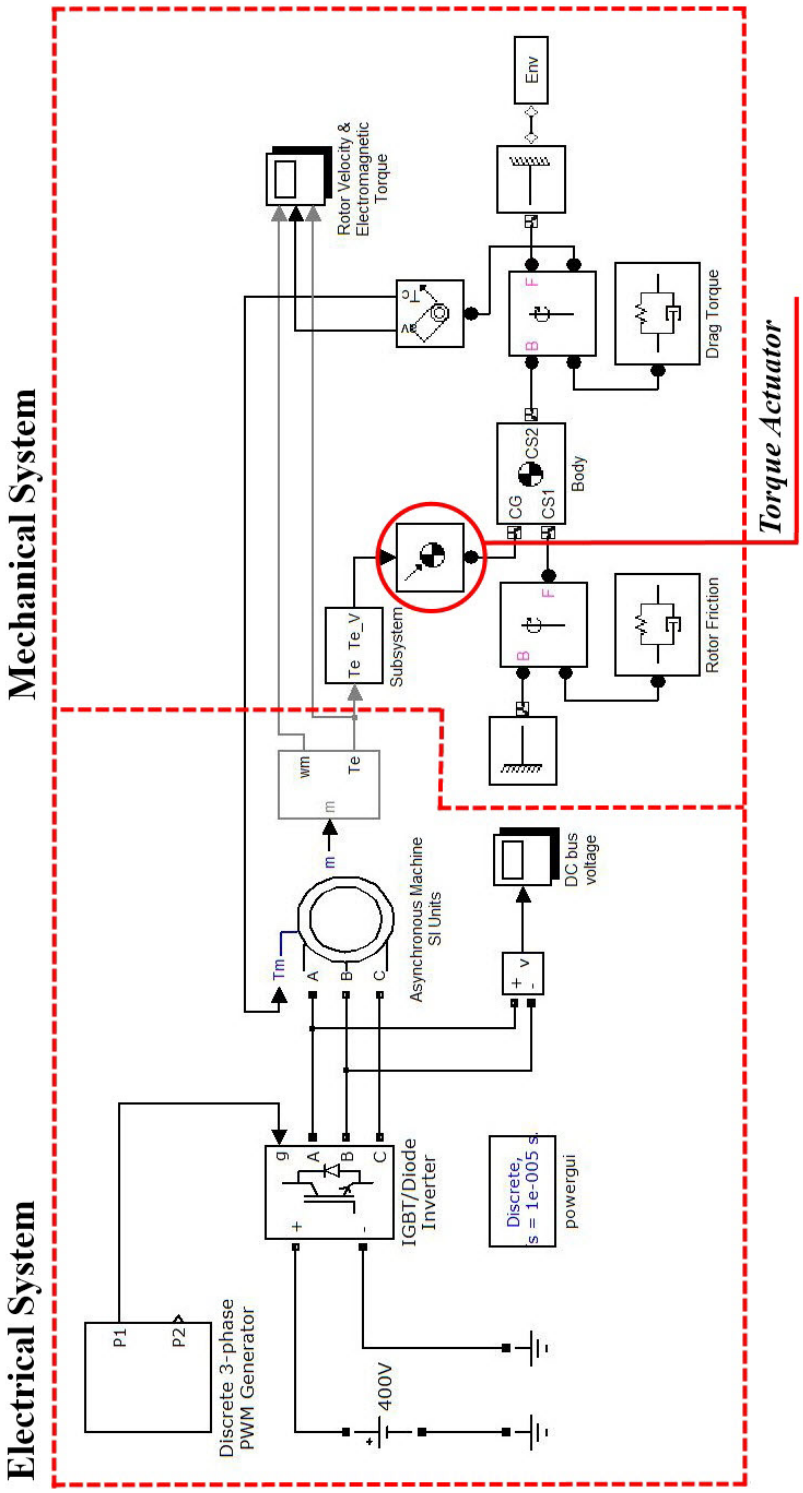

Fig. 27. Illustration for Interface Connections with Interface Method II. Two Rotor Model

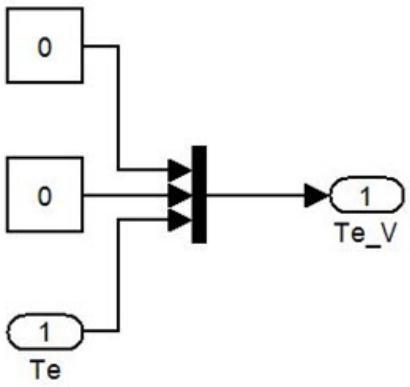

Fig. 28. Torque Vector Conversion

The simulation condition is set to be the same as that for model with SimPowerSystems only. The simulation results are presented in Fig. 29. The upper two figures show the rotor velocity from the induction motor block in electrical system and the velocity of the second rotor in mechanical system. By comparison, they are identically the same as expected.

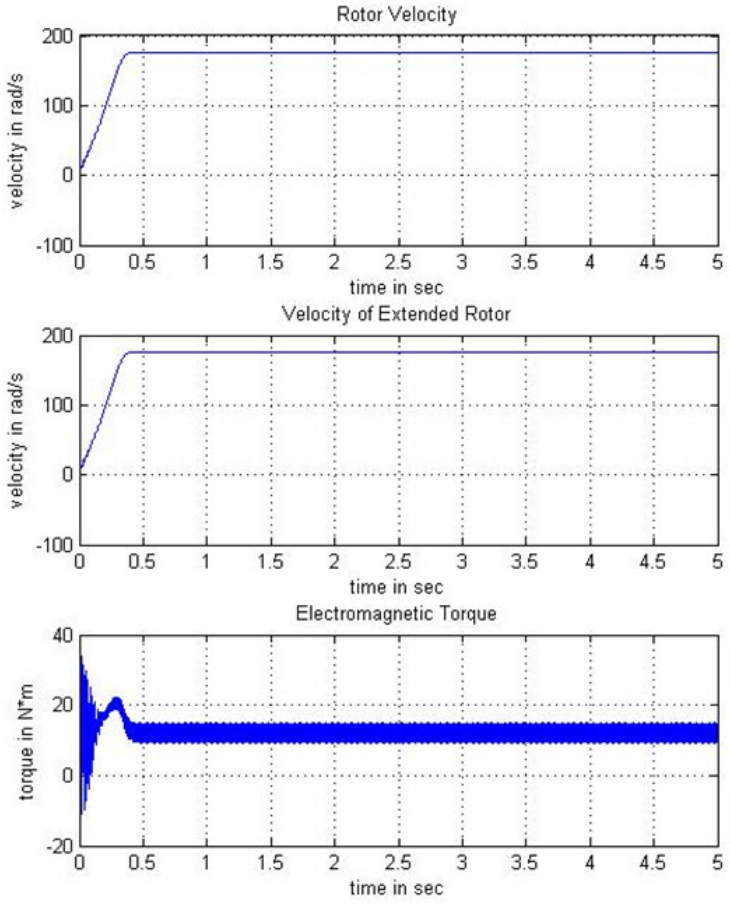

Fig. 29. Simulation Results for Model with Interface Method II.
Upper: Rotor Velocity from Induction Motor Block;
Middle: Velocity of Second Rotor;
Lower: Electromagnetic Torque

CHAPTER IV

ANALYSIS OF OPEN-LOOP CONTROL – VOLTS/HERTZ

In Chapter II, the open-loop Volts/Hertz control method has been discussed, note there is no feedback from the motor side. Fig. 30 presents the basic diagram for a machinery train driven by a VFD using open-loop Volts/Hertz control method.

In this thesis, the PWM generation method for open-loop Volts/Hertz is assumed to be carrier-based PWM generation.

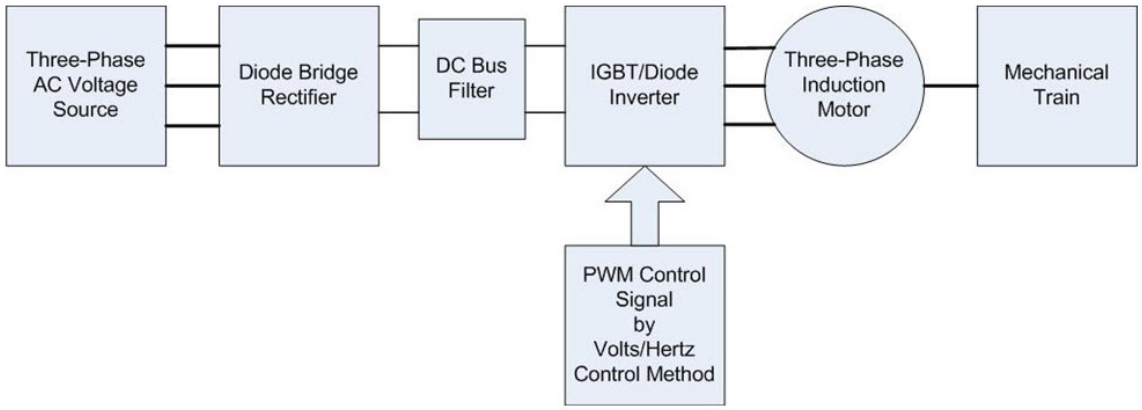

Fig. 30. Machinery Train Driven by VFD with Open-Loop Volts/Hertz Control

A. Analysis for Harmonic Sources

For the machinery train structure shown in Fig. 30, the following items are potential electrical harmonic sources which may induce harmonics in the electromagnetic torque and results in mechanical resonance.

- Non-balanced three-phase AC voltage source

- Non-ideal DC bus voltage fed to inverter (DC bus voltage is not a constant, but with ripples)
- Non-ideal characteristics of the power switches in rectifier and inverter
- Harmonics in the inverter output voltage fed to motor, which is due to the implementation of Volts/Hertz control and PWM signals

The first two harmonic sources all contributes to the DC bus voltage problem, since the diode rectifier is fed by the three-phase AC voltage source. The DC bus filter in Fig. 30 is used to smooth the DC bus ripple and tries to keep the DC bus voltage a constant. Thus the DC ripple value is relatively small with respect to the DC voltage.

Any type of power switches is not an ideal switch. A power switch cannot be turned on and off immediately. When an upper level pulse is given, the current in IGBTs needs some time to be established up from zero. When a "turn off" signal is given, the current in IGBTs needs time to decay away. However, these power switches are switched at a quite high frequency and the "turn on/off" time is quite small. The influence of these non-ideal characteristics is limited.

The fourth harmonic source plays the main role in the contribution of the electromagnetic torque harmonics and system vibrations. The implementation of Volts/Hertz control requires the using of PWM signals to control the power switches. The PWM control signals contain harmonics, which are reflected in the motor input voltage harmonics. These harmonic voltages feed into the motor directly and will result in ripples of electromagnetic torque. If the harmonic frequency of electromagnetic torque is near the natural frequency of the mechanical train, a resonance will be induced.

B. PWM Harmonic Identification

1. Carrier-Based PWM Generation

The PWM generation method used here is a carrier-based PWM. In order to generate a modulated signal containing the information of sinusoidal AC voltage, a triangular carrier signal is compared with a sinusoidal modulation signal, as shown in Fig.31.

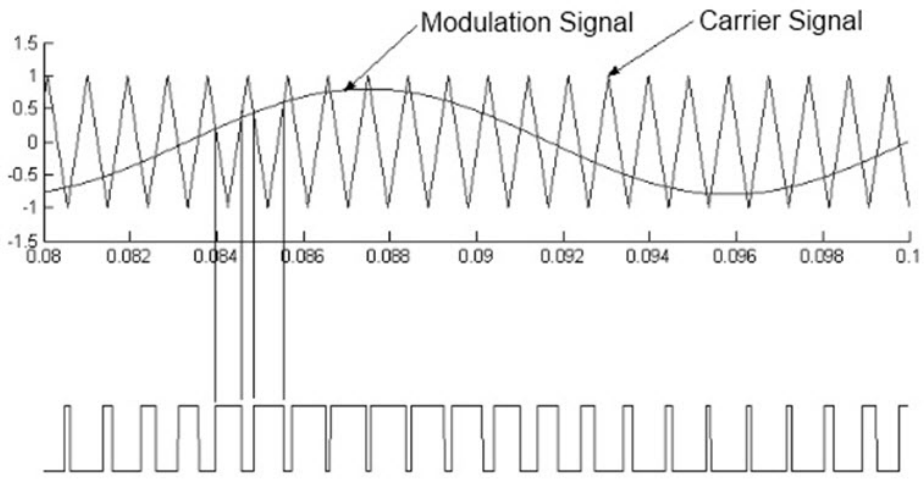

Fig. 31. Carrier-Based PWM Signal Generation [20]

The output pulses (PWM signals) from the PWM generator control the power switches of the inverter, whose input is a smoothed DC voltage as shown in Fig. 30. The inverter output voltage waveform is in the same pattern as the PWM signals.

When the value of the sinusoidal modulation signal is bigger than the value of the triangular carrier signal, the output is at the upper level. The corresponding power switch is turned on, and there is current flowing through it. When the sinusoidal modulation signal is smaller than the triangular carrier signal, the output is at its lower level. The corresponding power switch is turned off. There is no current flowing through it at this time.

The triangular carrier signal has the magnitude of 1 and a fixed high frequency. Thus the PWM signal and inverter output voltage are determined on the sinusoidal modulation signal. The fundamental component of the inverter output voltage has the same frequency as the sinusoidal modulation signal. The magnitude of the fundamental component is dependent on the magnitude ratio of the sinusoidal modulation signal and the triangular carrier signal. This magnitude ratio is called modulation index m.

$$m = \frac{A_{modulation}}{A_{carrier}} \tag{4.1}$$

2. Three-Phase Inverter and PWM Sidebands

Fig. 32 presents the electric circuit of a three-phase IGBT/Diode inverter. There are six IGBT/Diode switches Q1 to Q6. Six corresponding PWM signals are needed to control this inverter.

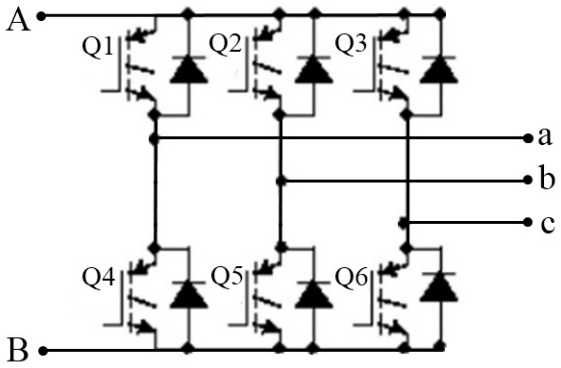

Fig. 32. Three-Phase IGBT/Diode Inverter

Each vertical connected IGBT/Diodes are called an arm. There are three arms in Fig. 32. The two power switches cannot be at their "on" state at the same time because in that case the DC bus would be shorted. Thus the PWM signals for the

two switches in the same arm are compensated to each other. An example for Q1 and Q4 is illustrated in Fig. 33.

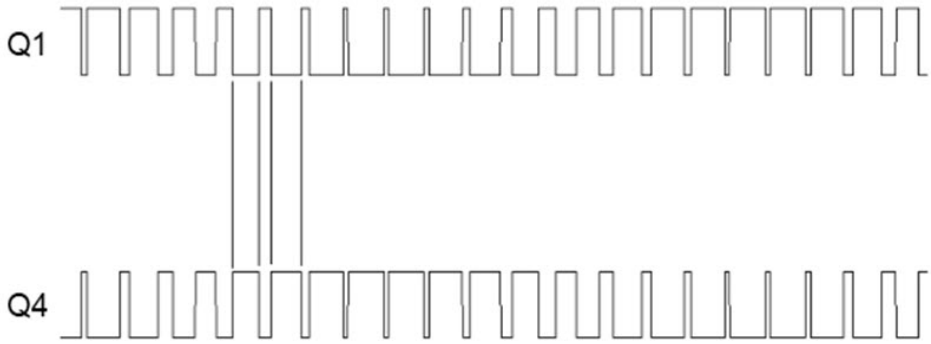

Fig. 33. Compensated Pulses for Switch Q1 and Q4 in Three-Arm Inverter [20]

For this three phase inverter, the PWM signals are generated by comparing the triangular carrier signal with three-phase AC sinusoidal modulation signals. Fig. 34 shows the six pulse for the six power switches Q1 – Q4.

If the inverter input DC voltage is V_{DC}, The magnitude of the output voltages has the following relationship with the modulation index m.

$$V_{LL-RMS} = \frac{m}{2} \times \frac{\sqrt{3}}{\sqrt{2}} V_{DC} \tag{4.2}$$

Let f_{PWM} presents the frequency of the triangular carrier signal, and the three-phase AC sinusoidal modulation signal has a frequency of f_e. Then the sideband frequencies of the output PWM signals and the output voltage of the inverter are

$$a \times f_{PWM} \pm b \times f_e \tag{4.3}$$

where $a + b$ is an odd integer.

The output voltage of the inverter contains the same sideband harmonics as the PWM signals. The electromagnetic torque sideband frequencies due to these input

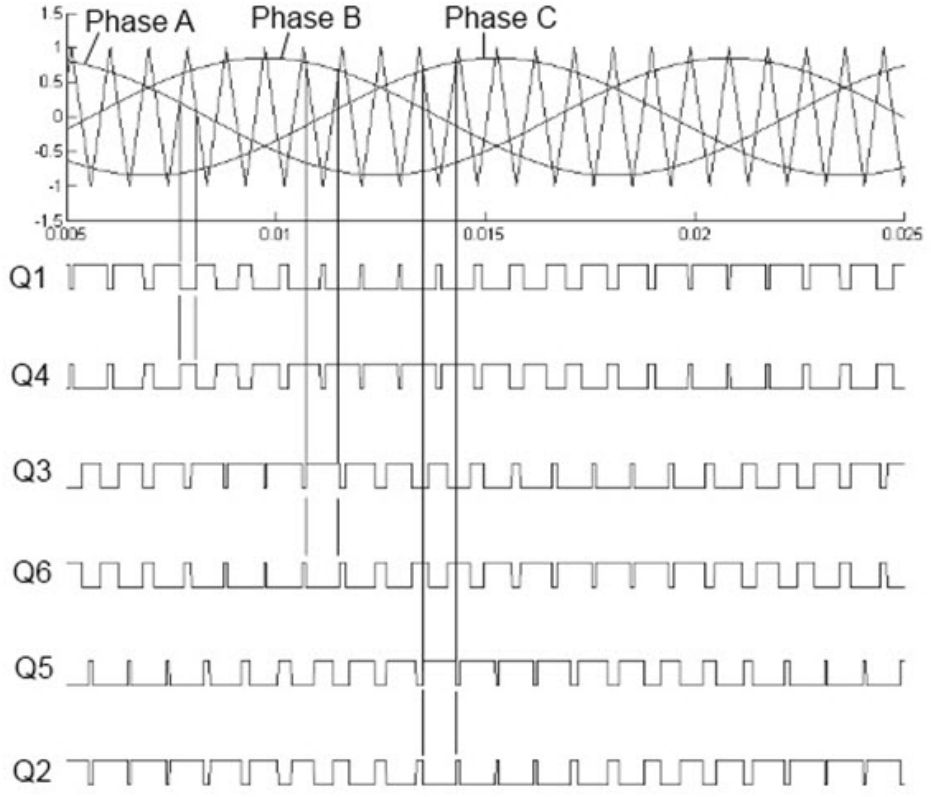

Fig. 34. PWM Generation for Three-Phase Three-Arm Inverter [20]

voltage sideband harmonics are

$$c \times f_{PWM} \pm d \times f_e \tag{4.4}$$

where $c + d$ is even integer.

If the sideband harmonics of the electromagnetic torque coincide with the torsional natural frequency of the mechanical train, a torsional resonance will occur.

C. Motor-Compressor Machinery Train

To study the open-loop Volts/Hertz control, a motor-compressor machinery train model is built. Fig. 35 shows its structure diagram. The system is driven by a VFD with open-loop control.

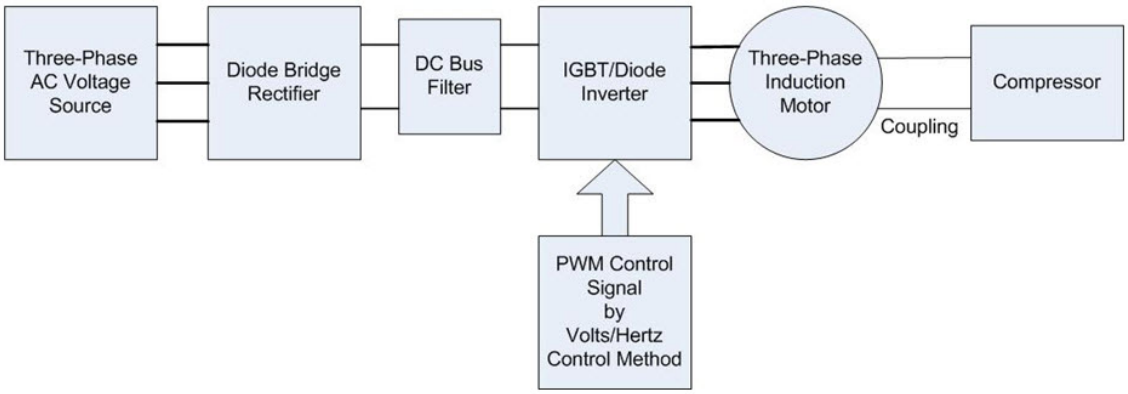

Fig. 35. Motor-Compressor Machinery Train

1. Electric Induction Motor

The squirrel-cage induction motor used here is 150 HP. The nominal parameters are listed in Table III. The detailed motor parameters are in Appendix B. From the nominal voltage and frequency, the Volts/Hertz ratio for this motor is 8 (= 400 V/50 Hz).

2. Mechanical Components

The mechanical system is illustrated in Fig. 36. The compressor is connected to the motor rotor via a coupling, where the coupling is assumed to be a spool piece. Suppose the compressor is subject to a mechanical load, which is proportional to the compressor rotating speed ω_c. The load torque ratio is denoted by b_l.

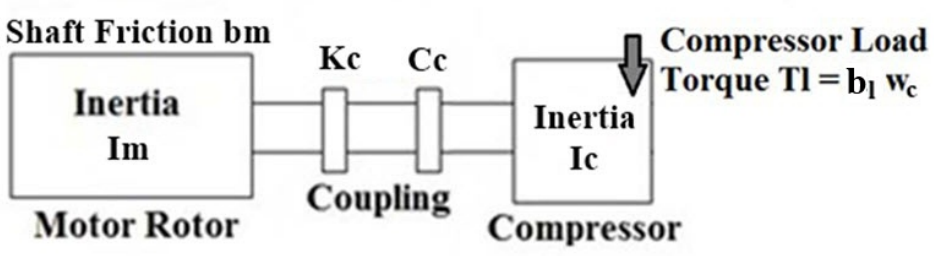

Fig. 36. Motor-Compressor Mechanical System

The parameters for this mechanical train are listed in Table IV. The shear stress of the coupling is calculated as Eq. (4.5).

$$\tau = T_t \frac{r}{(LK_c/G)} \tag{4.5}$$

where T_t is the transmitted torque from the motor, which is also the mechanical load torque acting on the motor.

D. Effects of Volts/Hertz Controller & PWM Sidebands

1. Assumptions

In order to see the effects of PWM sidebands on mechanical torsional vibration, the following assumptions are made.

- Ideal DC bus voltage = 800 V

Table III. 150 HP Motor Nominal Parameters

Motor Nominal Parameters	
Rotor Type	Squirrel-Cage
Power	150 HP
Voltage (phase-phase RMS)	400 V
Frequency	50 Hz
Number of Poles	4
Volts/Hertz Ratio	8

Table IV. Mechanical Parameters for Motor-Compressor Train

Induction Motor	
Rotor Inertia I_m	2.3 kg·m^2
Rotor Shaft Friction b_m	0.05421 N·m/(rad/s)
Coupling	
Stiffness K_c	31000 N·m/rad
Damping C_c	5.88 N·m/(rad/s)
Radius r	0.075 m
Length L	0.5 m
Shear Modulus G	2.136e9 N·m^2
Compressor	
Inertia I_c	13.8 kg·m^2
Compressor Load	
Torque/Speed Ratio b_l	4.5 N·m/(rad/s)
Natural Frequency	20 Hz

- Ideal power switches for inverter

These assumptions eliminate all the other harmonic sources for electromagnetic torque except PWM effects. Then motor-compressor train driven by VFD with Volts/Hertz is simplified as in Fig. 37.

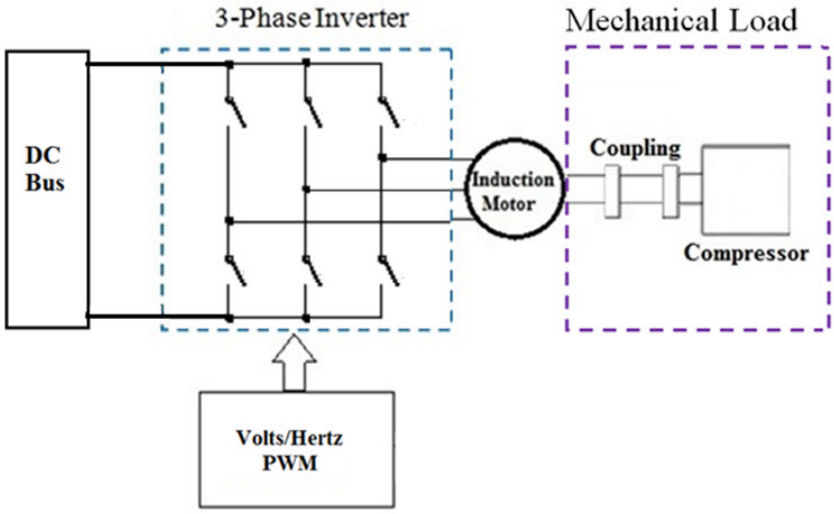

Fig. 37. VFD Driven Motor-Compressor Train with Open-Loop Volts/Hertz Control; Assumptions: Ideal DC Bus Voltage and Ideal Inverter Switches

2. System Model in SimPowerSystems and SimMechanics

The system shown in Fig. 37 is built with SimPowerSystems and SimMechanics, using the second interface method "two-rotor model", which is mentioned in Chapter III. The system model is shown in Fig. 38. The PWM carrier digital frequency is set to be 950 Hz. The simulator is set to be discrete. The time step is 1e-6 sec. This simulation setting is used for all the simulations in this thesis.

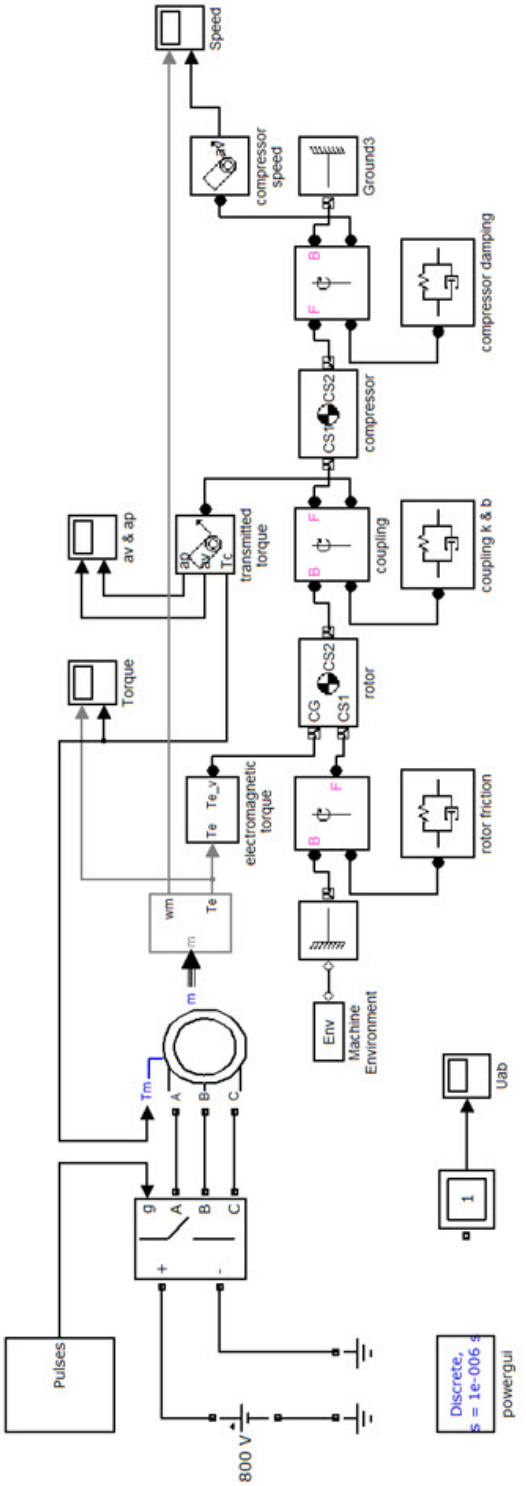

Fig. 38. SimPowerSystems and SimMechanics Model for VFD Driven Motor–Compressor Train with Open-Loop Volts/Hertz Control; Assumptions: Ideal DC Bus Voltage and Ideal Power Switches for Inverter

3. Running at Nominal Frequency

In this case, the motor is running at its nominal frequency 50 Hz. The simulation results are shown from Fig. 39 to Fig. 42. Spectrums are ploted for relative angular displacement and electromagnetic torque via Fast Fourier Transform (FFT). From Fig. 40(a), the peak to peak value of the relative angular displacement is approximate 0.0004 rad. In Fig. 42, the shear stress value (peak to peak) at steady state is about 1e5 N*m^2.

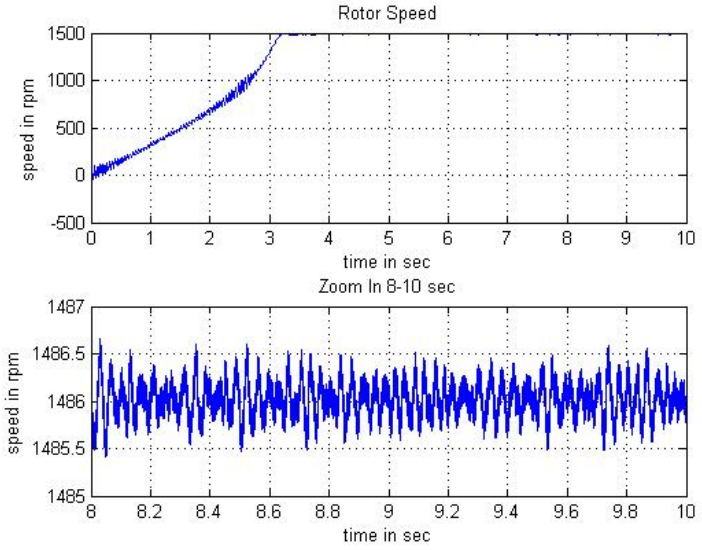

Fig. 39. Motor-Compressor Train with Volts/Hertz; Rotor Speed – Motor Operation Frequency 50 Hz; Assumptions: Ideal DC Bus Voltage and Ideal Switches

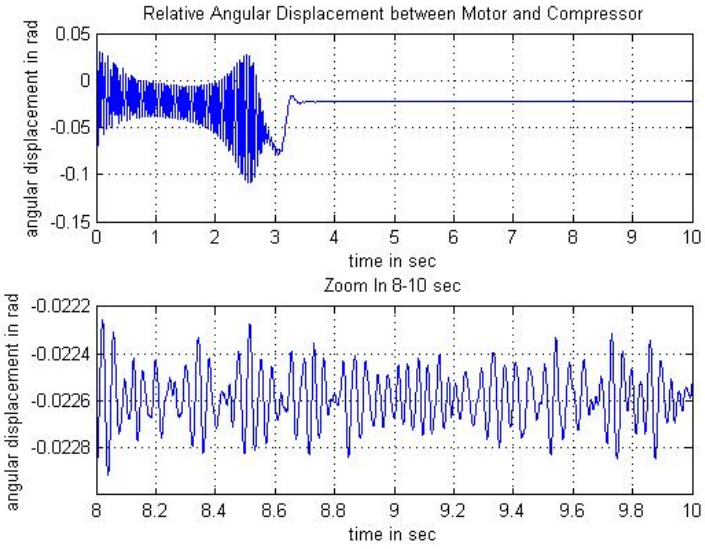

(a) Time Domain

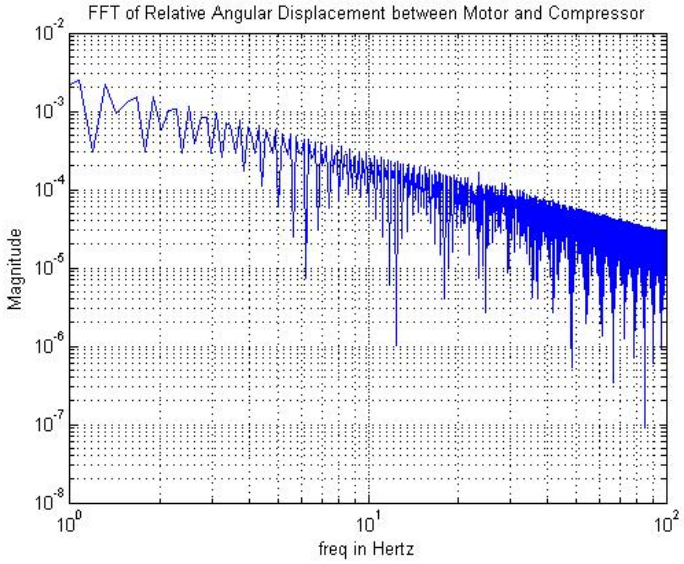

(b) Frequency Domain

Fig. 40. Motor-Compressor Train with Volts/Hertz; Relative Angular Displacement between Motor and Compressor – Motor Operation Frequency 50Hz; Assumptions: Ideal DC Bus Voltage and Ideal Switches

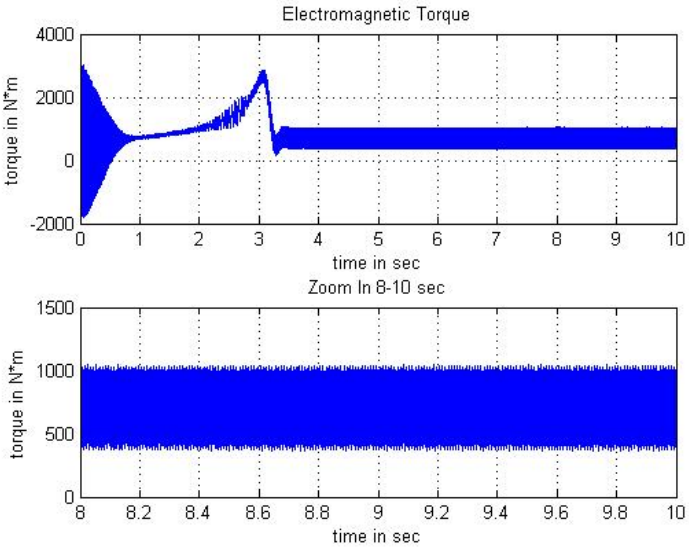

(a) Time Domain

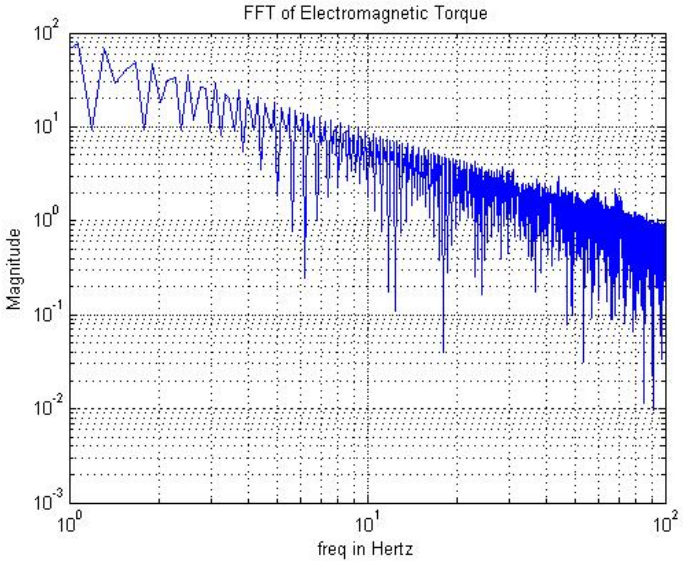

(b) Frequency Domain

Fig. 41. Motor-Compressor Train with Volts/Hertz; Electromagnetic Torque – Motor Operation Frequency 50 Hz; Assumptions: Ideal DC Bus Voltage and Ideal Switches

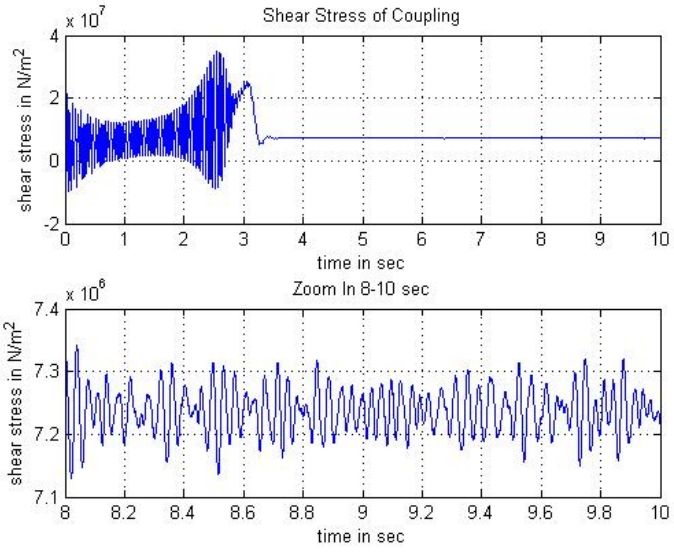

Fig. 42. Motor-Compressor Train with Volts/Hertz; Shear Stress of Coupling – Motor Operation Frequency 50 Hz; Assumptions: Ideal DC Bus Voltage and Ideal Switches

4. Resonance

In this case, the operating frequency of the motor is 32 Hz. The electrical frequency for the PWM output is 32 Hz. From Eq. (4.4), the torque harmonic frequencies have the form

$$c \times f_{PWM} \pm d \times f_e \tag{4.6}$$

where $c + d$ is an even integer.

In this case, $f_PWM = 950\,\text{Hz}$, $f_e = 32\,\text{Hz}$. One of the harmonic frequency of the electromagnetic torque is

$$1 * f_PWM - 29 * f_e = 22\,\text{Hz} \tag{4.7}$$

with $c = 1$, $d = 29$.

This frequency is quite near the mechanical natural frequency of the system, which is 20 Hz. The simulation results are shown in Fig. 43 to Fig. 46. From Fig. 44(a), the peak to peak value of the relative angular displacement is approximate 0.004 rad, while for 50 Hz case the value is 0.0004 rad. From Fig. 46, the shear stress peak to peak amplitude at steady state is about 1.25e6 N*m^2. Compared with that value of 1e5 N*m^2 in 50 Hz case, the torsional vibration is much bigger in this case. A resonance occurs in this system. A harmonic of 22 Hz is obvious in the spectrum of the electromagnetic torque and the relative angular displacement.

A comparison of oscillations of the two cases shown in Table V.

Table V. Comparison of Oscillation for Motor-Compressor Train with Open-Loop Volts/Hertz Running at 50 Hz and 32 Hz

Motor Operating Frequency	Relative Angular Displacement between Motor and Compressor (Peak to Peak, Steady State)	Shear Stress of Coupling (Peak to Peak, Steady State)
50 Hz	0.0004 rad	1e5 N/m^2
32 Hz	0.004 rad	12.5e5 N/m^2

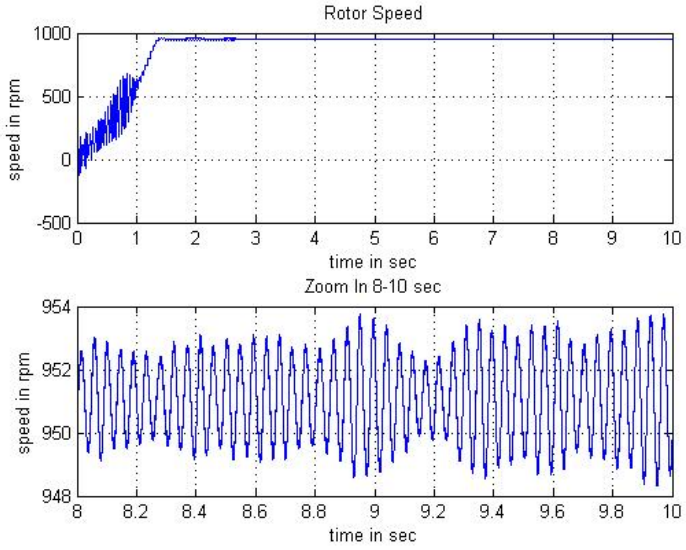

Fig. 43. Motor-Compressor Train with Volts/Hertz; Rotor Speed – Motor Operation Frequency 32 Hz; Assumptions: Ideal DC Bus Voltage and Ideal Switches

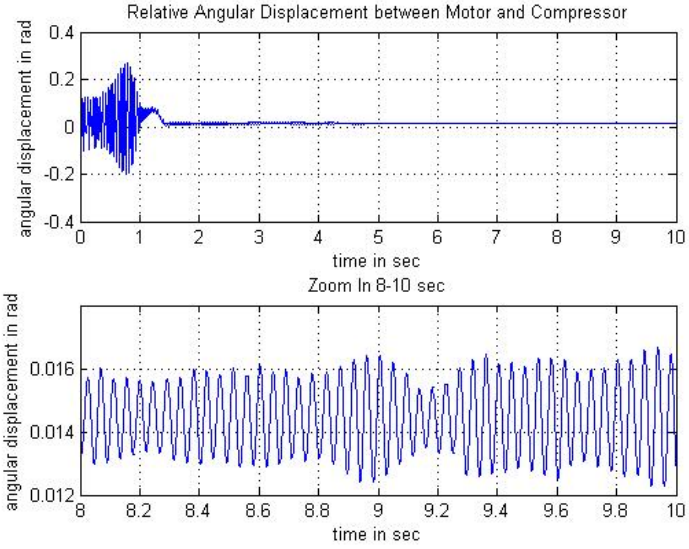

(a) Time Domain

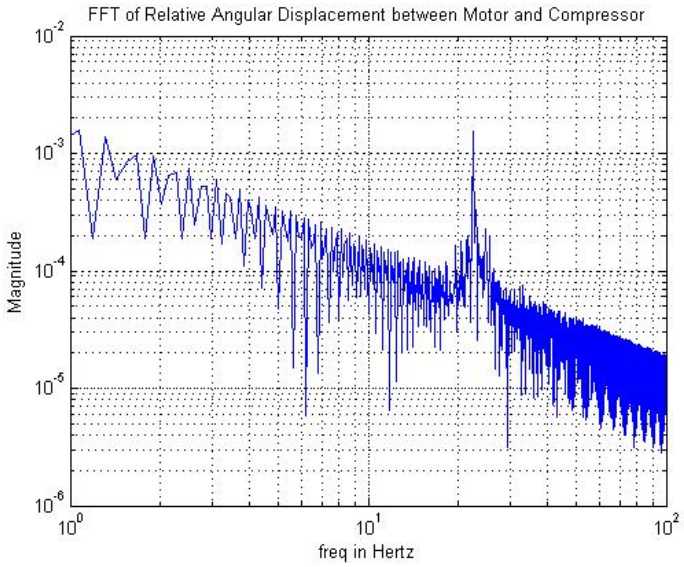

(b) Frequency Domain

Fig. 44. Motor-Compressor Train with Volts/Hertz; Relative Angular Displacement between Motor and Compressor – Motor Operation Frequency 32 Hz; Assumptions: Ideal DC Bus Voltage and Ideal Switches

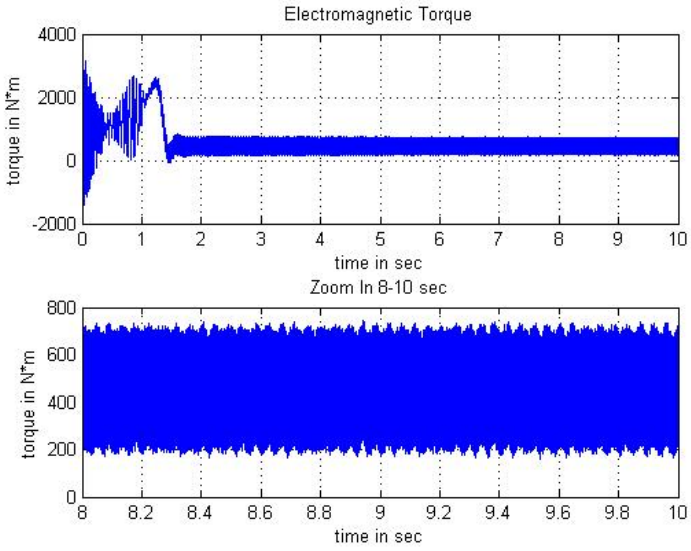

(a) Time Domain

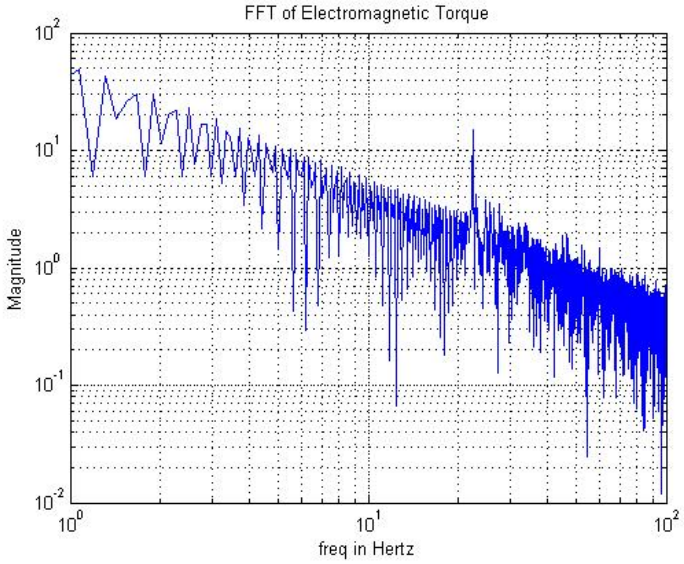

(b) Frequency Domain

Fig. 45. Motor-Compressor Train with Volts/Hertz; Electromagnetic Torque – Motor Operation Frequency 32 Hz; Assumptions: Ideal DC Bus Voltage and Ideal Switches

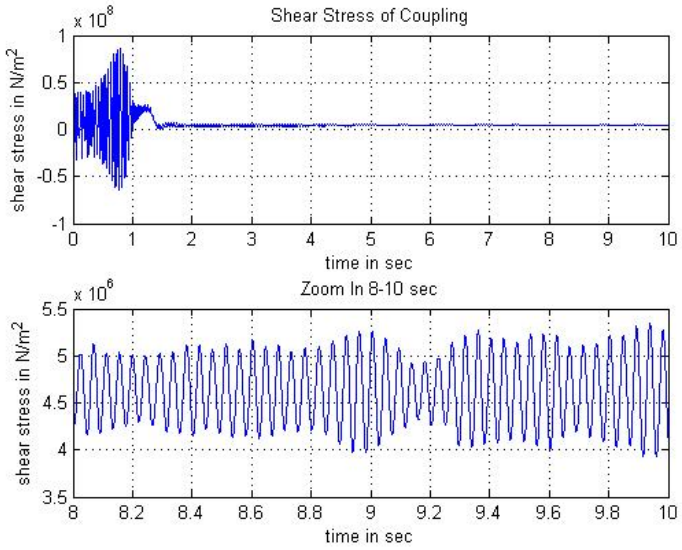

Fig. 46. Motor-Compressor Train with Volts/Hertz; Shear Stress of Coupling – Motor Operation Frequency 32 Hz; Assumptions: Ideal DC Bus Voltage and Ideal Switches

E. Effects of IGBT/Diodes with Non-Ideal Characteristics in Inverter

1. Assumptions

In order to find the effects of the non-ideal characteristics of IGBT/Diodes of the inverter, change the ideal switches in Fig. 37 to IGBT/Diodes. And the following assumption holds.

- Ideal DC bus voltage = 800 V

This ideal DC bus makes sure the change in simulation results come from the non-ideal characteristics of the power switches. The system diagram is shown in Fig. 47.

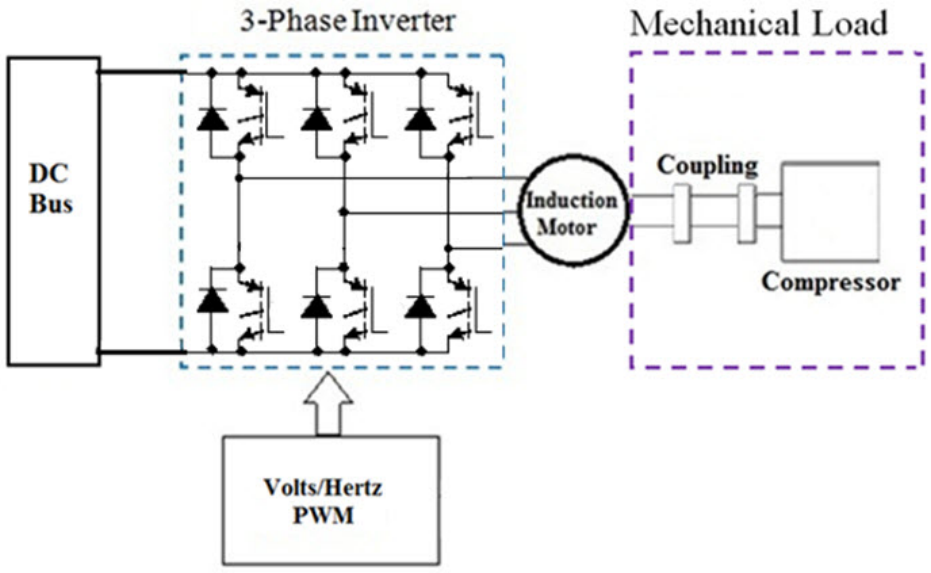

Fig. 47. VFD Driven Motor-Compressor Train with Open-Loop Volts/Hertz Control; Assumptions: Ideal DC Bus Voltage

The non-ideal characteristic of diode is modeled as shown in Fig. 48. A diode is modeled with a small forward voltage V_f and an internal resistance R_{on}. It will be turn on when the voltage across its terminal is less than V_f.

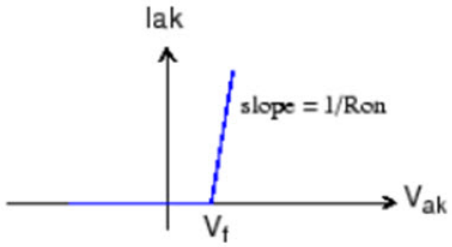

Fig. 48. Non-Ideal Characteristic of Diode [20]

Fig. 49 presents the IGBT model with non-ideal characteristics. For "turn-on" characteristic, it needs a turn-on forward voltage V_f. For "turn-off" characteristic, it has fall time and tail time. Fall time is the time it needs to let the current drop from the maxmum value to ten percents of that value. Additional tail time is required for the current to drop to zero.

2. System Model in SimPowerSystems and SimMechanics

The system model in SimPowerSystems and SimMechanics is shown in Fig. 50, which is the same as Fig. 37 except changing the ideal switches into IGBT/Diodes.

The detailed settings for IGBT/Diodes are listed in Table VI. These values are quite small compared with the voltage and resistance of the motor.

3. Simulation with Non-Ideal IGBT/Diodes

The motor is set to be operated at its nominal frequency 50 Hz. Except changing the ideal switches into IGBT/Diodes, all other parameters are identically the same as the

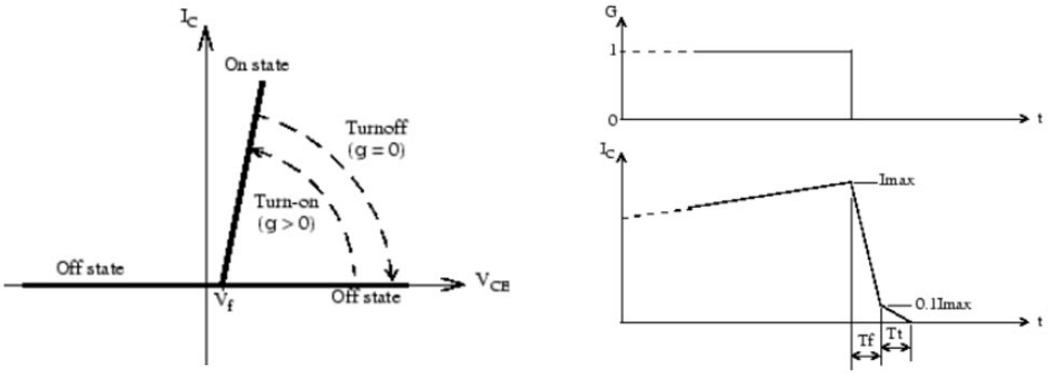

(a) Turn-On Characteristic (b) Turn-Off Characteristic

Fig. 49. Non-Ideal Characteristic Model of IGBT [20]

Table VI. IGBT/Diode Characteristics Setting

IGBT/Diode Parameters	
On-State Resistance R_on	1e-3 Ohm
IGBT Forward Voltage V_{f-IGBT}	0.8 V
Diode Forward Voltage $V_{f-Diode}$	0.8 V
IGBT Fall Time T_f	1e-6 sec
IGBT Tail Time T_t	2e-6 sec

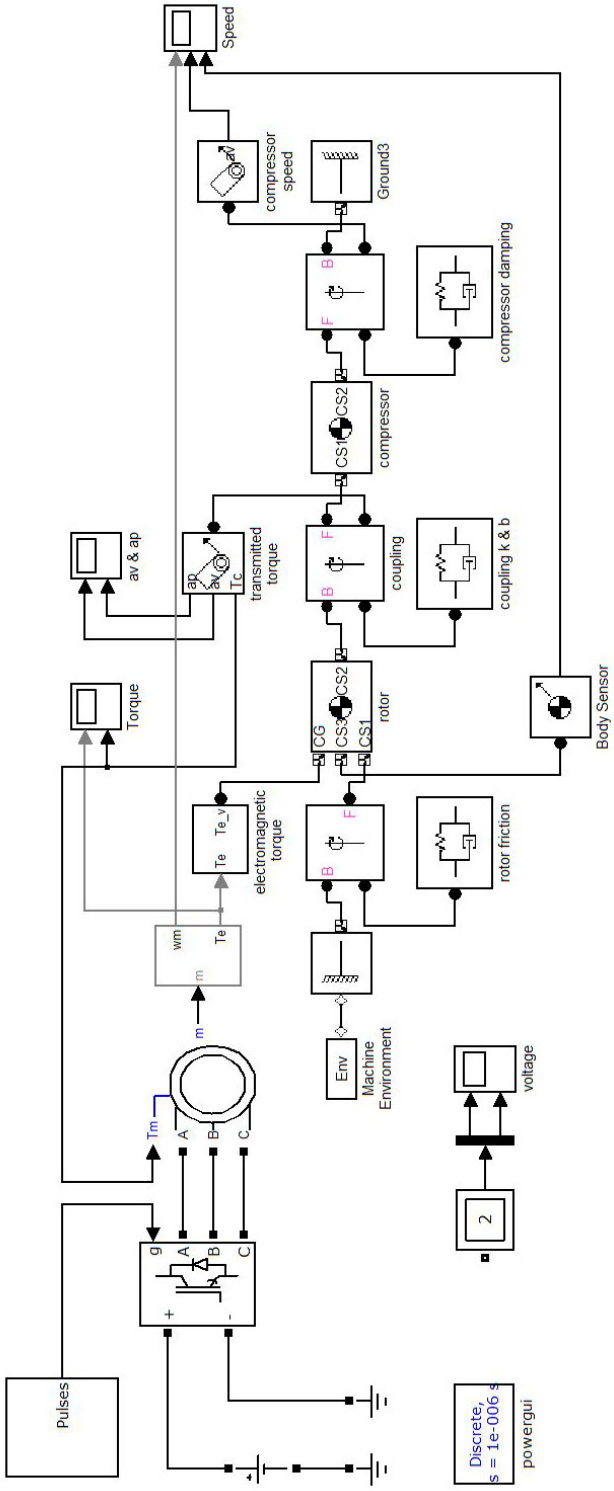

Fig. 50. SimPowerSystems and SimMechanics Model for Motor-Compressor Train with Open-Loop Volts/Hertz Control; IGBT/Diode Inverter Study

ideal switches case. The simulation results are shown in Fig. 51 to Fig. 54. Compared with the simulation results for the case of ideal switches, the two simulation results show no big differences.

From Fig. 51, the zoomed view of rotor speed in 8–10 sec, the rotor speed with IGBT/Diodes is a little smaller than the ideal switch case. This is because the non-ideal power switches consume energy.

The effects of the non-ideal characteristics of the power switches in system vibrations are relatively small with respect to the PWM harmonics, which is induced by the use of Volts/Hertz control method. This is because the voltage characteristics (the forward voltage of IGBTs and diodes) are quite small comparing with the motor operating voltage and the harmonics from the inverter. And the time characteristics (the fall time and tail time of IGBTs) are quite small compared with the PWM switching period (inverse of the PWM switching frequency).

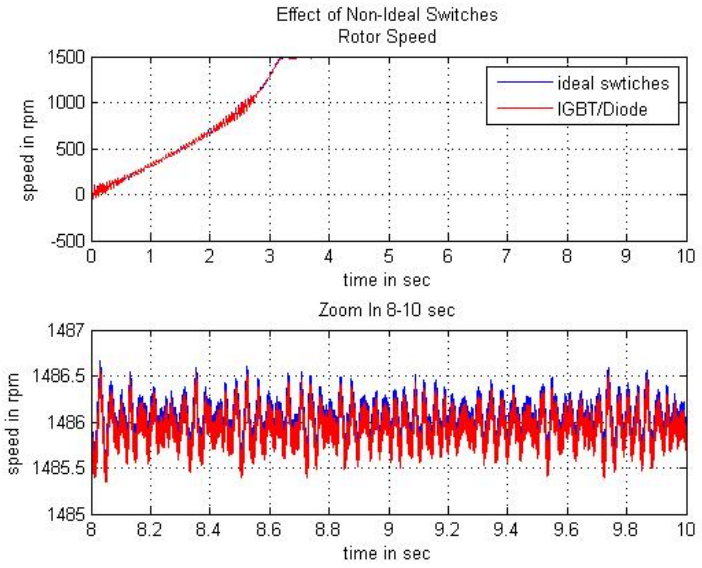

Fig. 51. Motor-Compressor Train with Volts/Hertz; Rotor Speed – Motor Operation Frequency 50 Hz; IGBT/Diode Inverter Case Compared with Ideal Switch Case

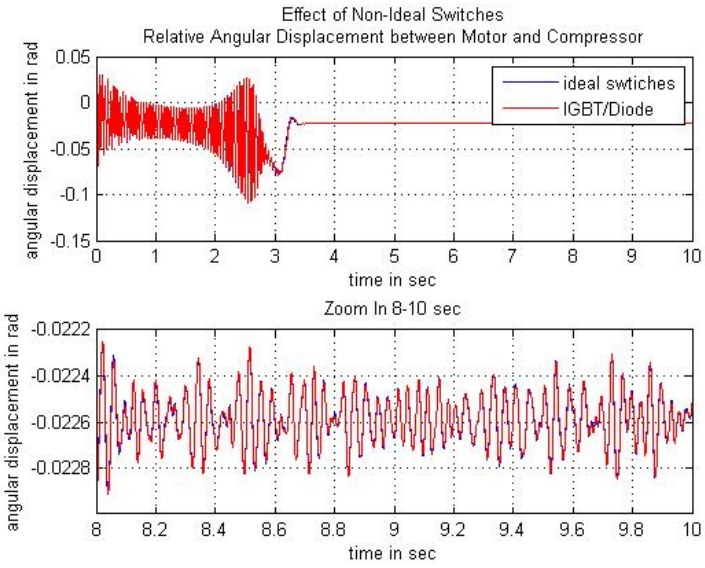

(a) Time Domain

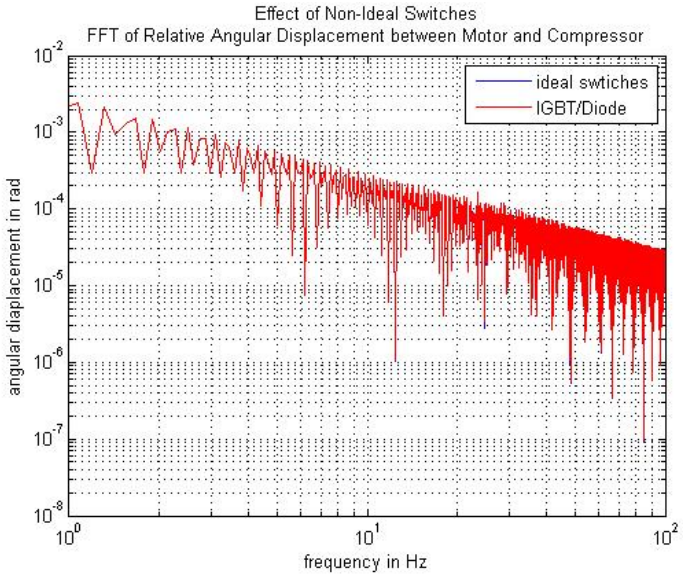

(b) Frequency Domain

Fig. 52. Motor-Compressor Train with Volts/Hertz; Relative Angular Displacement between Motor and Compressor – Motor Operation Frequency 50 Hz; IGBT/Diode Inverter Case Compared with Ideal Switch Case

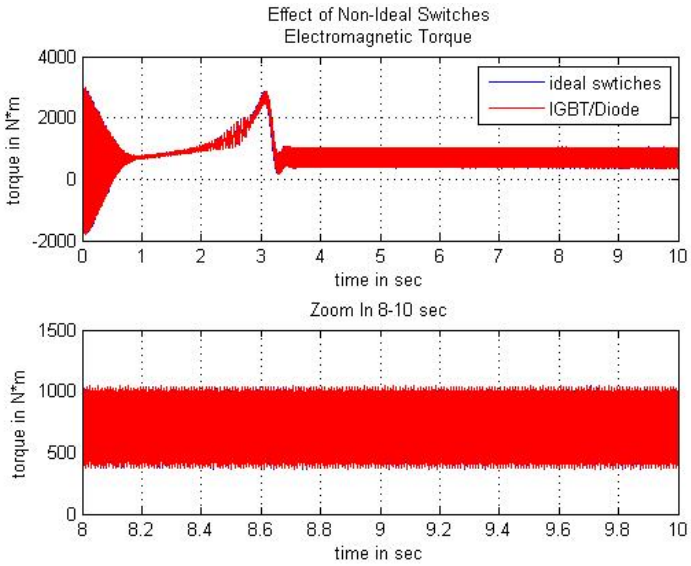

(a) Time Domain

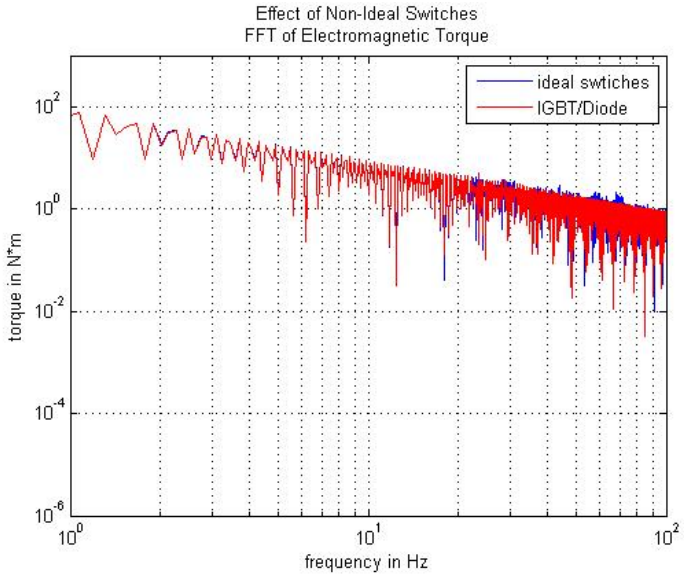

(b) Frequency Domain

Fig. 53. Motor-Compressor Train with Volts/Hertz; Electromagnetic Torque – Motor Operation Frequency 50 Hz; IGBT/Diode Inverter Case Compared with Ideal Switch Case

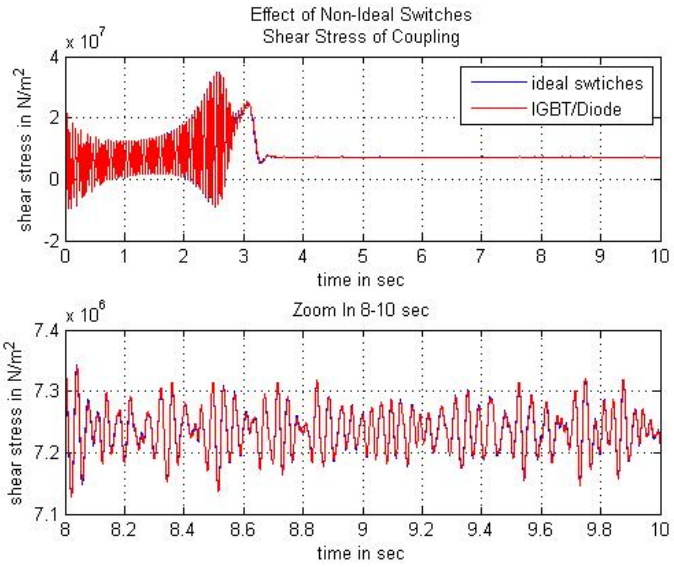

Fig. 54. Motor-Compressor Train with Volts/Hertz; Shear Stress of Coupling – Motor Operation Frequency 50 Hz; IGBT/Diode Inverter Case Compared with Ideal Switch Case

F. Effects of Non-Ideal DC Bus Voltage

Since the DC bus voltage is the output of the DC bus filter, the harmonics depends on the total effects of the input three-phase AC voltage, the inverter characteristic and the DC bus filter. It is hard to tell all the harmonic frequencies. In this thesis, three harmonic frequencies are studied.

- System characteristic frequencies
  - The three-phase AC voltage frequency of the motor input (motor operation frequency)
  - Mechanical system natural frequency
- 120 Hz (resonance)

1. System Model

Consider the system as shown in Fig. 47. Add a sinusoidal component V_h to the DC bus voltage.

$$V_{BUS} = V_{DC} + V_h \tag{4.8}$$

$$V_h = V_m sin(\omega_h t) \tag{4.9}$$

where

V_{BUS} = DC bus voltage;

V_h = DC bus harmonic component;

V_m = Amplitude of DC bus harmonic component;

ω_h = Frequency DC bus harmonic component.

The SimPowerSystems and SimMechanics model is shown in Fig. 55. The motor is set to run at its nominal frequency - 50 Hz for all the following DC bus harmonic cases.

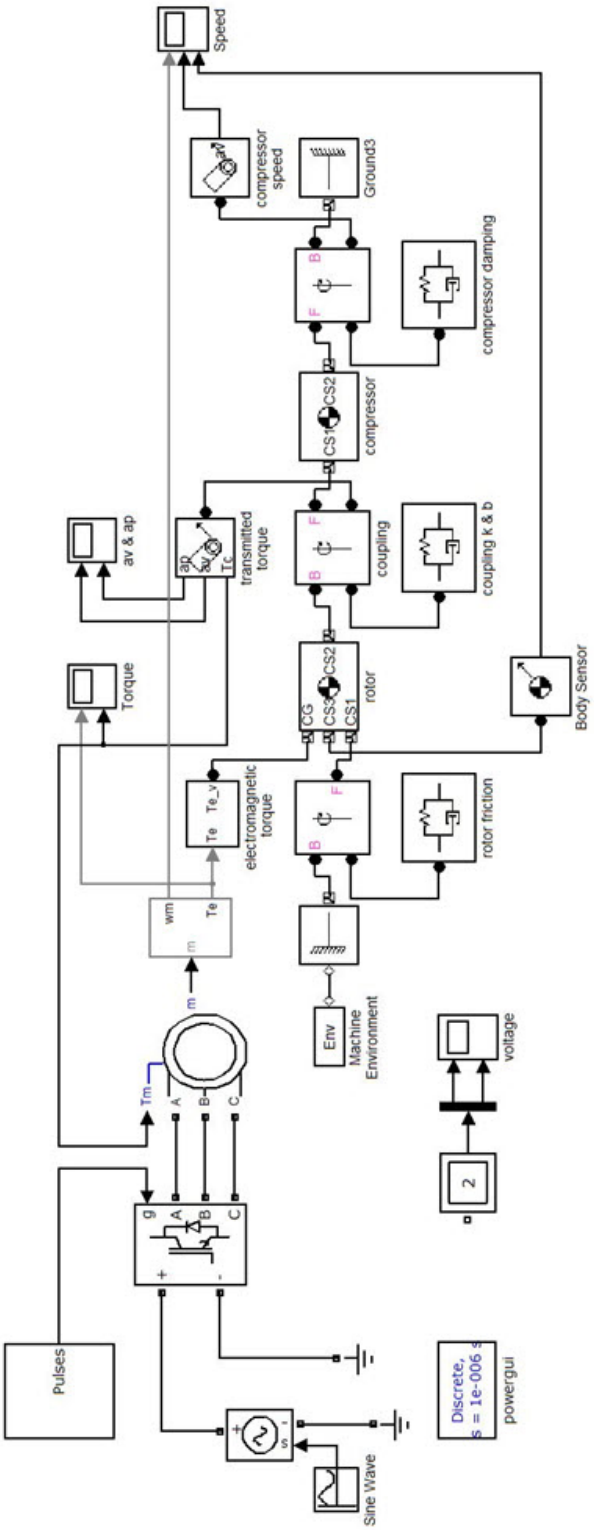

Fig. 55. SimPowerSystems and SimMechanics Model for Motor-Compressor Train with Open-Loop Volts/Hertz Control; DC Bus Harmonic Study

2. DC Bus Harmonic Frequency – Motor Operation Frequency

In this case, the DC bus harmonic frequency is equal to the motor operation frequency.

$$\omega_h = \omega_e \tag{4.10}$$

$$\omega_e = 2\pi f_e \tag{4.11}$$

where

ω_e is induction motor synchronous speed in electrical degree;

f_e is the motor operation frequency (the fundamental frequency of the inverter output).

Vary the amplitude V_m of the DC bus harmonic from 0 V (ideal DC bus, no harmonic) to 100 V, which are all relatively small with respect to the DC bus voltage 800 V. The results are shown in Fig. 56 to Fig. 59.

Comparing the simulation results, an obvious increase of torsional vibration is observed from the waveforms of relative angular displacement (Fig. 57(a)) and shear stress (Fig. 59)as the amplitude of DC bus harmonic increases. For this motor-compressor machinery train, when the harmonic peak to peak amplitude is 10% of the DC bus voltage (40 V×2/800 V), the magnitude of relative angular displacement is more than 10 times (0.0052 rad compared with 0.0004 rad) the oscillation magnitude with no DC bus harmonics.

From the spectrums of relative angular displacement (Fig. 57(b)) and electromagnetic torque (Fig. 58(b)), there is a dominant vibrating frequency at 8 Hz. This reflects the mechanical system is subject to a forced vibration. A harmonic of 8 Hz is observed in the electromagnetic torque waveform. This frequency may be a combined result of the PWM frequency, electrical frequency and mechanical torsional natural frequency. The simulation results of oscillation are compared in Table VII.

Table VII. Comparison of Oscillation with DC Bus Harmonic Frequency = Motor Operation Frequency 50 Hz for Motor-Compressor Train with Open-Loop Volts/Hertz

DC Bus Harmonic Amplitude	Relative Angular Dispalcement between Motor and Compressor (Peak-Peak, Steady State)	Shear Stress of Coupling (Peak-Peak, Steady State)
0 V	0.0004 rad	4.8186e5 N/m^2
10 V	0.0015 rad	14.689e5 N/m^2
20 V	0.0027 rad	26.937e5 N/m^2
30 V	0.0040 rad	39.410e5 N/m^2
40 V	0.0052 rad	51.91e5 N/m^2

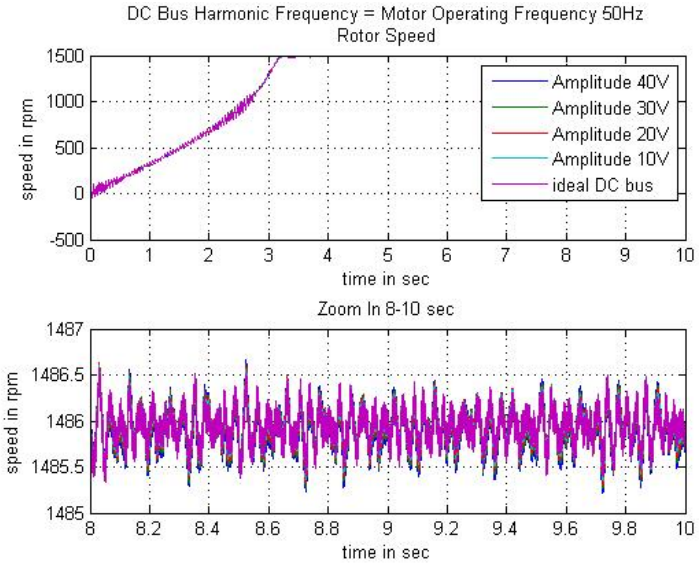

Fig. 56. Motor-Compressor Train with Volts/Hertz; Rotor Speed – Motor Operation Frequency 50 Hz; DC Bus Harmonic Frequency = Motor Operation Frequency 50 Hz

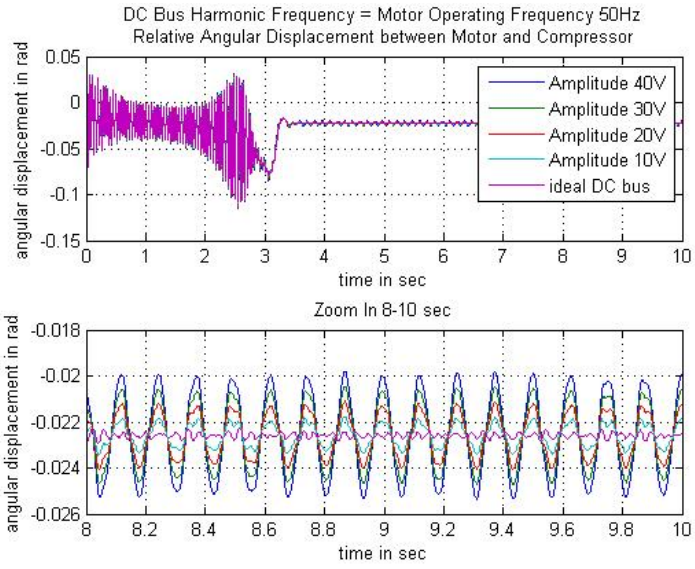

(a) Time Domain

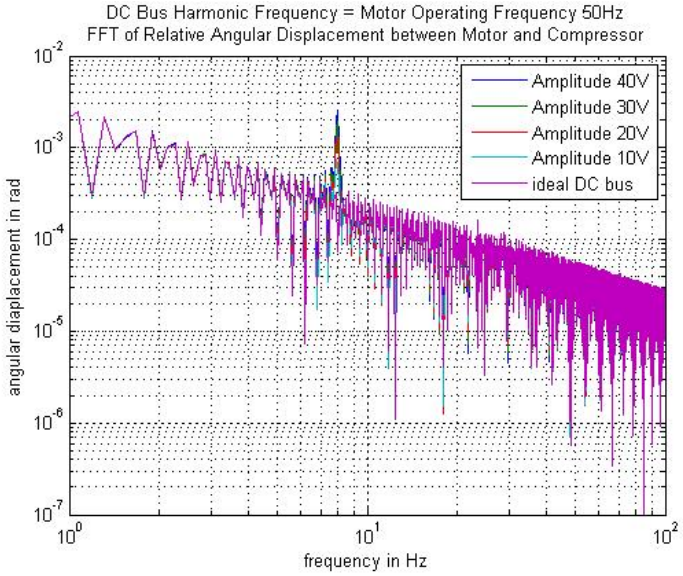

(b) Frequency Domain

Fig. 57. Motor-Compressor Train with Volts/Hertz; Relative Angular Displacement between Motor and Compressor – Motor Operation Frequency 50 Hz; DC Bus Harmonic Frequency = Motor Operation Frequency 50 Hz

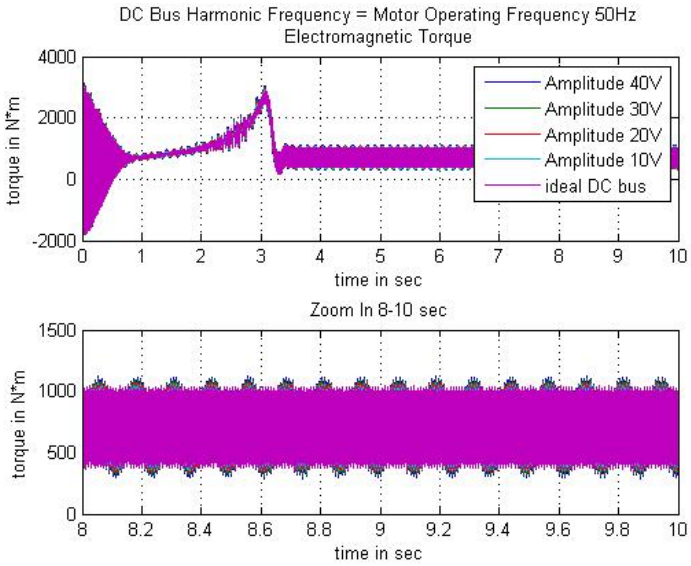

(a) Time Domain

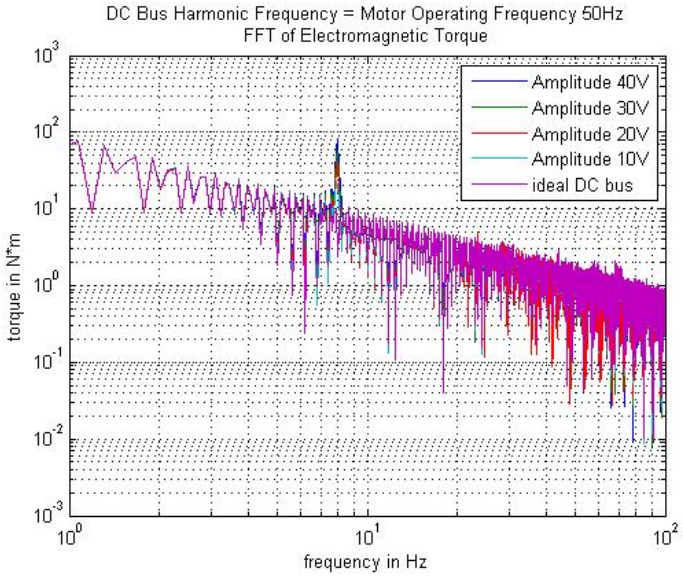

(b) Frequency Domain

Fig. 58. Motor-Compressor Train with Volts/Hertz; Electromagnetic Torque – Motor Operation Frequency 50 Hz; DC Bus Harmonic Frequency = Motor Operation Frequency 50 Hz

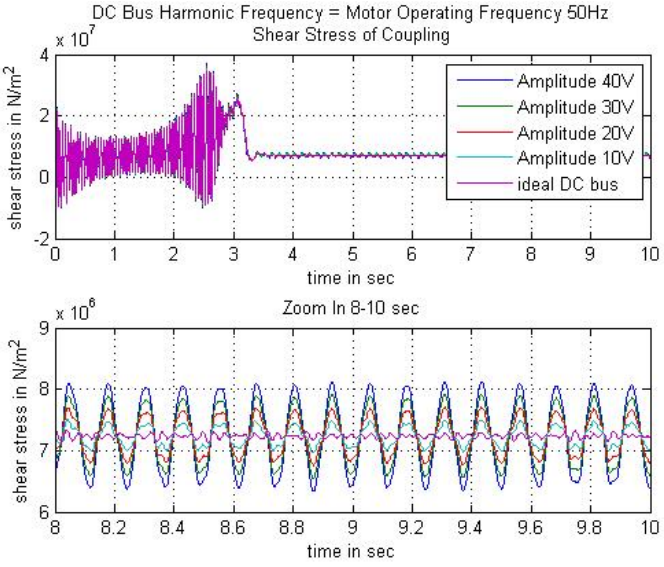

Fig. 59. Motor-Compressor Train with Volts/Hertz; Shear Stress of Coupling – Motor Operation Frequency 50 Hz; DC Bus Harmonic Frequency = Motor Operation Frequency 50 Hz

3. DC Bus Harmonic Frequency = Mechanical Torsional Natural Frequency

In this case, the DC bus harmonic is expressed as the following. The DC bus harmonic frequency is equal to the mechanical torsional natural frequency.

$$\omega_h = \omega_N F \tag{4.12}$$

$$\omega_N F = 2\pi f_N F \tag{4.13}$$

where ω_{NF} is the torsional natural frequency of the mechanical system in rad/s; $f_N F$ is the torsional natural frequency of the mechanical system.

For the motor-compressor machiner train shown in Fig. 36, the natural frequency is 20 Hz. Vary the amplitude of V_m and compare the simulation results with the ideal DC bus case. The simulation results are shown in Fig. 60 to Fig. 63.

With the DC bus harmonic amplitude increasing, there is an observable increase in the torsional vibration in the waveforms of relative angular displacement (Fig. 61) and shear stress (Fig. 63). The magnitude of relative angular displacement increases from 0.0004 rad to 0.0012 rad (3 times), when the DC bus harmonic peak to peak amplitude is 10% of the DC bus voltage (40 V×2/800 V).

By the observation of the responses of rotor speed, relative angular displacement and electromagnetic torque, it seems with a bigger harmonic amplitude at torsional natural frequency, the transient time of the system is shorter.

However, a harmonic equal to the torsional natural frequency does not induce a resonance. At steady state, a dominant oscillation frequency about 3.2 Hz is observed. This is also a forced vibration due to the electromagnetic torque harmonic of 3.2 Hz.

The simulation results of oscillation are compared in Table VIII.

Table VIII. Comparison of Oscillation with DC Bus Harmonic Frequency = Torsional Natural Frequency 20 Hz for Motor-Compressor Train with Open-Loop Volts/Hertz

DC Bus Harmonic Amplitude	Relative Angular Dispalcement between Motor and Compressor (Peak-Peak, Steady State)	Shear Stress of Coupling (Peak-Peak, Steady State)
0 V	0.0004 rad	4.8186e5 N/m^2
10 V	0.000643 rad	6.4220e5 N/m^2
20 V	0.000836 rad	8.3171e5 N/m^2
30 V	0.0011 rad	10.977e5 N/m^2
40 V	0.0012 rad	11.822e5 N/m^2

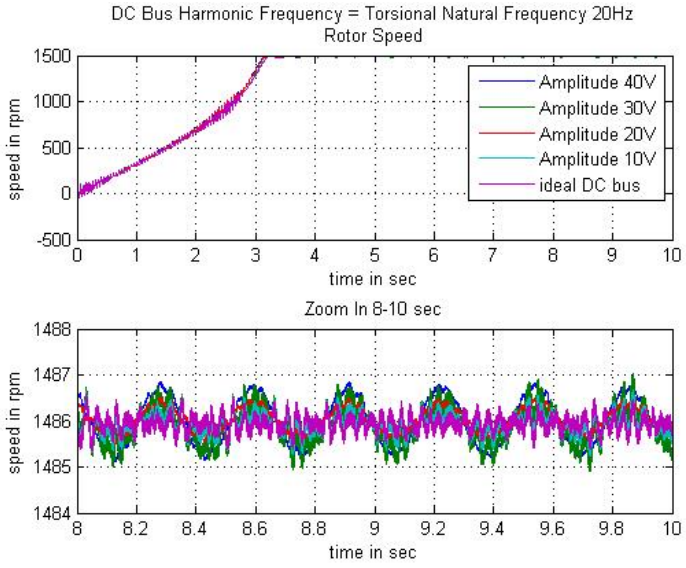

Fig. 60. Motor-Compressor Train with Volts/Hertz; Rotor Speed – Motor Operation Frequency 50 Hz; DC Bus Harmonic Frequency = Mechanical Torsional Natural Frequency 20 Hz

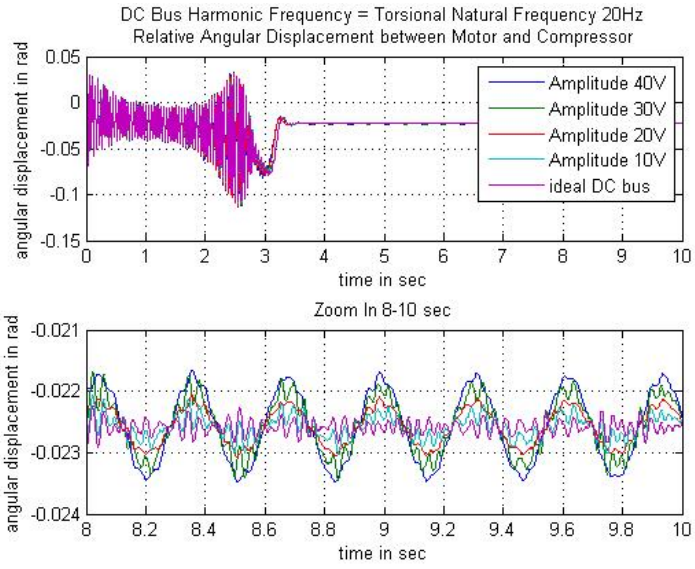

(a) Time Domain

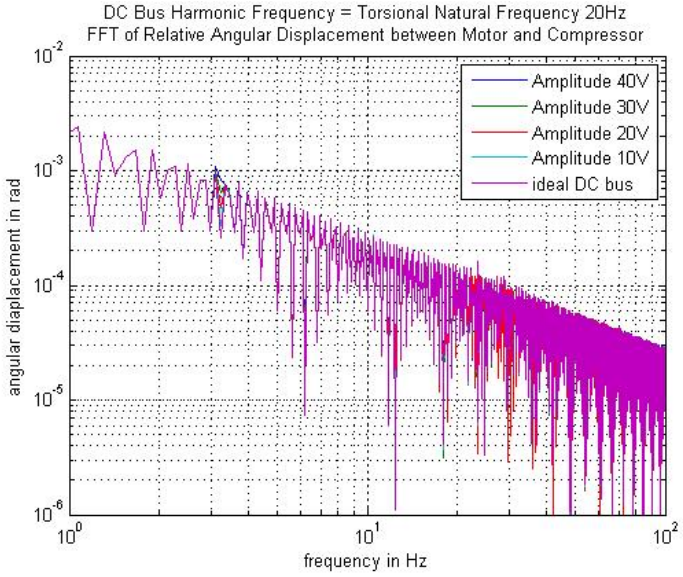

(b) Frequency Domain

Fig. 61. Motor-Compressor Train with Volts/Hertz; Relative Angular Displacement between Motor and Compressor – Motor Operation Frequency 50 Hz; DC Bus Harmonic Frequency = Mechanical Torsional Natural Frequency 20 Hz

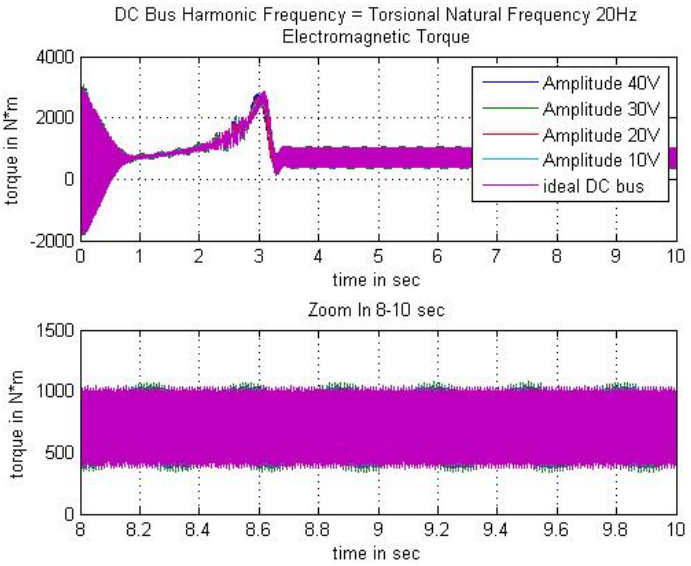

(a) Time Domain

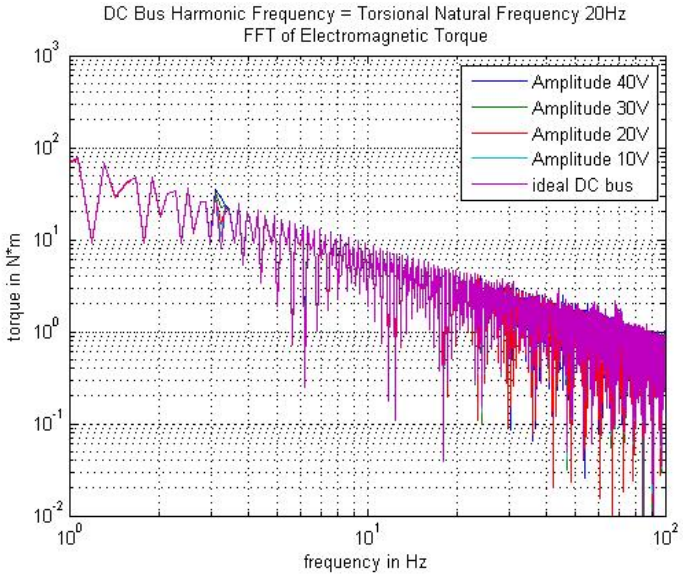

(b) Frequency Domain

Fig. 62. Motor-Compressor Train with Volts/Hertz; Electromagnetic Torque – Motor Operating Frequency 50 Hz; DC Bus Harmonic Frequency = Mechanical Torsional Natural Frequency 20 Hz

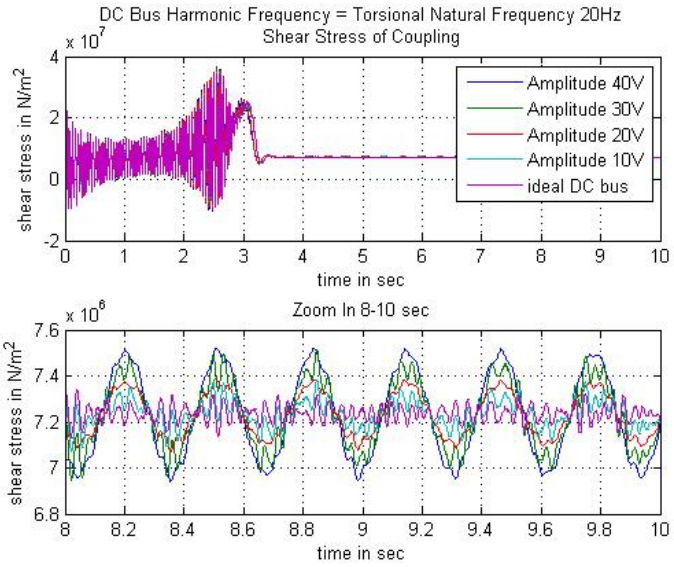

Fig. 63. Motor-Compressor Train with Volts/Hertz; Shear Stress of Coupling – Motor Operation Frequency 50 Hz; DC Bus Harmonic Frequency = Mechanical Torsional Natural Frequency 20 Hz

4. DC Bus Harmonic Frequency = 120 Hz

Let the DC bus harmonic component have the following form.

$$V_h = V_m sin(\omega t) \tag{4.14}$$

$$\omega = 2\pi \times 120 \tag{4.15}$$

Simulations are performed for the ideal DC bus harmonic case and 10 V harmonic amplitude case. The simulation results are shown in Fig. 64 to Fig. 67.

From Fig. 65(a) and Fig. 67, at steady state, the system is subject to a big oscillation. And by Fig. 65(b) and Fig. 66(b), the spectrums of relative angular displacement and electromagnetic torque show the oscillation frequency is near 20Hz, which is the torsional natural frequency of the mechanical system. The steady state peak-to-peak relative angular displacement between motor and compressor increases from 0.0004 rad to 0.0069 rad (17 times) while the peak-to-peak DC bus ripple of 120 Hz is just 2.5% of the DC bus voltage (10 V×2/800 V).

DC harmonic with non-characteristic frequency can also cause resonance of the mechanical system. The simulation results of oscillation are compared in Table IX.

Table IX. Comparison of Oscillation with DC Bus Harmonic Frequency = 120 Hz for Motor-Compressor Train with Open-Loop Volts/Hertz

DC Bus Harmonic Amplitude	Relative Angular Dispalcement between Motor and Compressor (Peak-Peak, Steady State)	Shear Stress of Coupling (Peak-Peak, Steady State)
0 V	0.0004 rad	4.8186e5 N/m^2
10 V	0.0069 rad	68.560e5 N/m^2

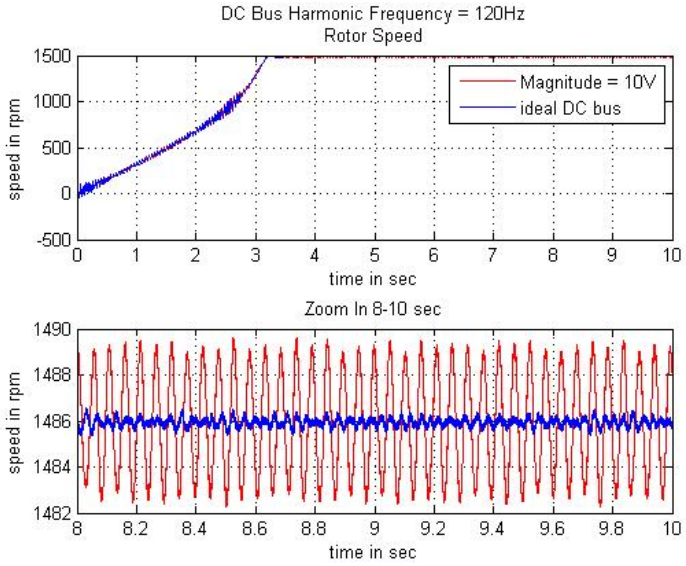

Fig. 64. Motor-Compressor Train with Volts/Hertz; Rotor Speed – Motor Operation Frequency 50 Hz; DC Bus Harmonic Frequency = 120 Hz

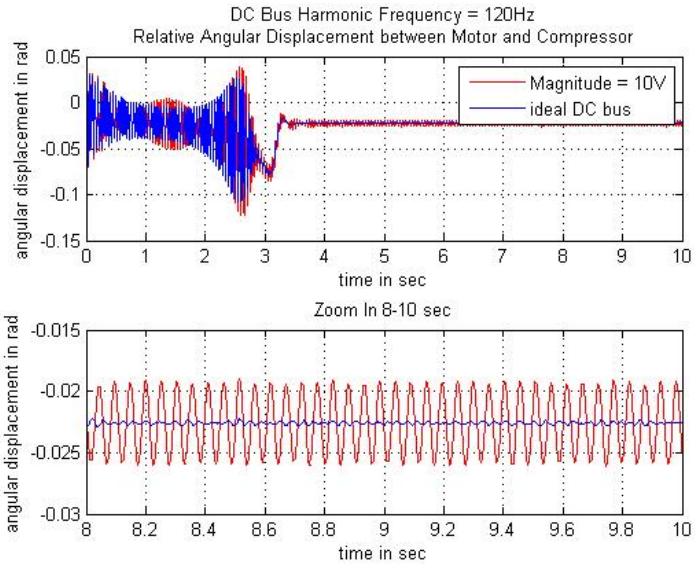

(a) Time Domain

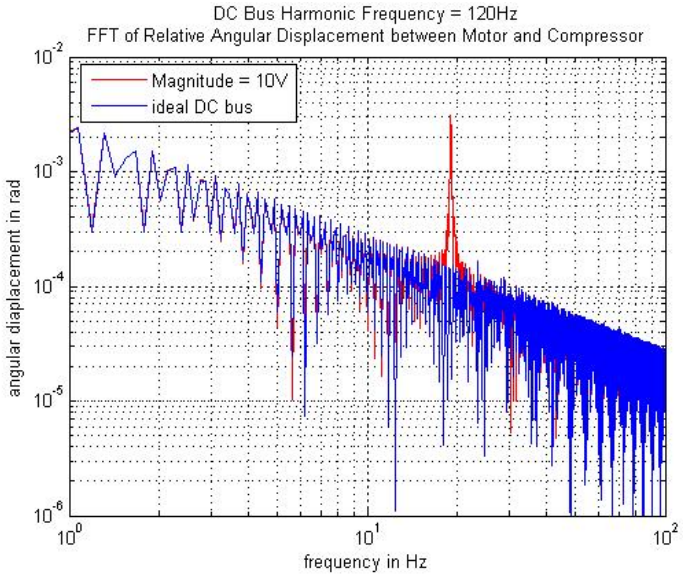

(b) Frequency Domain

Fig. 65. Motor-Compressor Train with Volts/Hertz; Relative Angular Displacement between Motor and Compressor – Motor Operationg Frequency 50 Hz; DC Bus Harmonic Frequency = 120 Hz

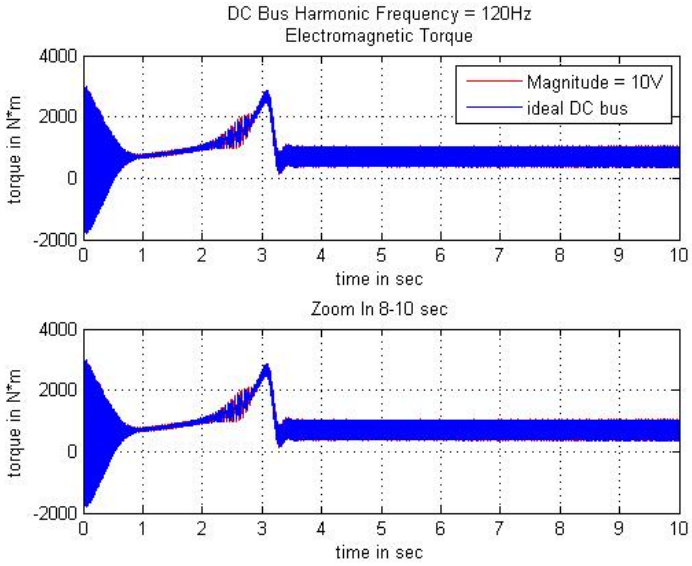

(a) Time Domain

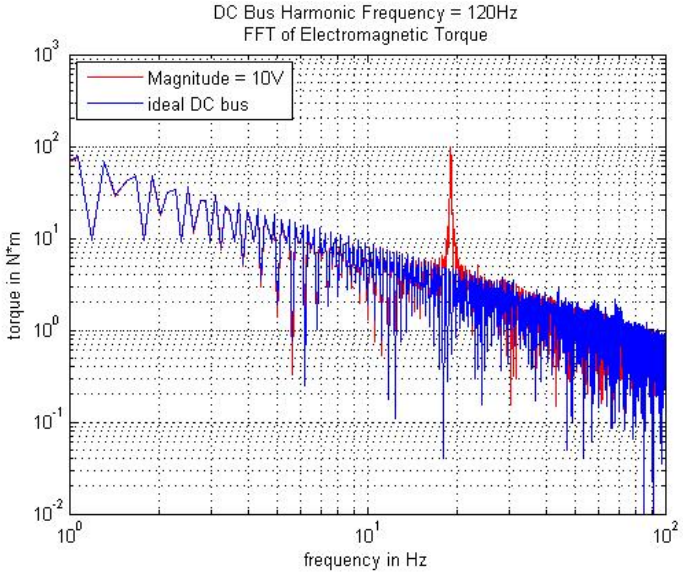

(b) Frequency Domain

Fig. 66. Motor-Compressor Train with Volts/Hertz; Electromagnetic Torque – Motor Operation Frequency 50 Hz; DC Bus Harmonic Frequency = 120 Hz

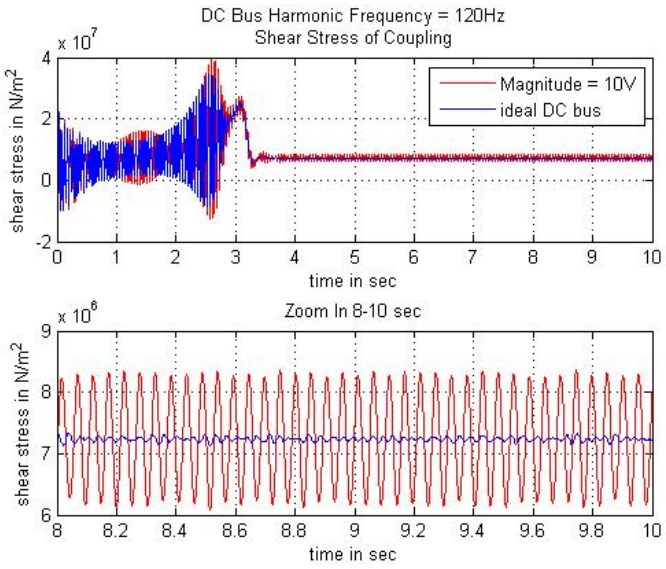

Fig. 67. Motor-Compressor Train with Volts/Hertz; Shear Stress of Coupling – Motor Operating Frequency 50 Hz; DC Bus Harmonic Frequency = 120 Hz

CHAPTER V

ANALYSIS OF CLOSED-LOOP CONTROL-FOC

In Chapter II the closed-loop FOC control method has been discussed. Fig. 68 presents the diagram for a machinery train driven by a VFD using closed-loop FOC control method.

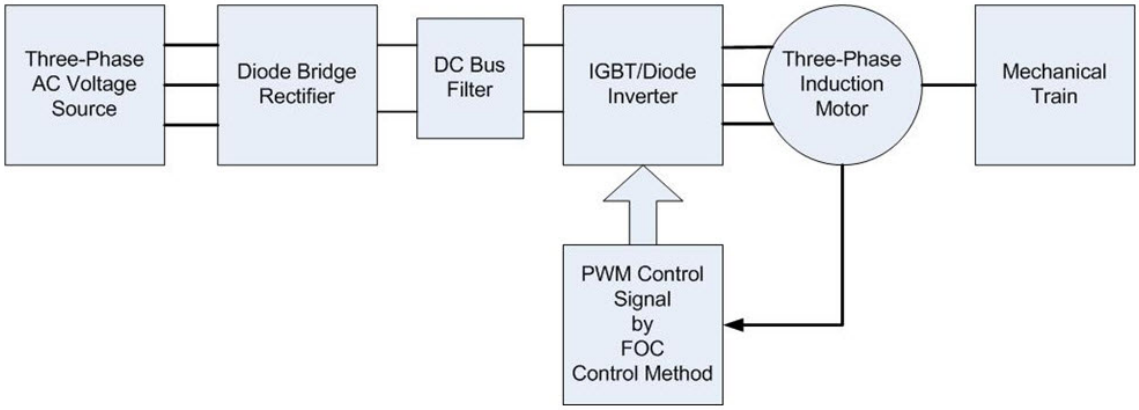

Fig. 68. Diagram for a Machinery Train Driven by Closed-Loop FOC Control VFD

A. Analysis for Harmonic Sources

For VFDs with FOC control method, the following items are potential electric harmonic sources to induce harmonics in electromagnetic torque and results in a resonance.

- Non-ideal Three-Phase AC Voltages
- Non-ideal DC Bus Voltages
- Non-ideal characteristics of the power switches in rectifier and inverter

- Harmonics in the inverter output voltage fed to motor, which is due to FOC control method and PWM switching
- Parametric Settings of the FOC Controller

The first three sources have been generally discussed in Chapter IV. The FOC algorithm is discussed in Chapter II . For this control method, it is hard to obtain a closed form of the output PWM control signals. This algorithm is a closed-loop control with the feedbacks of rotor speed and rotor flux, which makes the control system complex. And the implementations of the current regulator, PWM generator and flux calculator also make it hard to get the closed form expression of the inverter output. However, because of the closed-loop control, the harmonics are much more less than the open-loop Volts/Hertz control method.

The parametric settings of the FOC controller also play an important role in the performance of the VFD. Impropriate settings may induce instability, like the proportional gain of PI controllers. The common FOC controller setting parameters are list below.

- Speed regulator
  - Proportional gain
  - Integral gain
  - Speed ramps
- Flux controller
  - Proportional gain
  - Integral gain
  - Flux controller output limit (positive and negative)

- FOC controller
  - Flux nominal value
  - Current hysteresis band
  - Maximum switching frequency

B. Motor-Gearbox-Compressor Machinery Train

A motor-gearbox-compressor machinery train is built to study VFDs using FOC. Fig. 69 shows the machinery train diagram.

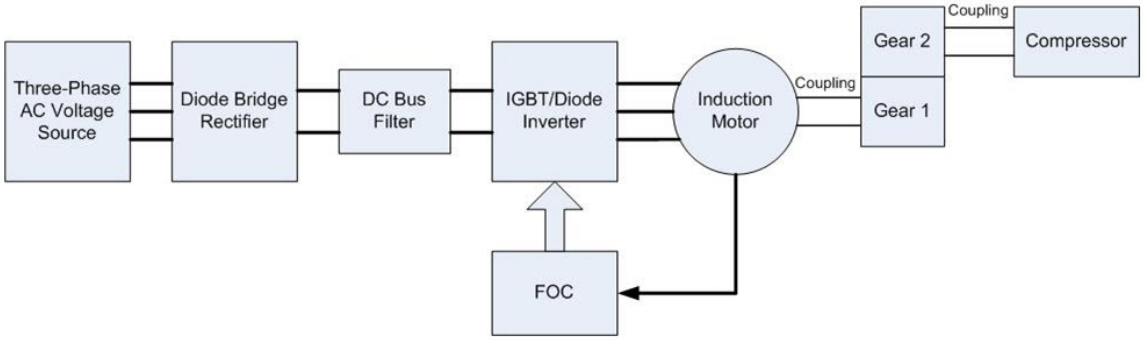

Fig. 69. Motor-Gearbox-Compressor Train

1. Electric Induction Motor

The squirrel-cage induction motor used here is 200 HP. The nominal parameters are listed in Table X. The detailed motor parameters are in Appendix B.

2. Mechanical Components

Fig. 70 presents the mechanical system. The coupling is assumed to be a spool piece. Suppose the compressor is subject to a mechanical load, which is proportional to

Table X. 200HP Motor Nominal Parameters

Motor Nominal Parameters	
Rotor Type	Squirrel Cage
Power	200 HP
Voltage (phase-phase RMS)	460 V
Frequency	60 Hz
Number of Poles	4

the compressor rotating speed ω_c. The load torque ratio is denoted by b_l. The two couplings are supposed to be spool pieces.The parameters for this mechanical train are shown in Table XI.

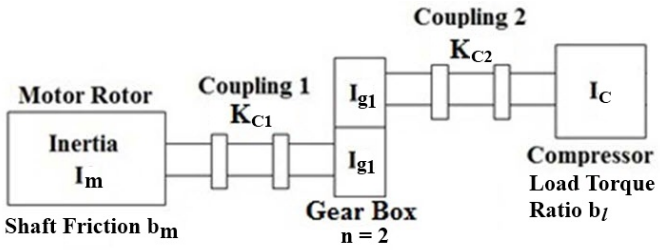

Fig. 70. Motor-Gearbox-Compressor Mechanical System

C. FOC Controller with Ideal DC Bus Voltage and Ideal Switch in Inverter

1. Assumptions

In order to study the effects of FOC controller and eliminate all the other possible harmonic sources, the following assumptions are made.

- Ideal DC bus voltage = 621.46 V

Table XI. Mechanical Parameters for Motor-Gearbox-Compressor Train

Induction Motor	
Rotor Inertia I_m	$3.1\,\mathrm{kg{\cdot}m^2}$
Rotor Shaft Friction b_m	$0.08\,\mathrm{N{\cdot}m/(rad/s)}$
Coupling#1	
Stiffness K_{c1}	$10000\,\mathrm{N{\cdot}m/rad}$
Radius r	$0.075\,\mathrm{m}$
Length L	$0.5\,\mathrm{m}$
Shear Modulus G	$2.136\mathrm{e}9\,\mathrm{N{\cdot}m^2}$
Gearbox	
Gear#1 Inertia I_{g1}	$0.124\,\mathrm{kg{\cdot}m^2}$
Gear#2 Inertia I_{g2}	$0.031\,\mathrm{kg{\cdot}m^2}$
Gear Ratio n	2
Compressor	
Inertia I_c	$13.8\,\mathrm{kg{\cdot}m^2}$
Coupling#2	
Stiffness K_{c2}	$10000\,\mathrm{N{\cdot}m/rad}$
Compressor Load	
Torque/Speed Ratio b_l	$0.2\,\mathrm{N{\cdot}m/(rad/s)}$
Natural Frequency	
1st Natural Frequency NF_1	$10.7\,\mathrm{Hz}$
2nd Natural Frequency NF_2	$72\,\mathrm{Hz}$

- Ideal power switches for inverter

Fig. 71 shows the simplified model.

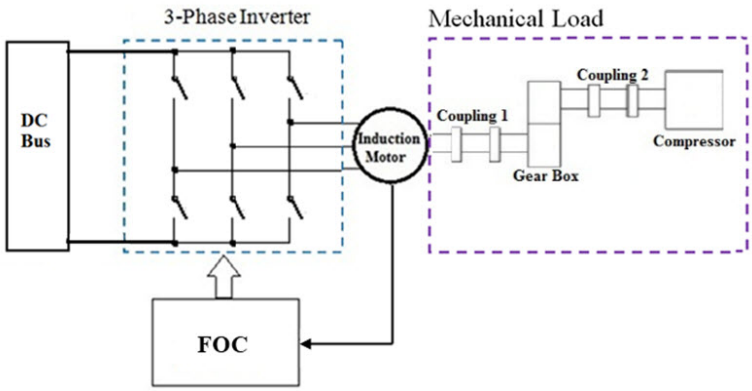

Fig. 71. VFD Driven Motor-Gearbox-Compressor Train with FOC;
Assumptions: Ideal DC Bus Voltage and Ideal Inverter Power Switches

2. System Model in SimPowerSystems and SimMechanics

The Field Oriented Control electric drive block in SimPowerSystems is used for the controller model. Fig. 72 shows the system model in SimPowerSystems and SimMechanics.

The detailed parameter settings for the FOC controller are listed in Table XII. These parameters are already turned by Matlab.

3. Simulation Results

The simulation time step is 1e-6 sec. The simulation time span is set to 0 – 8 sec. These settings are used for all the simulations in this chapter.

The reference speed of the motor is set to be 1750 rpm, which is the nominal speed for this 200 HP induction motor. The simulation results are shown in Fig. 73 to Fig. 76. The spectrums for the relative angular velocity and electromagnetic torque

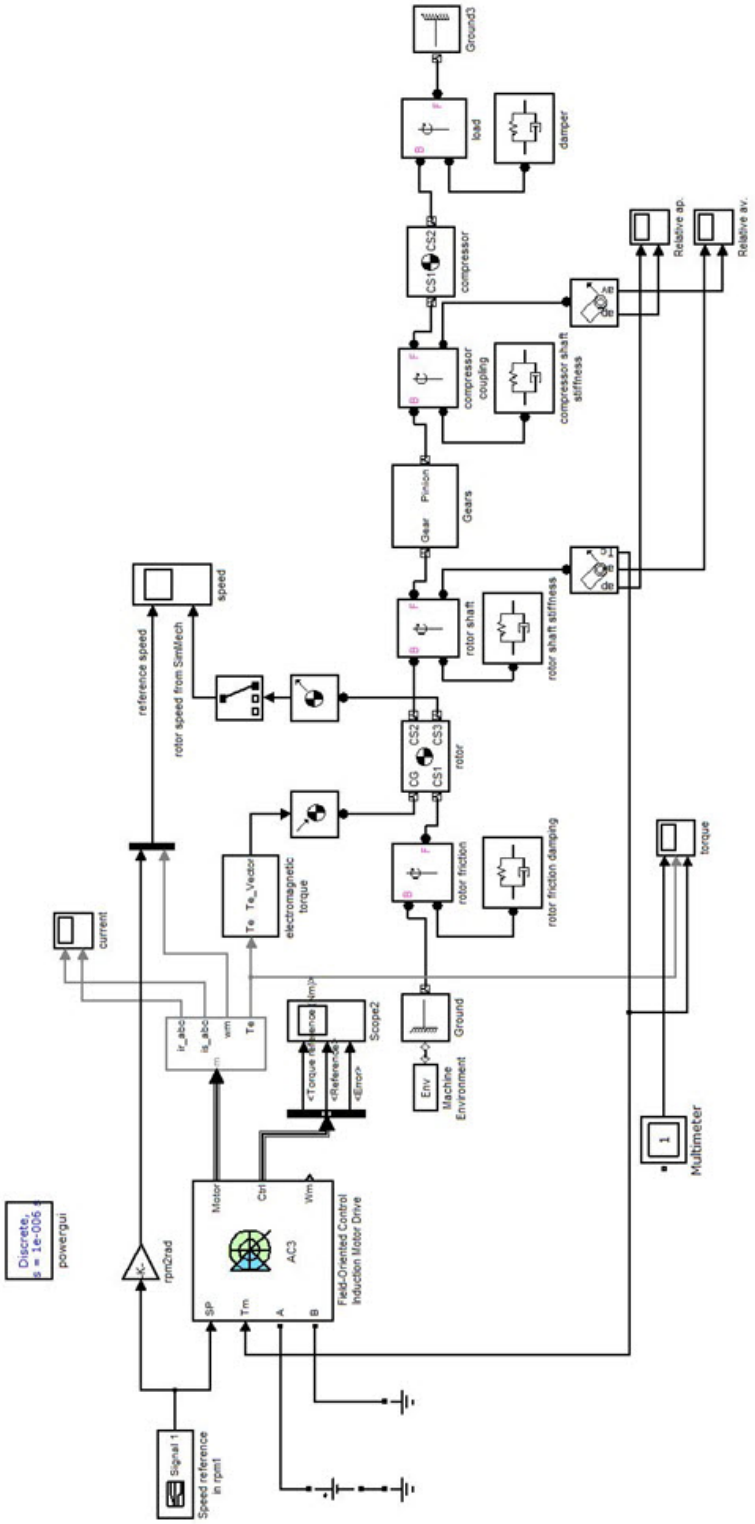

Fig. 72. SimPowerSystems and SimMechanics Model for VFD Driven Motor-Gearbox-Compressor Train with FOC; Assumptions: Ideal DC Bus Voltage and Ideal Inverter Power Switches

Table XII. Controller Settings for FOC

Speed Regulator	
Proportional Gain	300
Integral Gain	2000
Speed Ramps	900 rpm/s
Torque Limit	1200 N m
Flux Controller	
Proportional Gain	100
Integral Gain	30
Output Limit	2 Wb
FOC Controller	
Current Hysteresis Band	10 A
Maximum Switching Frequency	20000 Hz

are obtained with respect to the oscillation, the DC component is not included. This rule applies to all the following studies of FOC.

The motor ramps to its target speed at the acceleration rate of 900 rpm/s. At steady state, the speed nearly maintains the reference speed with small high frequency oscillations.

From the simulation results, the two stages – ramping up and steady state are clearly shown in the waveforms. In the spectrum of relative angular displacement and shear stress, two vibration frequencies are observed. The lower frequency is around 7 Hz, which is lower than the first natural frequency. This vibration frequency switch is due to the proportional controller in the speed regulator, which will be discussed in the part of parametric study. The second vibration frequency is around 72 Hz, which is the same as the second natural frequency.

The electromagnetic torque mainly contains high frequency harmonics, which influences the mechanical system not much.

D. Complete VFD Model with FOC

1. Motor-Gearbox-Compressor Machinery Train Model with FOC

The complete VFD model with FOC is shown in Fig. 77. Compared with the model in Fig. 71 of previous section, there is no assumption in this complete model. The system input is three-phase AC voltage source. The DC bus voltage is smoothed and filtered by a capacitor and dynamic braking chopper. IGBT/Diodes are used for the inverter.

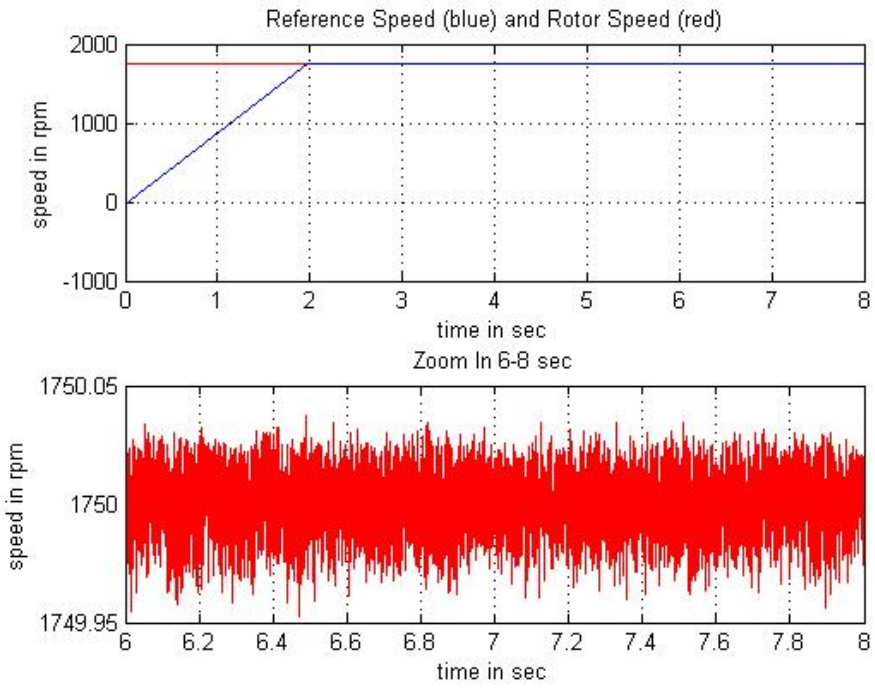

Fig. 73. Motor-Gearbox-Compressor Train with FOC; Rotor Speed – Motor Target Speed 1750 rpm; Assumptions: Ideal DC Bus Voltage and Ideal Inverter Power Switches

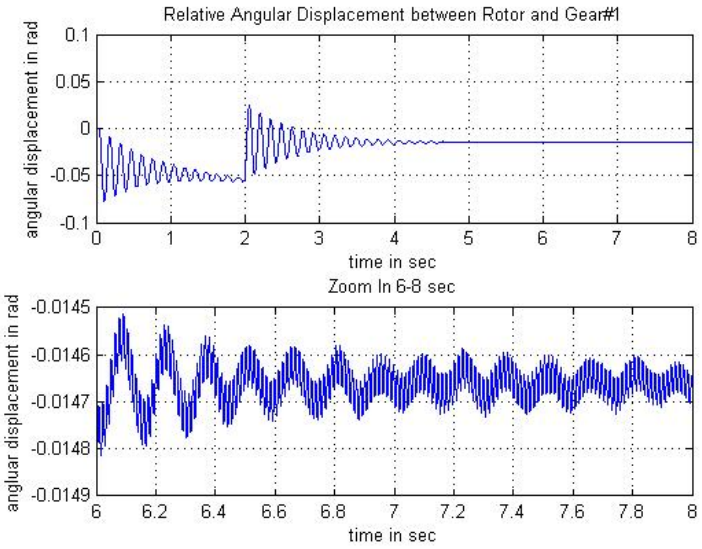

(a) Time Domain

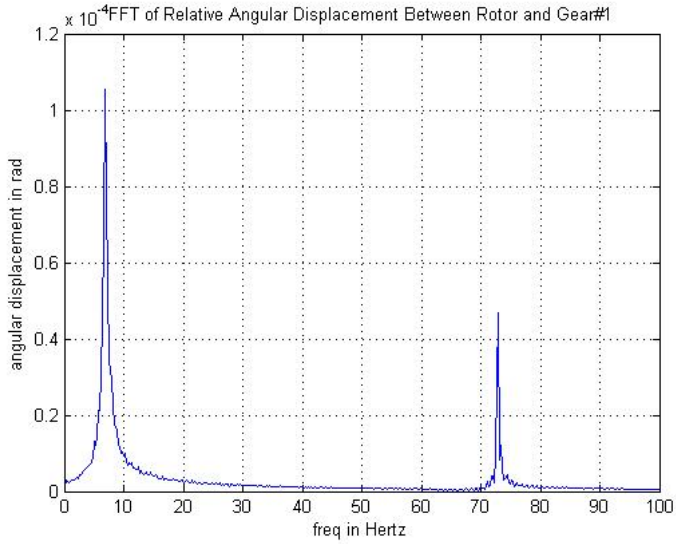

(b) Frequency Domain

Fig. 74. Motor-Gearbox-Compressor Train with FOC; Relative Angular Displacement between Motor and Gear#1 – Motor Target Speed 1750 rpm; Assumptions: Ideal DC Bus Voltage and Ideal Inverter Power Switches

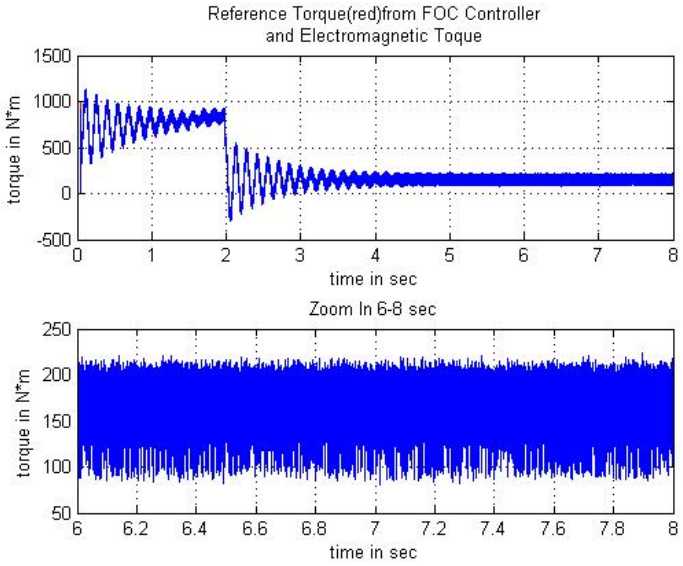

(a) Time Domain

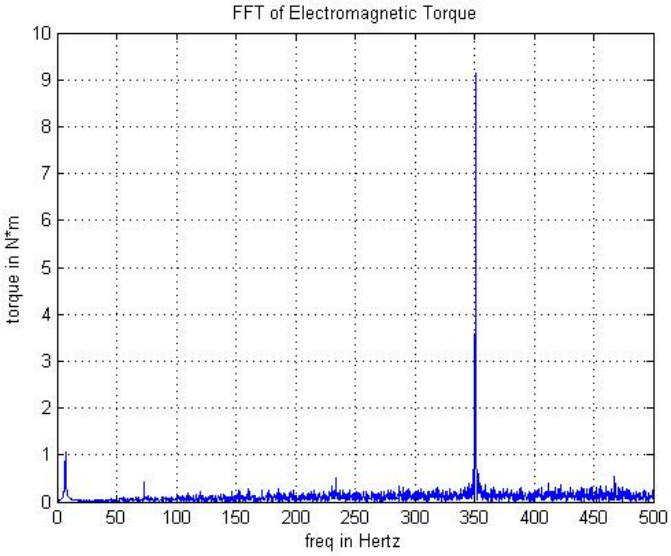

(b) Frequency Domain

Fig. 75. Motor-Gearbox-Compressor Train with FOC; Electromagnetic Torque – Motor Target Speed 1750 rpm; Assumptions: Ideal DC Bus Voltage and Ideal Inverter Power Switches

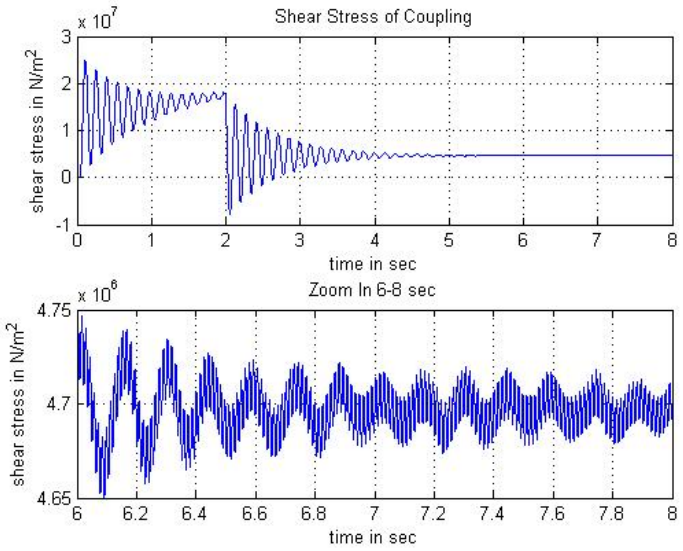

Fig. 76. Motor-Gearbox-Compressor Train with FOC; Shear Stress of Coupling#1 – Motor Target Speed 1750 rpm; Assumptions: Ideal DC Bus Voltage and Ideal Inverter Power Switches

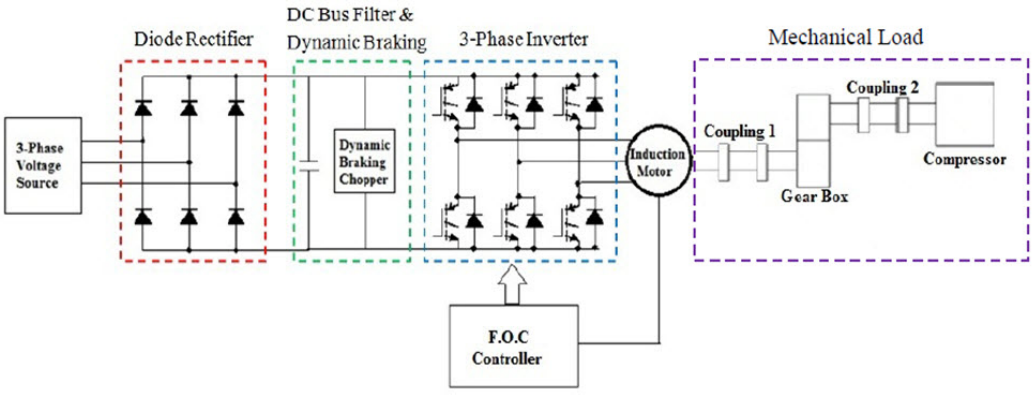

Fig. 77. VFD Driven Motor-Gearbox-Compressor Machinery Train with FOC

2. System Model in SimPowerSystems and SimMechanics

The system model in SimPowerSystems and SimMechanics is shown in Fig. 3. The three-phase AC voltage source is set to be the same as the motor nominal voltage 460 V (peak-peak RMS). The detailed parameters for the diode rectifier, DC bus capacitor, dynamic braking chopper and IGBT/Diode inverter are listed in Appendix B.

3. Simulation Results

The motor reference speed is also 1750 rpm. The simulation results are compared with the case under the assumptions of ideal DC bus voltage and ideal switches in inverter. The simulation results of oscillation are compared in Table XIII. Fig. 79 to Fig. 83 present the results.

With the capacitor and dynamic braking chopper, the DC bus is expected to be constant. From Fig. 83(a) and Fig. 83(b), at steady state, the DC bus only contains high frequency harmonics, which has little influence on the mechanical system.

From Fig. 80(a) and Fig. 82, the steady state relative angular displacement and shear stress along motor shaft are all smaller for the complete VFD train than the case with ideal DC bus and ideal switches. From the spectrums, the lower vibration magnitude is the same, while the second vibration magnitude is smaller. This means a lighter vibration in a complete VFD train. But the vibration frequency and pattern are identically the same.

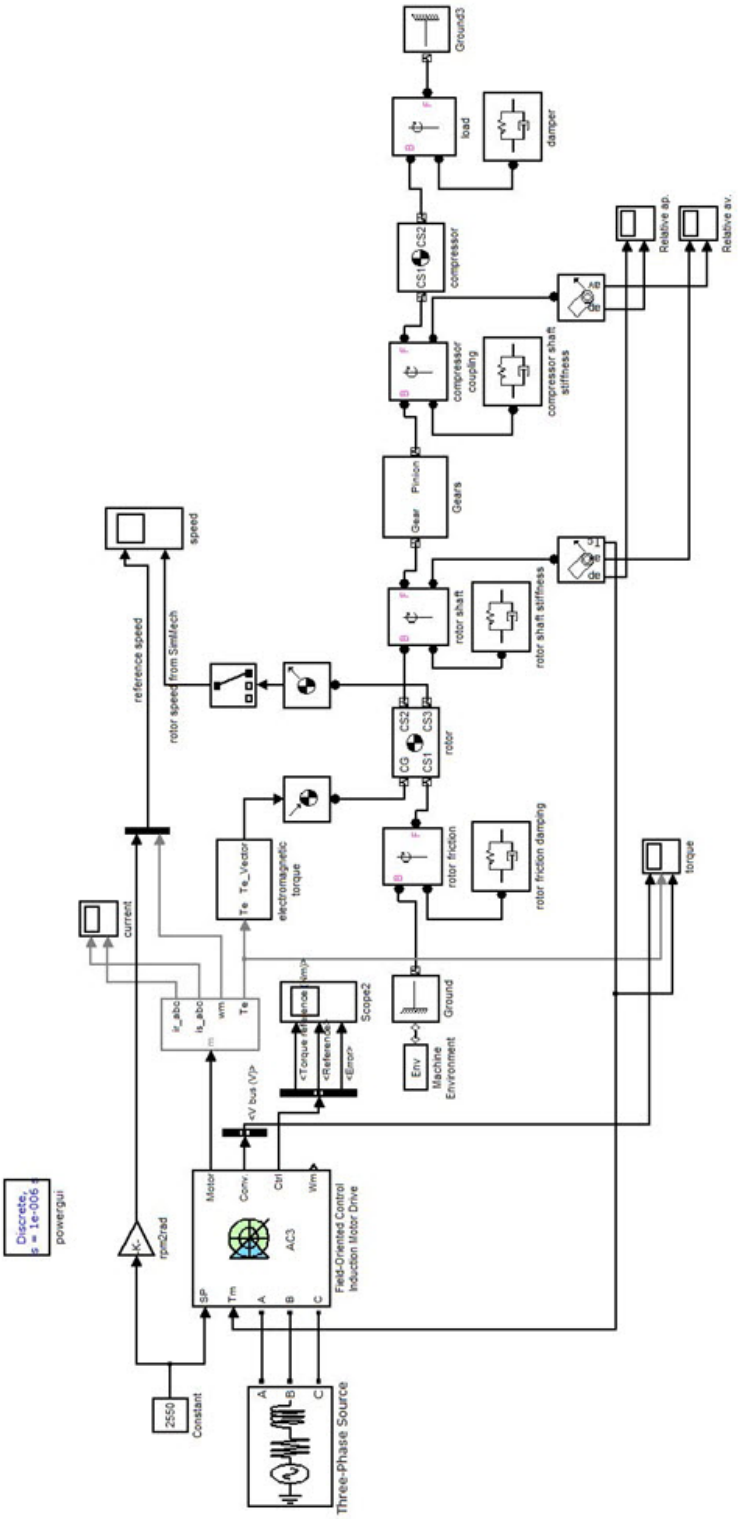

Fig. 78. SimPowerSystems and SimMechanics Model for VFD Driven Motor-Gearbox-Compressor Machinery Train with FOC

Table XIII. Comparison of Oscillation for Motor-Compressor Train with Closed-Loop FOC; Complete VFD Case Compared with Ideal DC Bus/Switches Case

FOC	Relative Angular Dispalcement between Motor and Gear#1 (Peak-Peak, Steady State)	Shear Stress of Coupling (Peak-Peak, Steady State)
Ideal DC Bus/ Inverter Switch	0.000171 rad	3.6405e4 N/m^2
Complete VFD Train	0.0000654 rad	1.6023e4 N/m^2

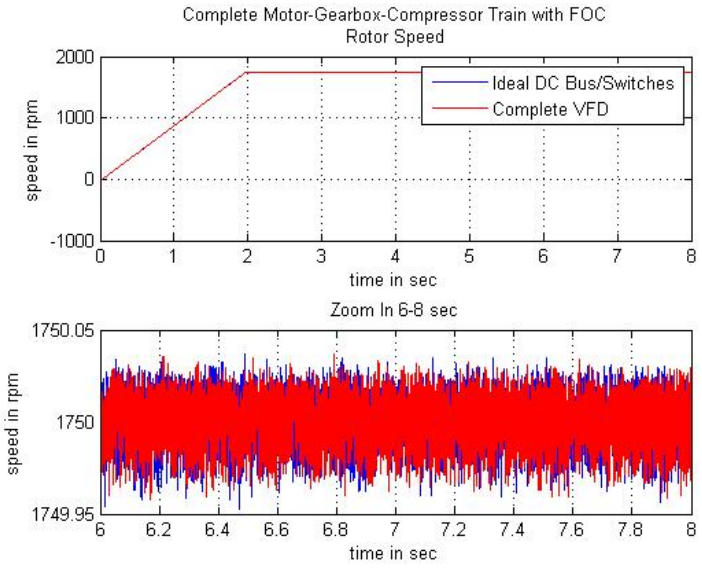

Fig. 79. Motor-Gearbox-Compressor Train with FOC; Rotor Speed – Motor Target Speed 1750 rpm; Complete VFD Case Compared with Ideal DC Bus/Switches Case

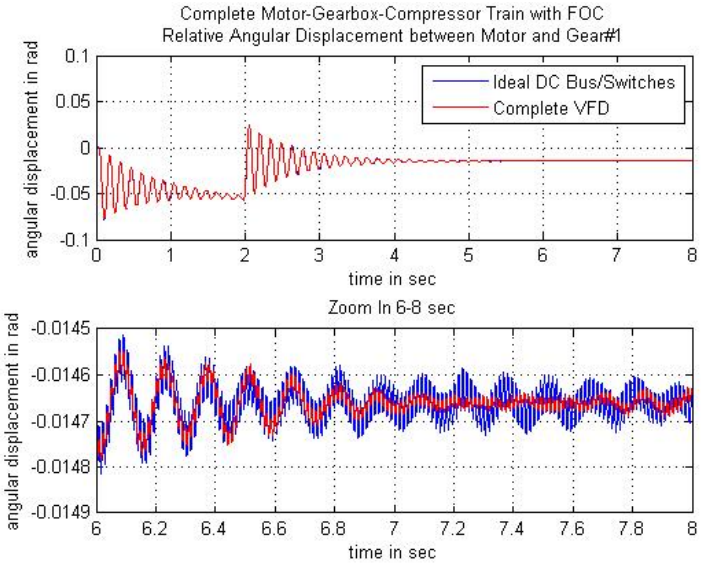

(a) Time Domain

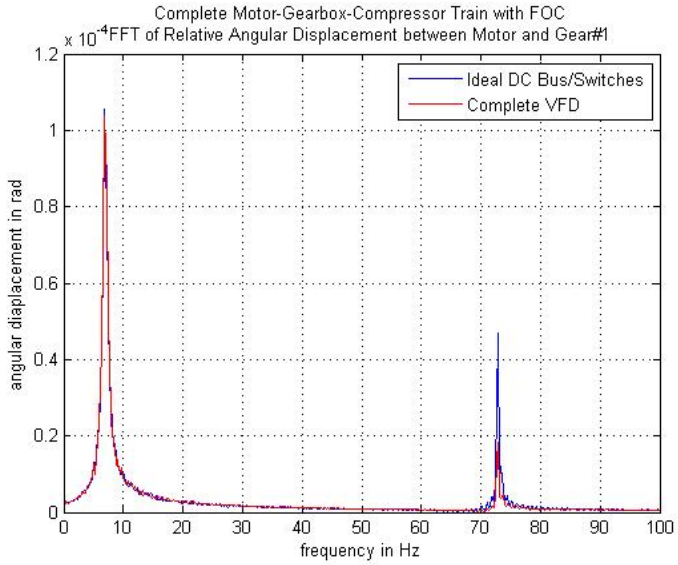

(b) Frequency Domain

Fig. 80. Motor-Gearbox-Compressor Train with FOC; Relative Angular Displacement between Motor and Gear#1 – Motor Target Speed 1750 rpm; Complete VFD Case Compared with Ideal DC Bus/Switches Case

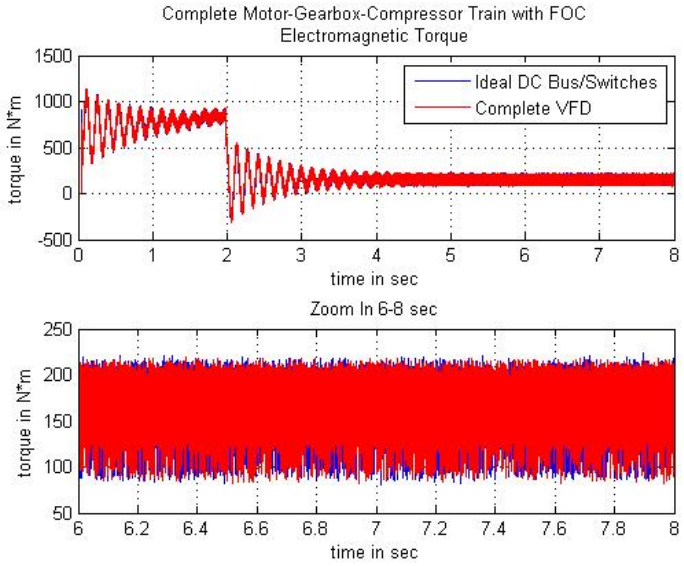

(a) Time Domain

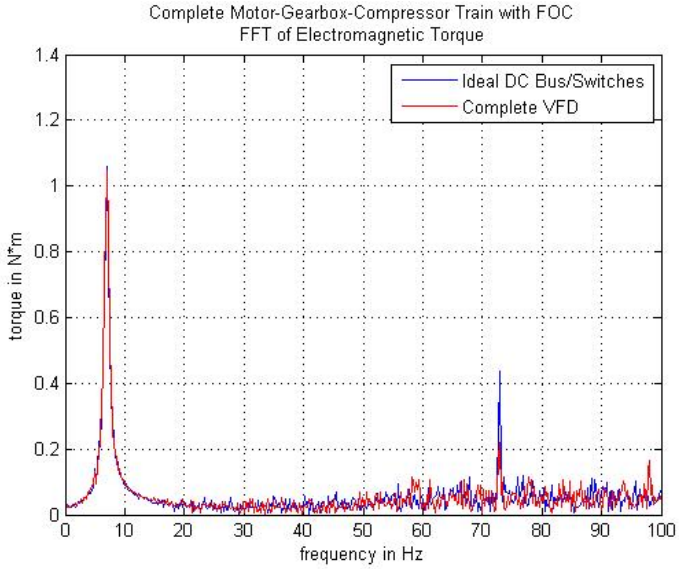

(b) Frequency Domain

Fig. 81. Motor-Gearbox-Compressor Train with FOC; Electromagnetic Torque – Motor Target Speed 1750 rpm; Complete VFD Case Compared with Ideal DC Bus/Switches Case

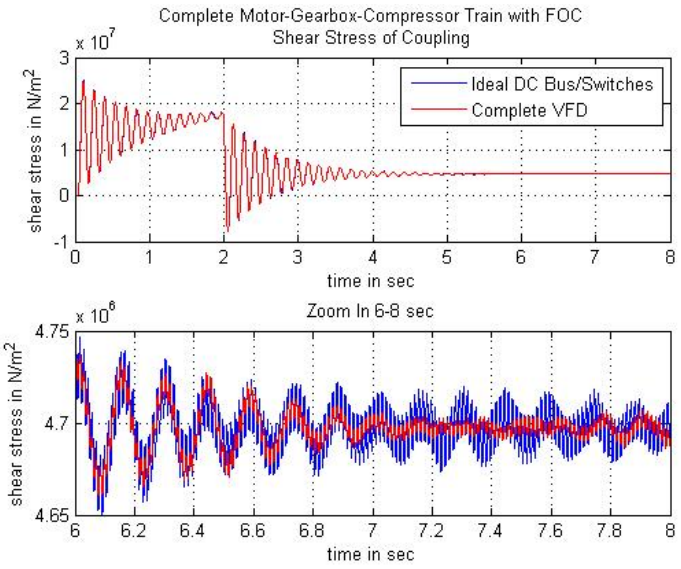

Fig. 82. Motor-Gearbox-Compressor Train with FOC; Shear Stress of Coupling#1 – Motor Target Speed 1750 rpm; Complete VFD Case Compared with Ideal DC Bus/Switches Case

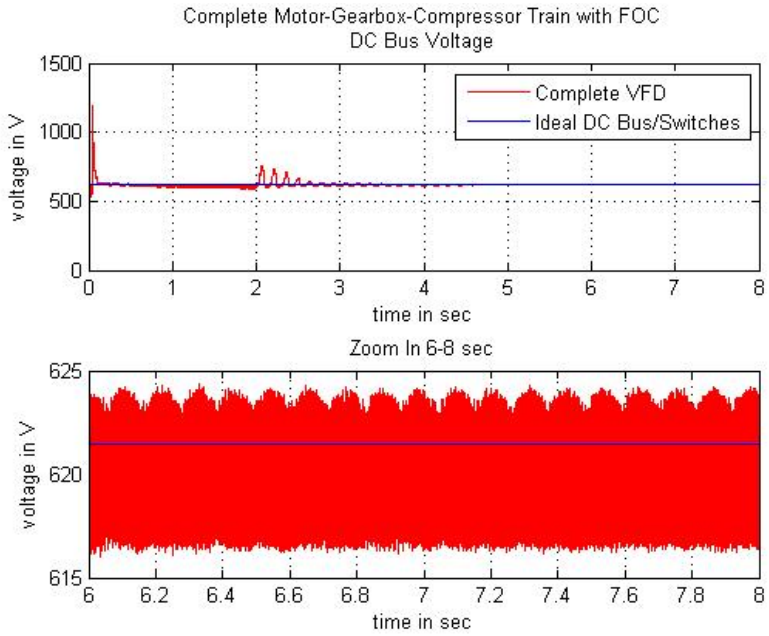

(a) Time Domain

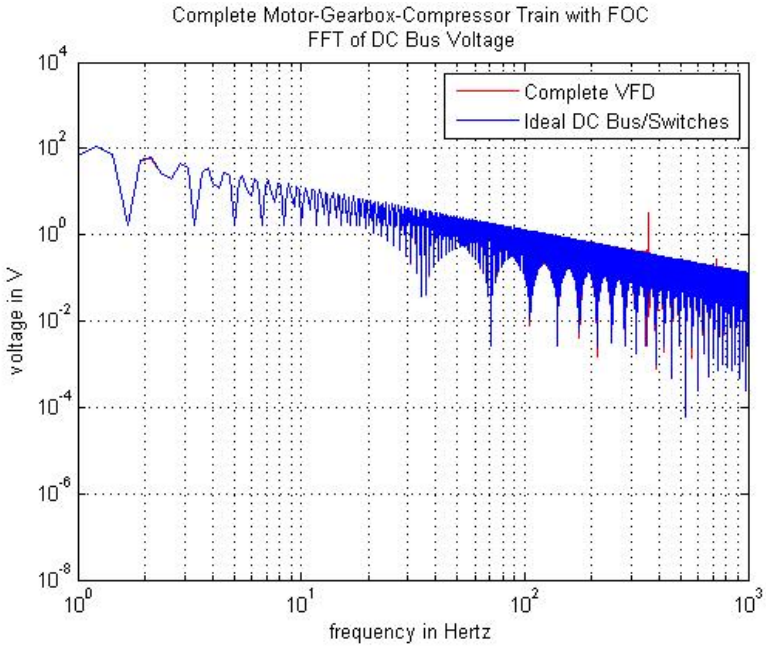

(b) Frequency Domain

Fig. 83. Motor-Gearbox-Compressor Train with FOC; DC Bus Voltage – Motor Target Speed 1750 rpm; Complete VFD Case Compared with Ideal DC Bus/Switches Case

E. Parametric Study of the Controller

1. Speed Regulator

For speed regulator, the following four parameters should be set.

- Proportional gain
- Integral gain
- Speed ramps
- Torque limit (positive and negative)

The proportional gain and integral grain affect the output of the PI controller, which is the reference electromagnetic torque.

The speed ramps controls the maximum and minimum acceleration rate of the motor.

The torque limit limits the maximum and minimum reference torque.

a. Speed PI Controller

Speed PI controller regulates the reference speed of the drive system. Its output is the reference electromagnetic torque. Simulations are performed for three cases: with full speed PI controller, without speed P controller (setting proportional gain to zero, only integration component) and without speed I controller (setting integral grain to zero, only proportional component). The simulation results of oscillation are compared in Table XIV, which are shown in Fig. 84 to Fig. 87.

Comparing the three cases, both speed P controller and speed I controller influence the system vibration. From the spectrum of the relative angular displacement

Fig. 85(b), without speed P controller or speed I controller results in bigger oscillation on the mechanical component for both the lower and upper vibration frequency, compared with a system with full speed PI controller. And the speed P controller has much more influence on the system torsional response than the speed I controller.

From Fig. 84, at steady state, the system without speed I controller has a steady state speed error, which shows the function of integration in controllers.

On the other hand, the speed P controller does not only affect the vibration magnitude greatly, it also affects the lower vibration frequency. From Fig. 85(b) and Fig. 87(b), when there is no speed P controller, the system's lower vibration frequency is the first torsional natural frequency of the mechanical system. While for the full speed PI controller case and without speed I controller (only speed P controller) case, the lower vibration frequency is switched to around 7 Hz, as mentioned previously.

Fig. 88 and Fig. 89 shows the comparison of relative angular displacement and electromagnetic torque for three different values of the speed proportional gain – 300, 150 and 50. From the results, a lower value for speed P controller means a shorter transient response time but a relatively bigger steady state oscillation.

Table XIV. Comparison of Oscillation for Motor-Compressor Train with Closed-Loop FOC; Speed PI Controller Study

Speed PI Controller		Relative Angular Dispalcement between Motor and Gear#1 (Peak-Peak, Steady State)	Shear Stress of Coupling#1 (Peak-Peak, Steady State)
P	I		
300	2000	0.0000654 rad	1.6023e4 N/m^2
150	2000	0.0000708 rad	2.0059e4 N/m^2
50	2000	0.0001275 rad	4.3437e4 N/m^2
0	2000	0.0575 rad	3688.9e4 N/m^2
300	0	0.0001006 rad	2.4784e4 N/m^2

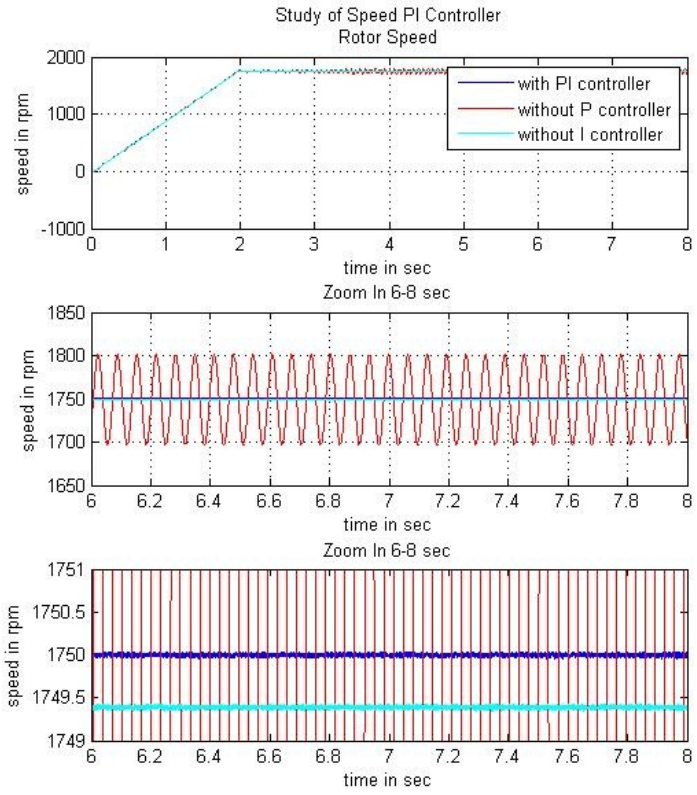

Fig. 84. Motor-Gearbox-Compressor Train with FOC; Rotor Speed – Motor Target Speed 1750 rpm; Speed PI Controller Study

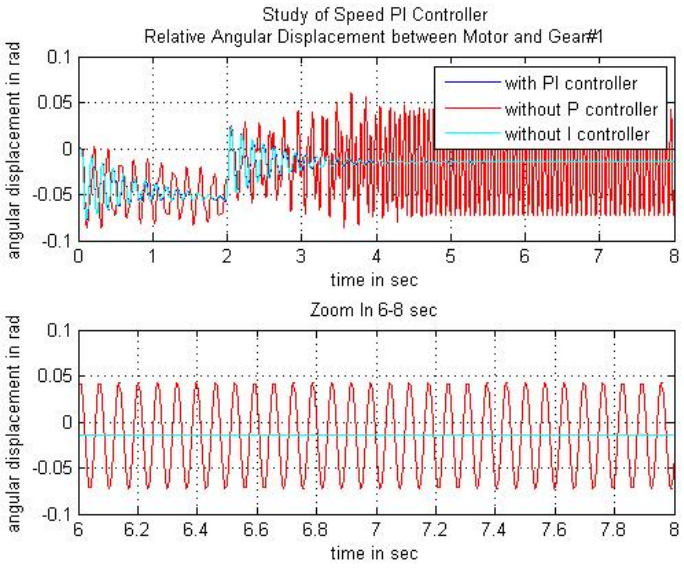

(a) Time Domain

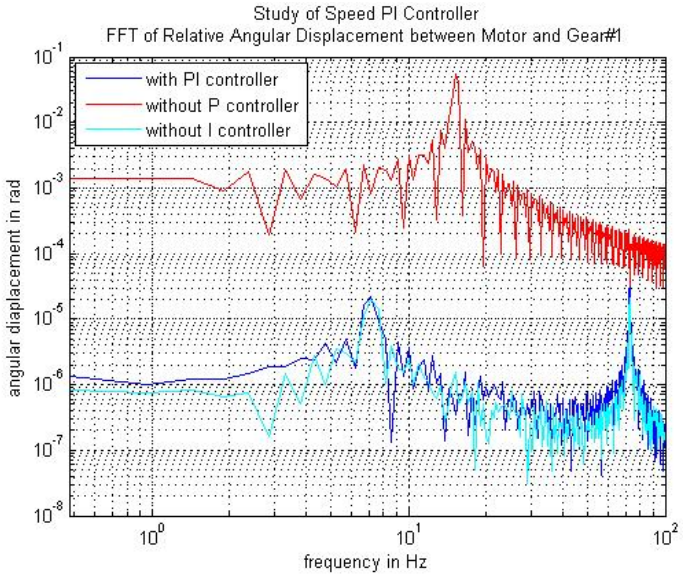

(b) Frequency Domain

Fig. 85. Motor-Gearbox-Compressor Train with FOC; Relative Angular Displacement between Motor and Gear#1 – Motor Target Speed 1750 rpm; Speed PI Controller Study

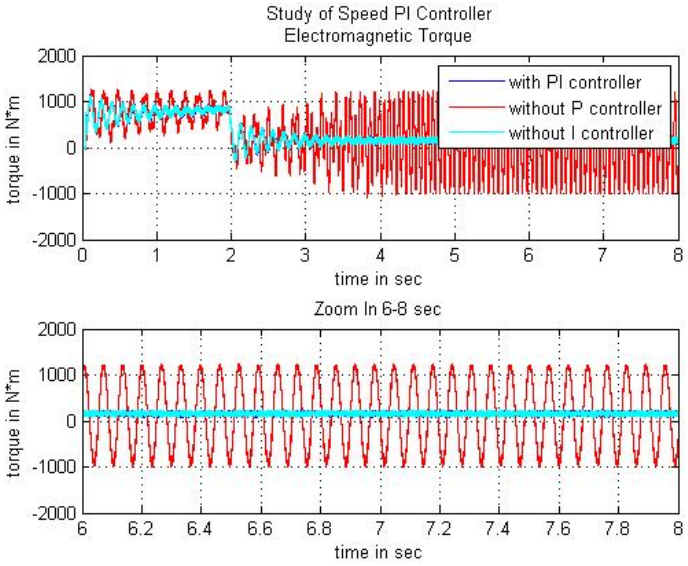

(a) Time Domain

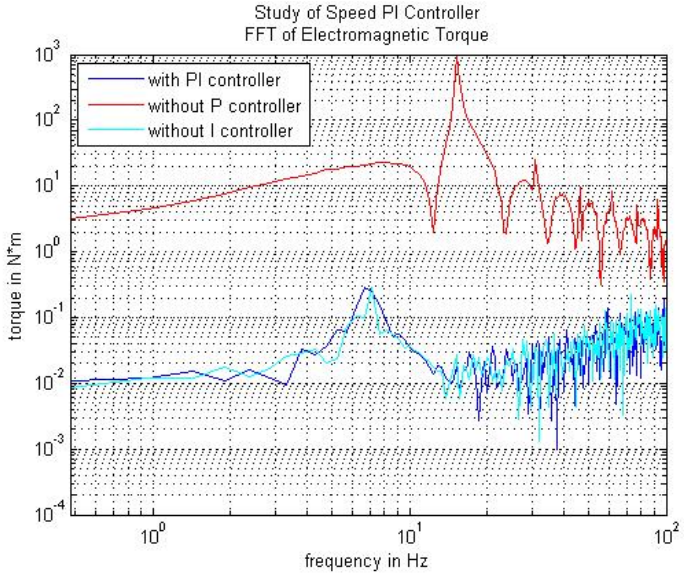

(b) Frequency Domain

Fig. 86. Motor-Gearbox-Compressor Train with FOC; Electromagnetic Torque – Motor Target Speed 1750 rpm; Speed PI Controller Study

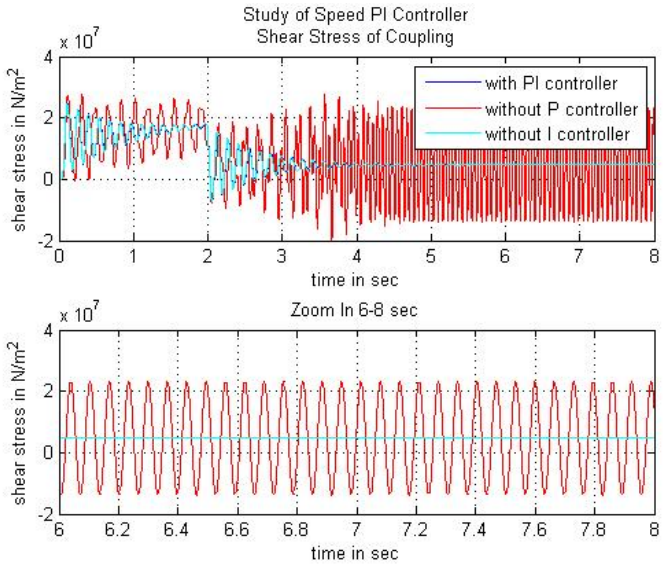

Fig. 87. Motor-Gearbox-Compressor Train with FOC; Shear Stress of Coupling#1 – Motor Target Speed 1750 rpm; Speed PI Controller Study

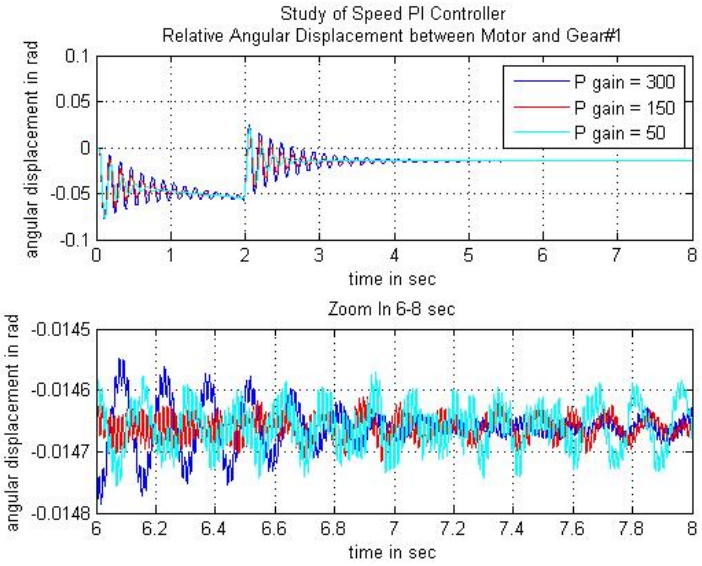

(a) Time Domain

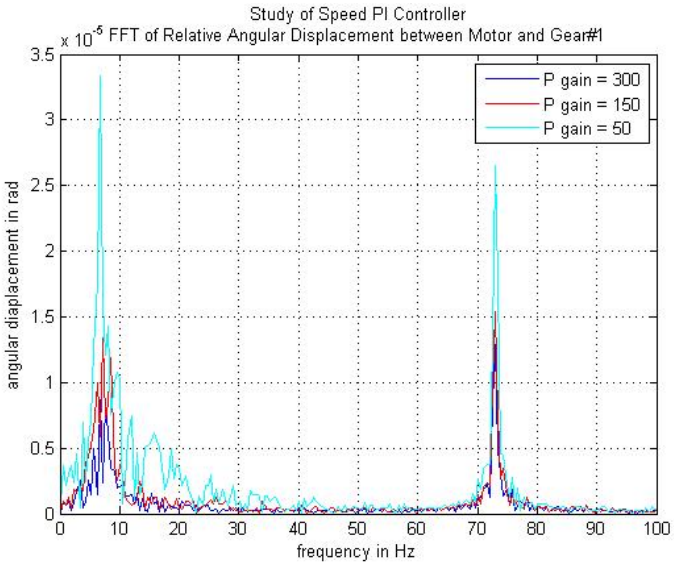

(b) Frequency Domain

Fig. 88. Motor-Gearbox-Compressor Train with FOC; Relative Angular Displacement between Motor and Gear#1 – Motor Target Speed 1750 rpm; Speed P Controller Study – P = 300, 150 and 50

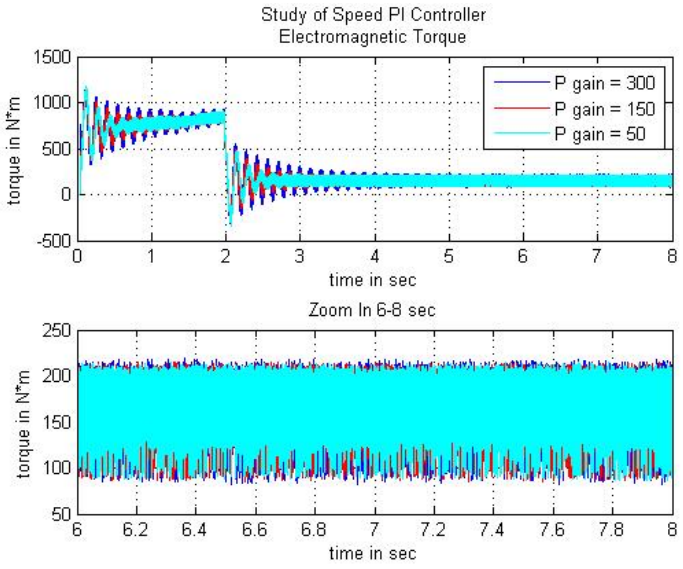

Fig. 89. Motor-Gearbox-Compressor Train with FOC; Electromagnetic Torque – Motor Target Speed 1750 rpm; Speed P Controller Study – P = 300, 150 and 50

b. Torque Limit

The simulations are performed for torque limit of 12000 N·m and 20000 N·m. The simulation results are shown in Fig. 90 to Fig. 93. Because the torque limit is used to regulate the maximum (positive) and minimum (negative) torque value of the torque controller, it is expected to influence the transient state of the system response when the acceleration or deceleration requires big torque. Since at steady state, the mechanical train is supposed to working at a normal torque level. The simulation results show that for this system, the required torque at any time is smaller than the maximum torque.

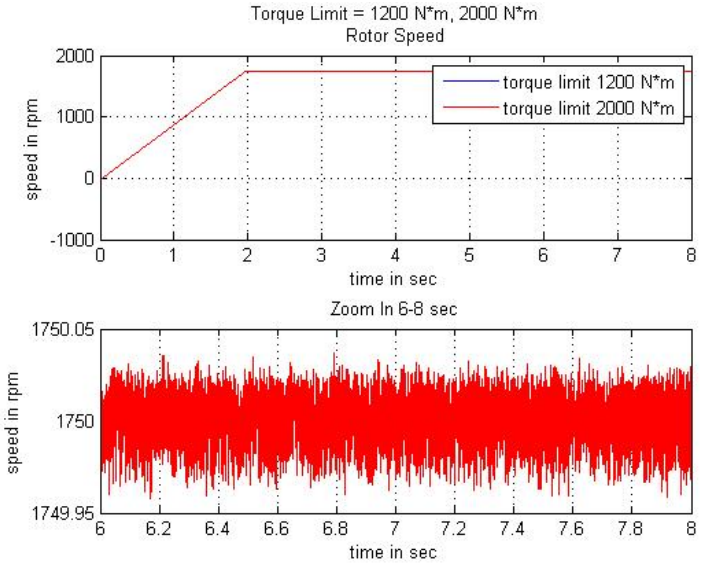

Fig. 90. Motor-Gearbox-Compressor Train with FOC; Rotor Speed – Motor Target Speed 1750 rpm; Torque Output Limit = 12000 N·m and 20000 N·m

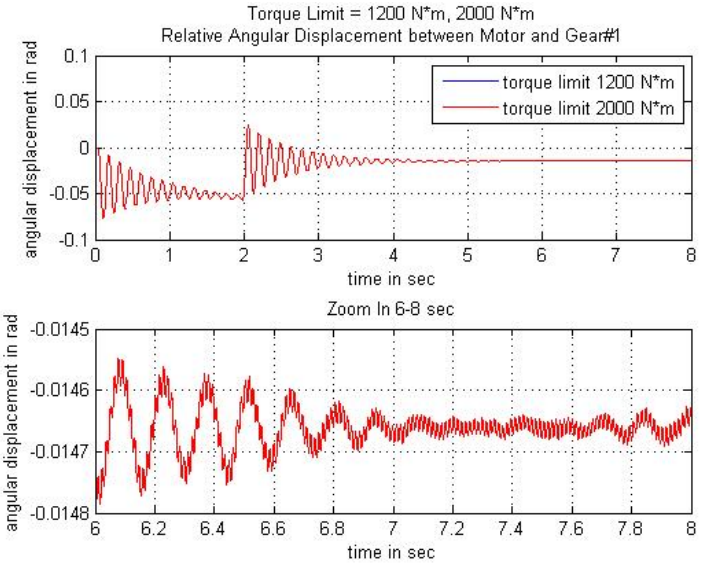

(a) Time Domain

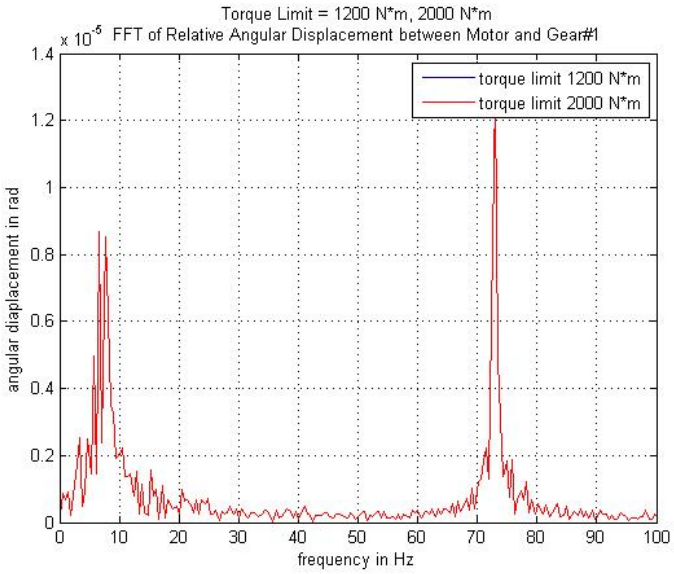

(b) Frequency Domain

Fig. 91. Motor-Gearbox-Compressor Train with FOC; Relative Angular Velocity between Motor and Gear#1 – Motor Target Speed 1750 rpm; Torque Output Limit = 12000 N·m and 20000 N·m

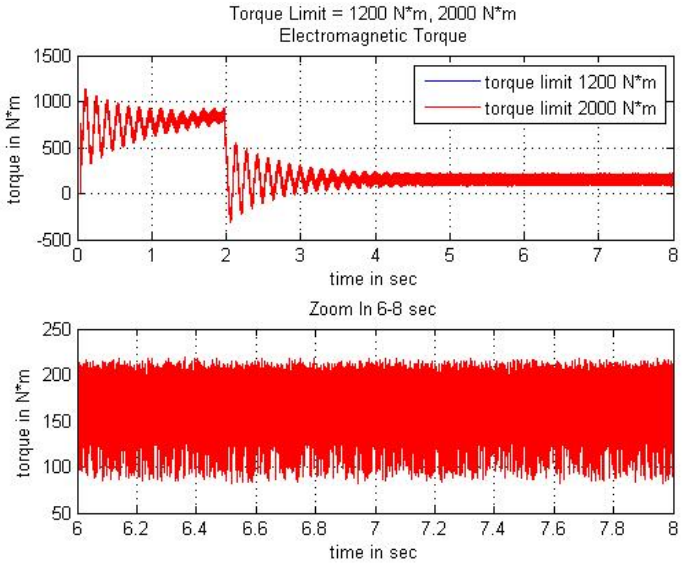

(a) Time Domain

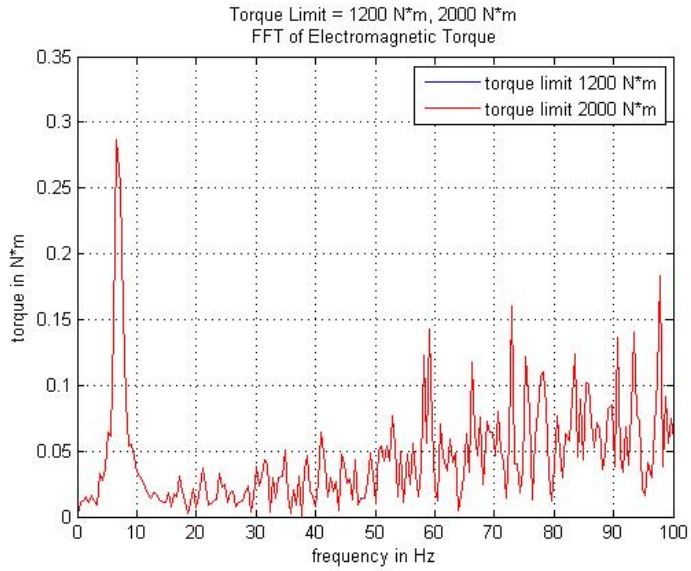

(b) Frequency Domain

Fig. 92. Motor-Gearbox-Compressor Train with FOC; Electromagnetic Torque – Motor Target Speed 1750 rpm; Torque Output Limit = 12000 N·m and 20000 N·m

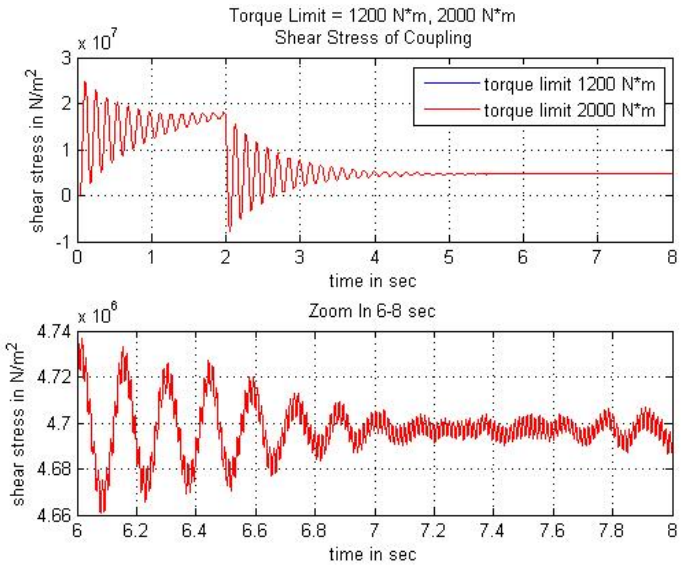

Fig. 93. Motor-Gearbox-Compressor Train with FOC; Shear Stress of Coupling#1– Motor Target Speed 1750 rpm; Torque Output Limit = 12000 N·m and 20000 N·m

c. Speed Ramps

Simulations are performed for speed ramps of 900 rpm/s and 1700 rpm/s. All the other parameters are the same as in Table XII. The simulation results are shown in Fig. 94 to Fig. 97.

From the results, the speed ramp value is not only related to the acceleration, but also influences the steady state vibration. In this machinery train, a high speed ramp means relative big oscillation at the upper vibration frequency. The simulation results of oscillation are compared in Table XV.

Table XV. Comparison of Oscillation for Motor-Compressor Train with Closed-Loop FOC; Speed Ramps = 900 rpm/s and 1700 rpm/s

Speed Ramp	Relative Angular Dispalcement between Motor and Gear#1 (Peak-Peak, Steady State)	Shear Stress of Coupling#1 (Peak-Peak, Steady State)
900 rpm/s	0.0000654 rad	1.6023e4 N/m^2
1700 rpm/s	0.0003095 rad	5.5720e4 N/m^2

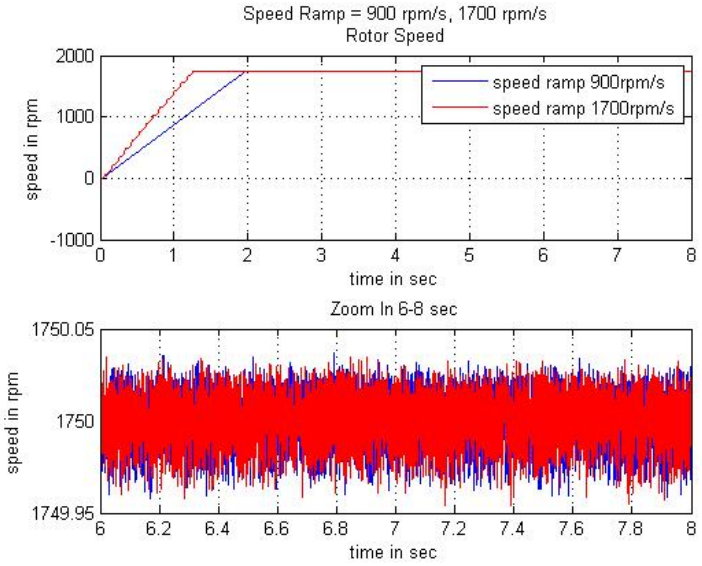

Fig. 94. Motor-Gearbox-Compressor Train with FOC; Rotor Speed – Motor Target Speed 1750 rpm; Speed Ramps = 900 rpm/s and 1700 rpm/s

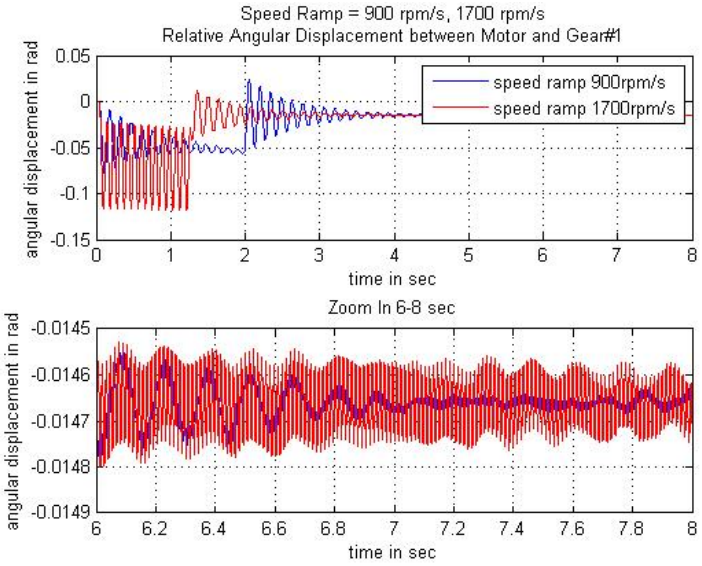

(a) Time Domain

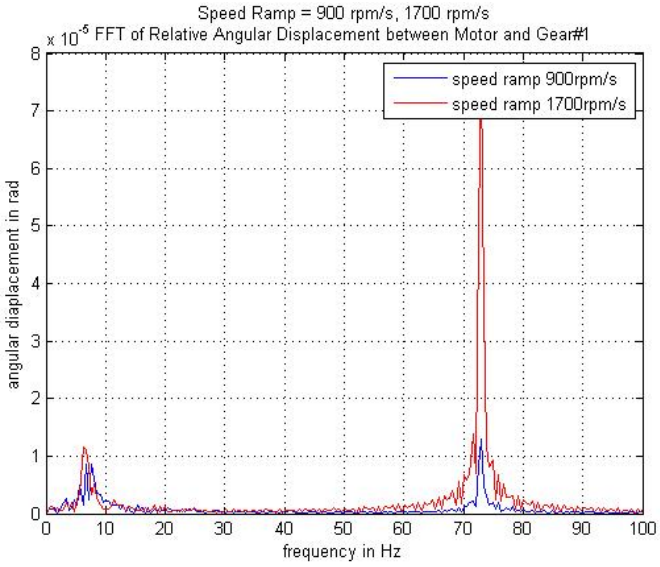

(b) Frequency Domain

Fig. 95. Motor-Gearbox-Compressor Train with FOC; Relative Angular Displacement between Motor and Gear#1 – Motor Target Speed 1750 rpm; Speed Ramps = 900 rpm/s and 1700 rpm/s

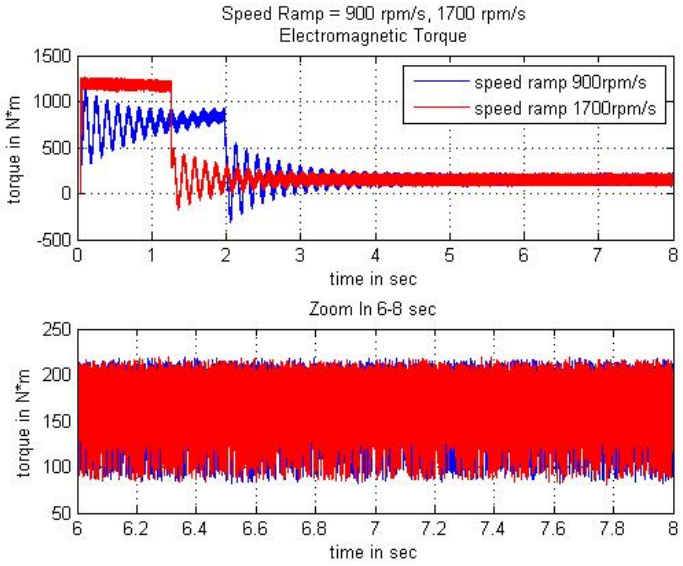

(a) Time Domain

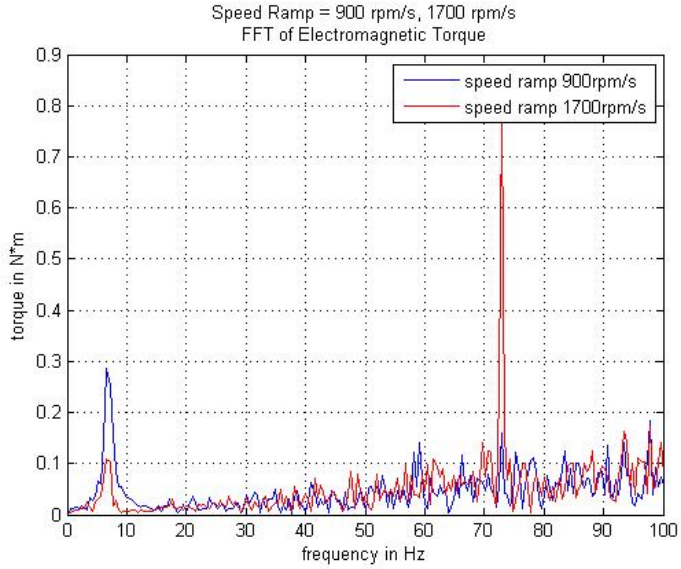

(b) Frequency Domain

Fig. 96. Motor-Gearbox-Compressor Train with FOC; Electromagnetic Torque – Motor Target Speed 1750 rpm; Speed Ramps = 900 rpm/s and 1700 rpm/s

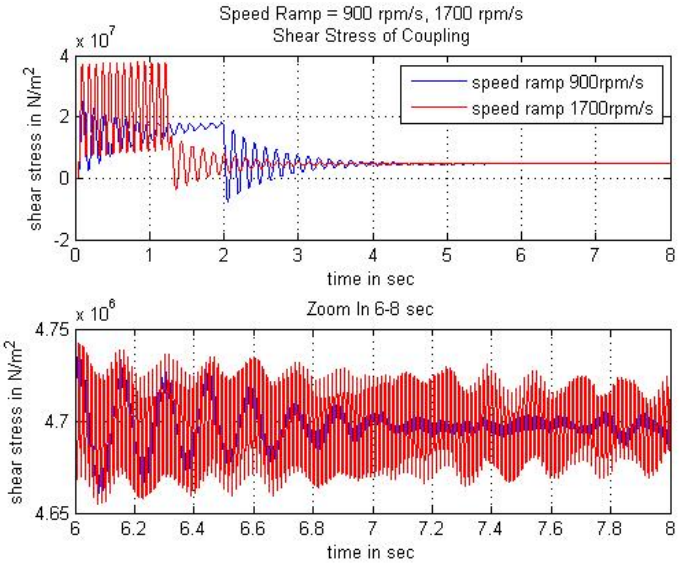

Fig. 97. Motor-Gearbox-Compressor Train with FOC; Shear Stress of Coupling#1 – Motor Target Speed 1750 rpm; Speed Ramps = 900 rpm/s and 1700 rpm/s

d. Torque Limit

The simulations are performed for torque limit of 12000 N·m and 20000 N·m. The simulation results are shown in Fig. 98 to Fig. 101. Because the torque limit is used to regulate the maximum (positive) and minimum (negative) torque value of the torque controller, it is expected to influence the transient state of the system response when the acceleration or deceleration requires big torque. Since at steady state, the mechanical train is supposed to working at a normal torque level. The simulation results show that for this system, the required torque at any time is smaller than the maximum torque.

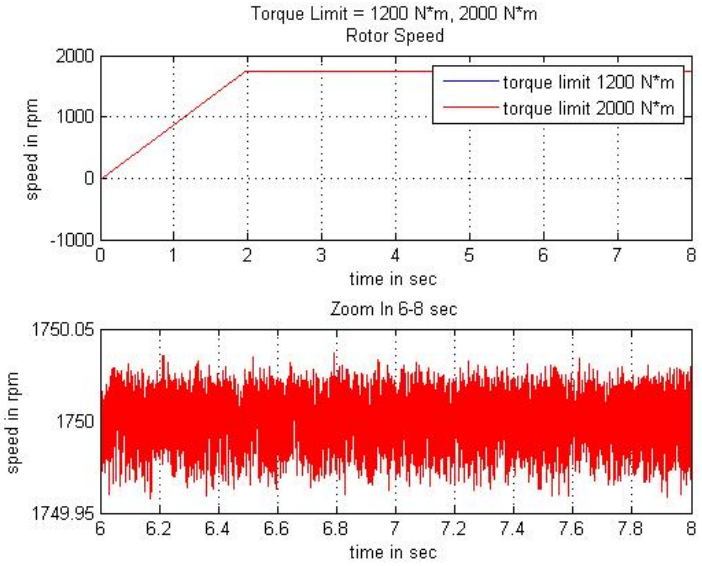

Fig. 98. Motor-Gearbox-Compressor Train with FOC; Rotor Speed – Motor Target Speed 1750 rpm; Torque Output Limit = 12000 N·m and 20000 N·m

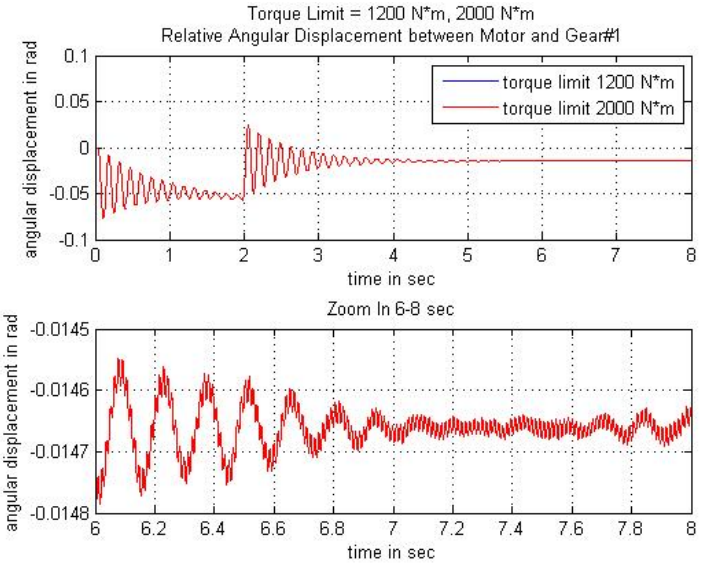

(a) Time Domain

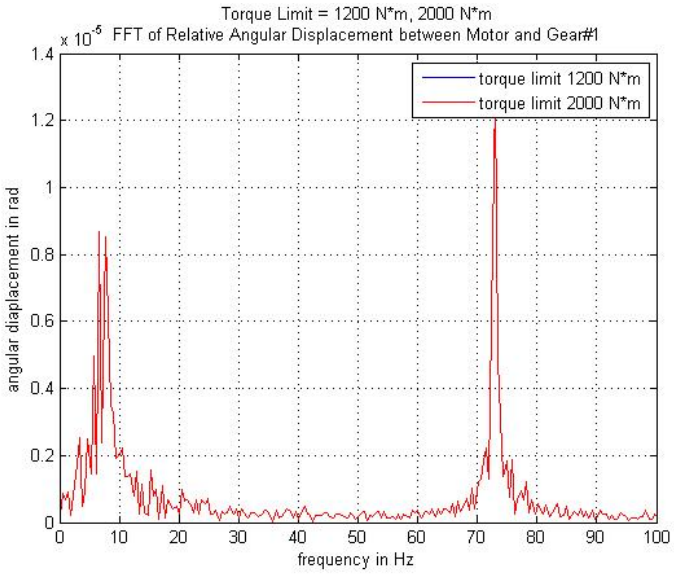

(b) Frequency Domain

Fig. 99. Motor-Gearbox-Compressor Train with FOC; Relative Angular Velocity between Motor and Gear#1 – Motor Target Speed 1750 rpm; Torque Output Limit = 12000 N·m and 20000 N·m

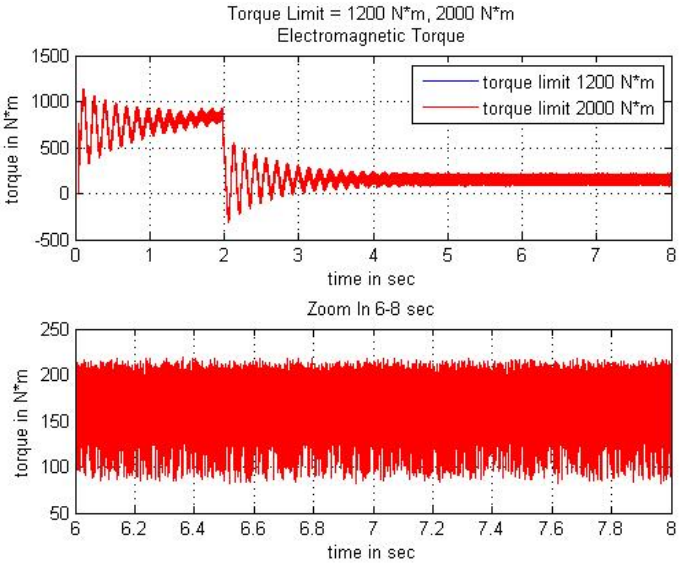

(a) Time Domain

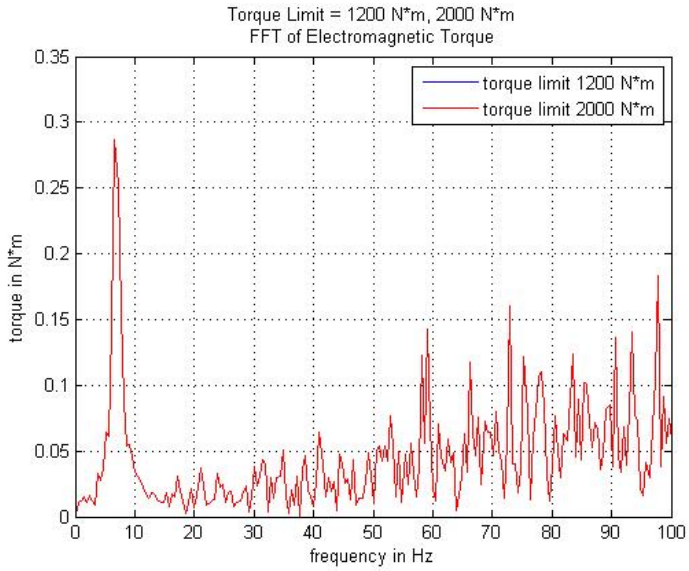

(b) Frequency Domain

Fig. 100. Motor-Gearbox-Compressor Train with FOC; Electromagnetic Torque – Motor Target Speed 1750 rpm; Torque Output Limit = 12000 N·m and 20000 N·m

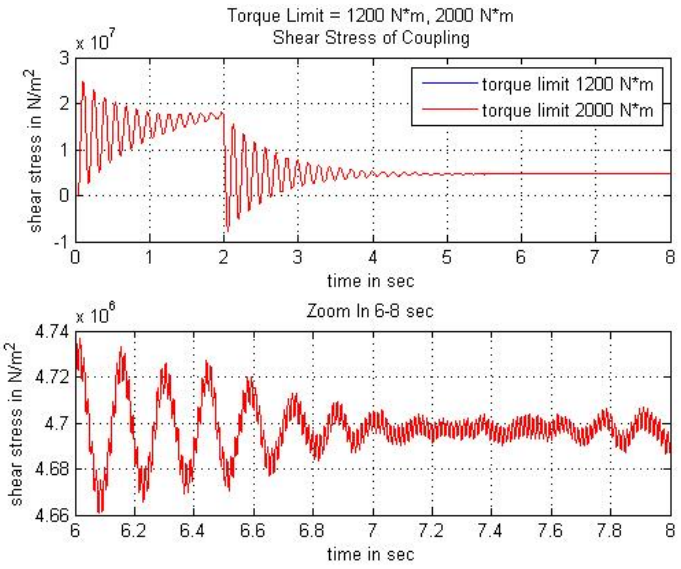

Fig. 101. Motor-Gearbox-Compressor Train with FOC; Shear Stress of Coupling#1 – Motor Target Speed 1750 rpm; Torque Output Limit = 12000 N·m and 20000 N·m

2. Flux Controller

There are three parameters related to the flux controller.

- Proportional gain
- Integral gain
- Output limit (positive and negative)

The proportional gain and integral gain influence the output of the PI controller, which is the reference flux.

The flux output limit controls the maximum and minimum value of the flux controller.

a. Flux PI Controller

The flux PI controller regulates the reference flux. Its output is the regulated reference flux value. As done in the study of the speed PI controller, simulations are performed for the three cases: with full flux PI controller, without flux P controller (the flux proportional gain is set to zero, only integration component) and without flux I controller (the flux integral gain is set to zero, only proportional component). The simulation results are shown in Fig. 102 to Fig. 105.

From the results, both flux P and I controllers affect the system torsional response. However, the flux PI controller does not have as much influence as the speed PI controller. As shown in the spectrums of the relative angular displacement and electromagnetic torque, the flux P controller has more influence on the mechanical oscillation than the flux I controller.

The simulation results of oscillation are compared in Table XVI.

Table XVI. Comparison of Oscillation for Motor-Compressor Train with Closed-Loop FOC; Flux PI Controller Study

Flux PI Controller	Relative Angular Dispalcement between Motor and Gear#1 (Peak-Peak, Steady State)	Shear Stress of Coupling#1 (Peak-Peak, Steady State)
PI Controller	0.0000654 rad	1.6023e4 N/m^2
No P Controller	0.0001101 rad	2.4500e4 N/m^2
No I Controller	0.0001093 rad	2.4114e4 N/m^2

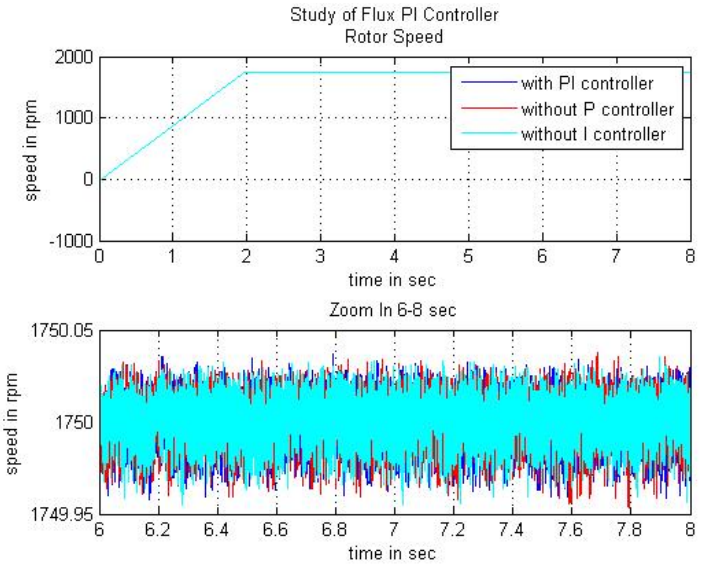

Fig. 102. Motor-Gearbox-Compressor Train with FOC; Rotor Speed – Motor Target Speed 1750 rpm; Flux PI Controller Study

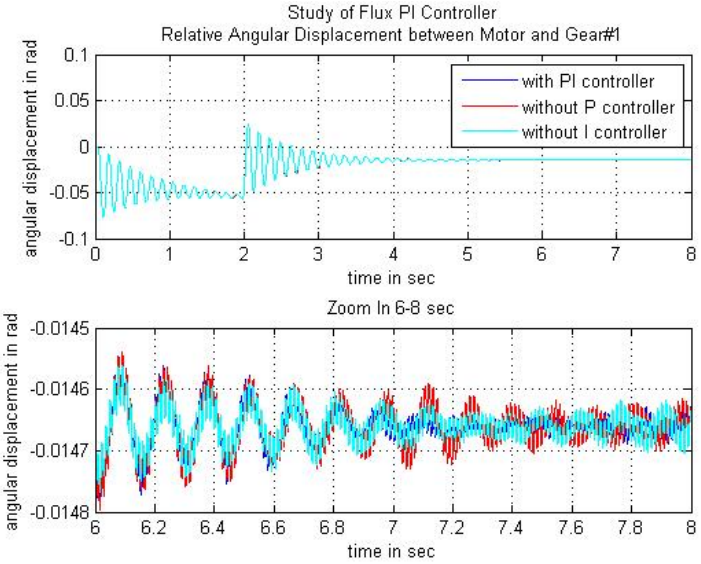

(a) Time Domain

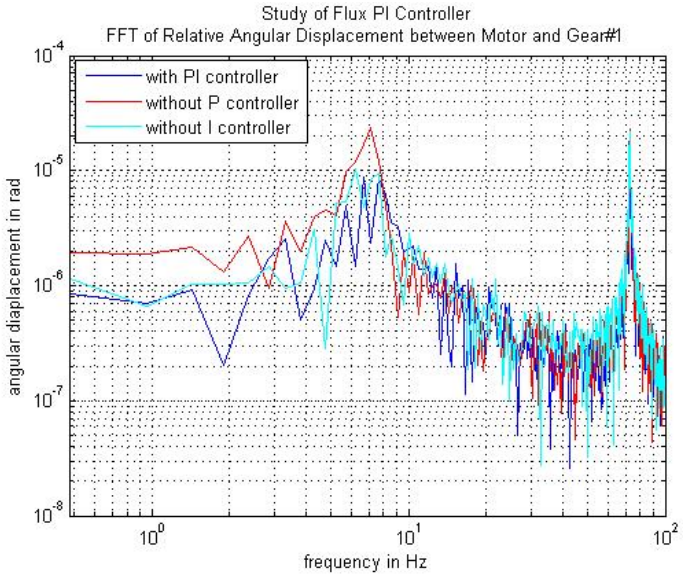

(b) Frequency Domain

Fig. 103. Motor-Gearbox-Compressor Train with FOC; Relative Angular Displacement between Motor and Gear#1 – Motor Target Speed 1750 rpm; Flux PI Controller Study

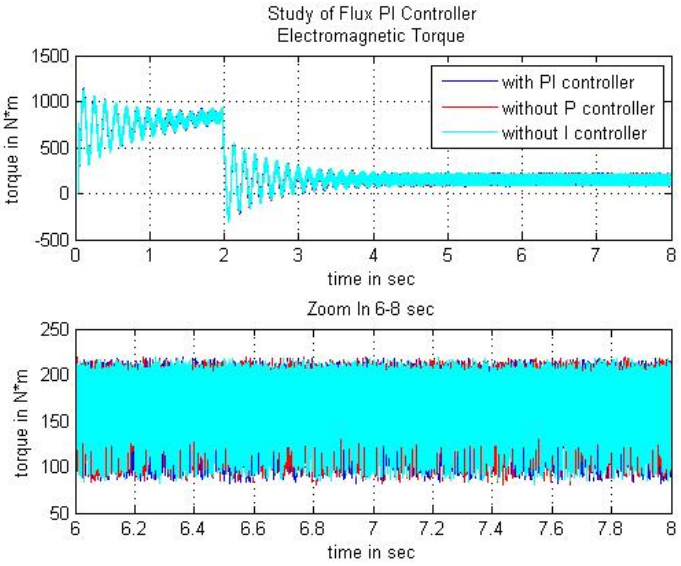

(a) Time Domain

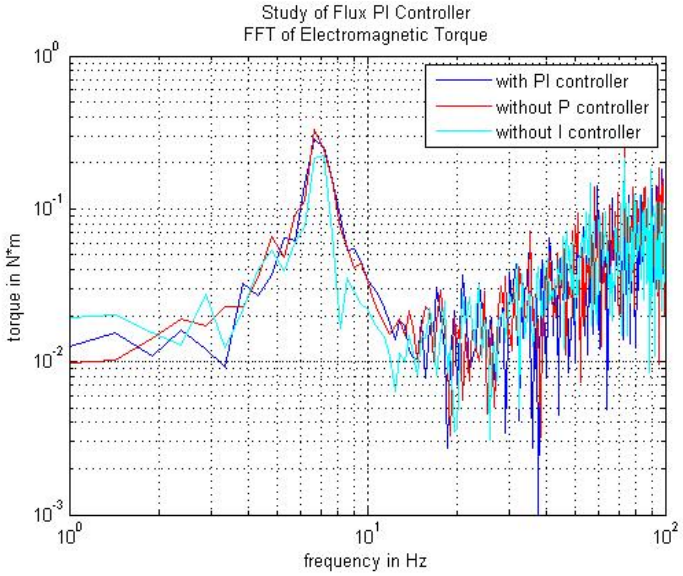

(b) Frequency Domain

Fig. 104. Motor-Gearbox-Compressor Train with FOC; Electromagnetic Torque – Motor Target Speed 1750 rpm; Flux PI Controller Study

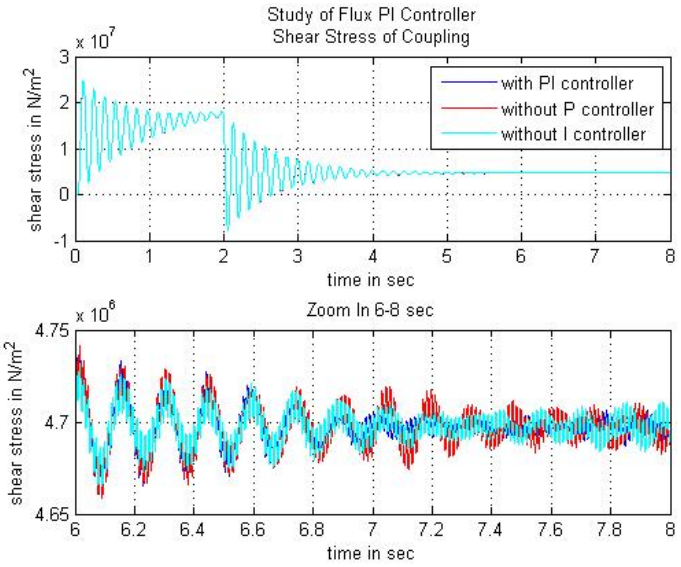

Fig. 105. Motor-Gearbox-Compressor Train with FOC; Shear Stress of Coupling#1 – Target Speed 1750 rpm; Flux PI Controller Study

b. Flux Output Limit

Simulations are performed for the flux output limit 1Wb and 2Wb. The simulation results are shown in Fig. 106 to Fig. 109. From the responses of relative angular velocity and shear stress along motor shaft, setting flux controller output limit to 1 Wb induces bigger oscillation than the setting of 2 Wb, especially for the lower vibration frequency.

The simulation results of oscillation are compared in Table XVII.

Table XVII. Comparison of Oscillation for Motor-Compressor Train with Closed-Loop FOC; Flux Output Limit = 1 Wb and 2 Wb

Flux Output Limit	Relative Angular Dispalcement between Motor and Gear#1 (Peak-Peak, Steady State)	Shear Stress of Coupling (Peak-Peak, Steady State)
1 Wb	0.00008594 rad	2.5077e4 N/m^2
2 Wb	0.0000654 rad	1.6023e4 N/m^2

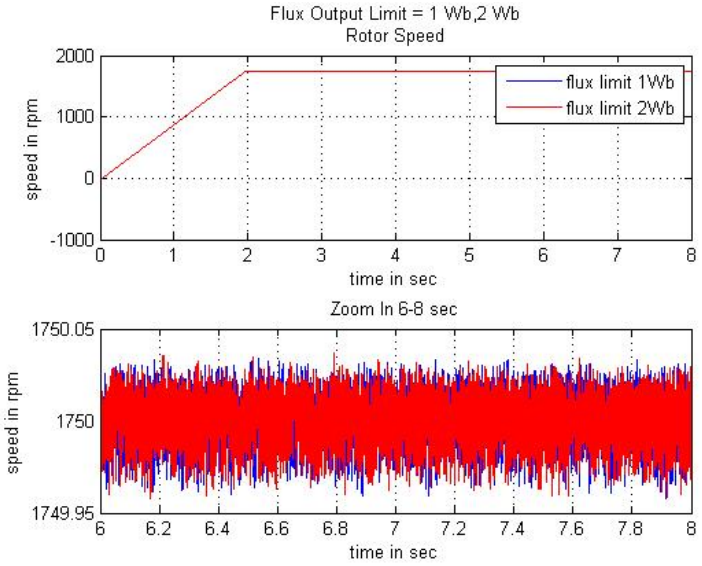

Fig. 106. Motor-Gearbox-Compressor Train with FOC; Rotor Speed – Motor Target Speed 1750 rpm; Flux Output Limit = 1 Wb and 2 Wb

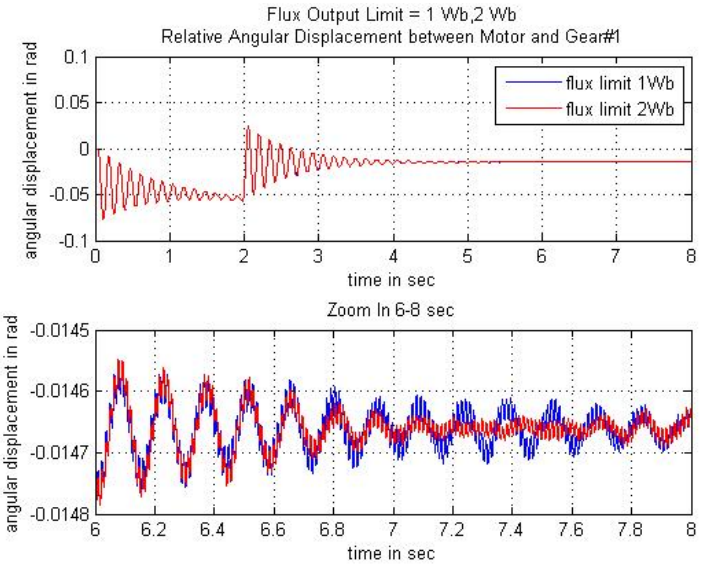

(a) Time Domain

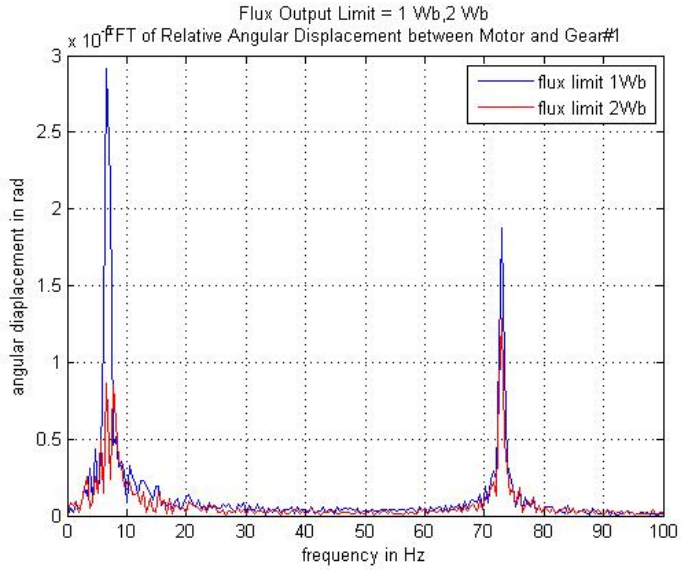

(b) Frequency Domain

Fig. 107. Motor-Gearbox-Compressor Train with FOC; Relative Angular Displacement between Motor and Gear#1 – Motor Target Speed 1750 rpm; Flux Output Limit = 1 Wb and 2 Wb

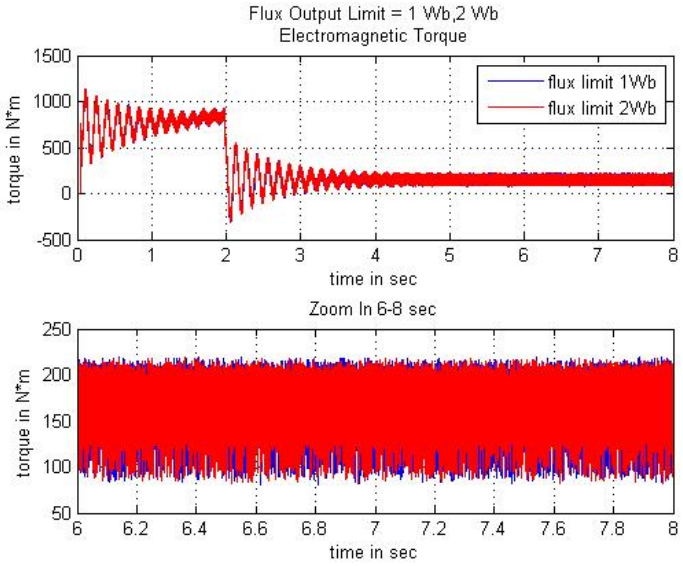

(a) Time Domain

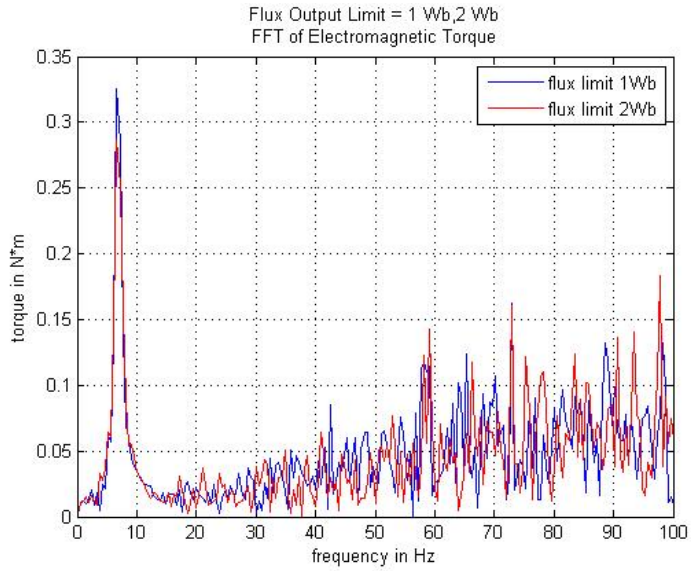

(b) Frequency Domain

Fig. 108. Motor-Gearbox-Compressor Train with FOC; Electromagnetic Torque – Motor Target Speed 1750 rpm; Flux Output Limit = 1 Wb and 2 Wb

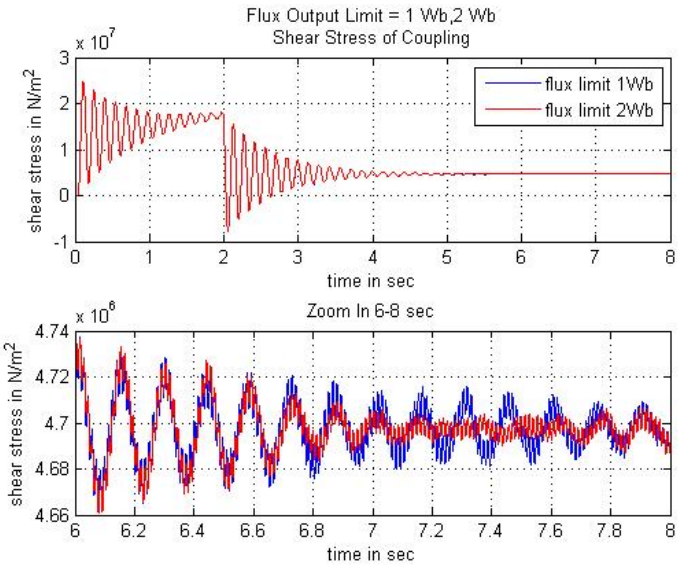

Fig. 109. Motor-Gearbox-Compressor Train with FOC; Shear Stress of Coupling#1 – Motor Target Speed 1750 rpm; Flux Output Limit = 1 Wb and 2 Wb

3. FOC Controller

Two parameters are for FOC controller settings.

- Current hysteresis band
- Maximum switching frequency

The current hysteresis band controls the maximum and minimum current error with respect to the reference current value.

The maximum switching frequency decides the maximum switching frequency of IGBT/Diode in the inverter.

a. Current Hysteresis Band

Simulations are performed for the current hysteresis band being 10 A and 30 A. The simulation results are shown in Fig. 110 to Fig. 113. From the results, it is obvious that with a bigger current hysteresis band, the oscillation of the mechanical system is bigger. This is because the current hysteresis band is the allowable error of the actual current with respect to the reference. The smaller the band, the smaller the error, which means a better control of the system.

The simulation results of oscillation are compared in Table XVIII.

Table XVIII. Comparison of Oscillation for Motor-Compressor Train with Closed-Loop FOC; Current Hysteresis Band = 10 A and 30 A

Current Hysteresis Band	Relative Angular Dispalcement between Motor and Gear#1 (Peak-Peak, Steady State)	Shear Stress of Coupling (Peak-Peak, Steady State)
10 A	0.0000654 rad	1.6023e4 N/m^2
30 A	0.0001068 rad	2.6235e4 N/m^2

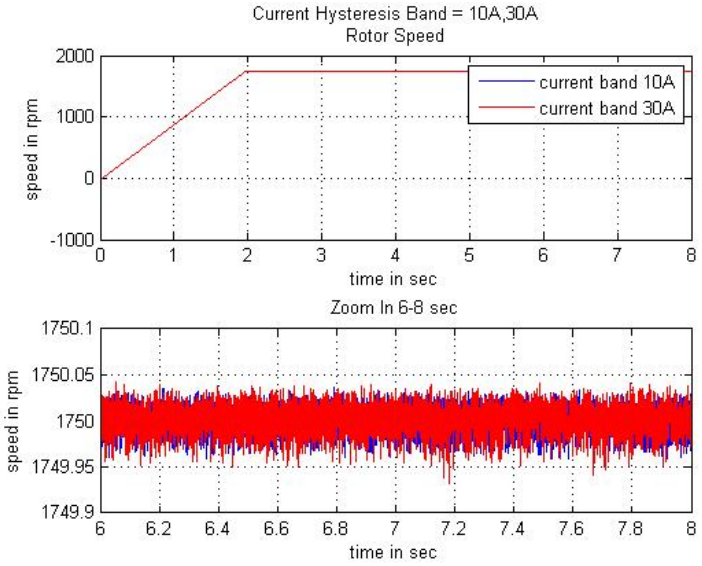

Fig. 110. Motor-Gearbox-Compressor Train with FOC; Rotor Speed – Motor Target Speed 1750 rpm; Current Hysteresis Band = 10 A and 30 A

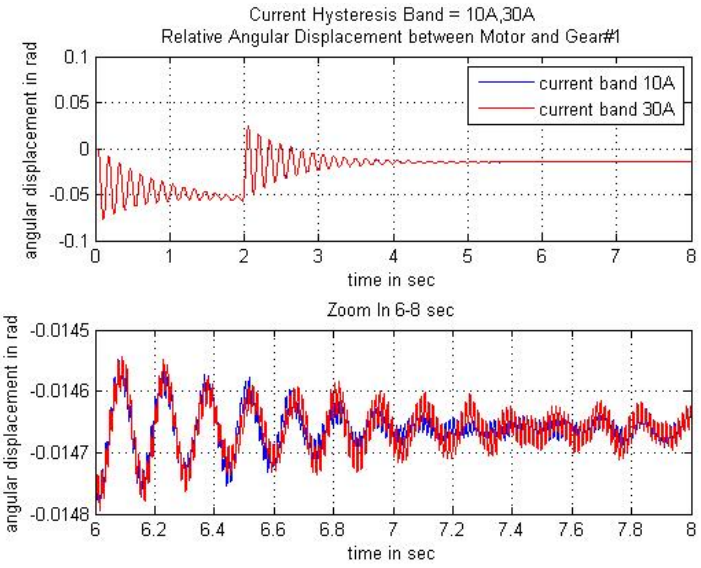

(a) Time Domain

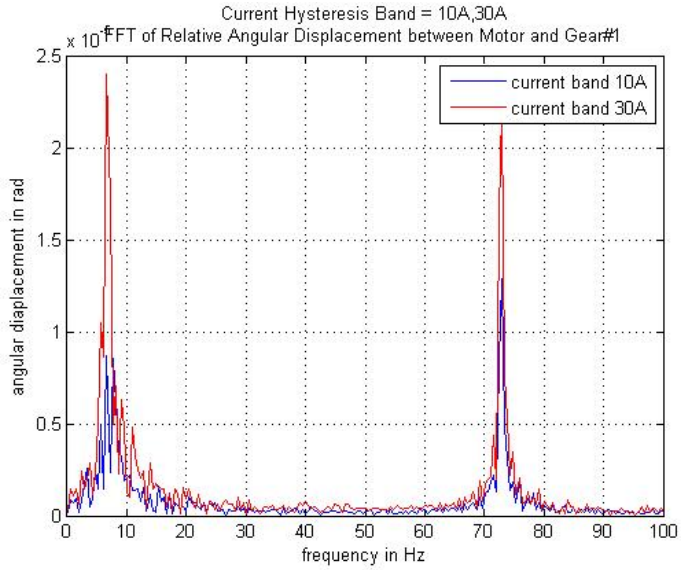

(b) Frequency Domain

Fig. 111. Motor-Gearbox-Compressor Train with FOC; Relative Angular Displacement between Motor and Gear#1 – Motor Target Speed 1750 rpm; Current Hysteresis Band = 10 A and 30 A

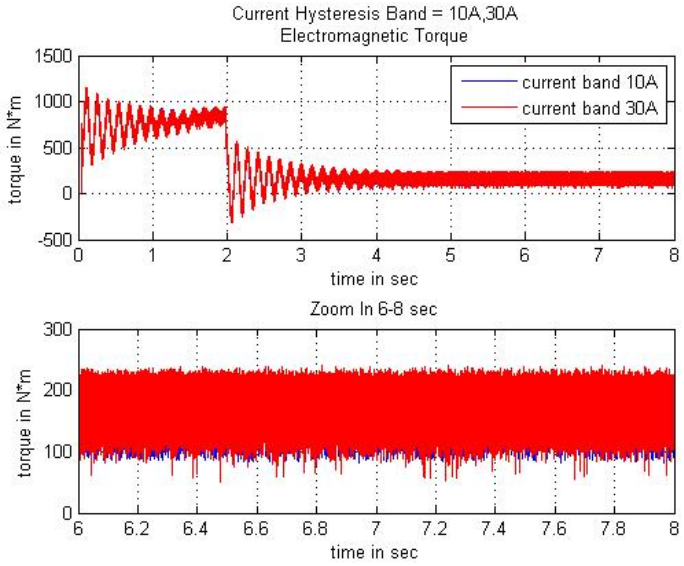

(a) Time Domain

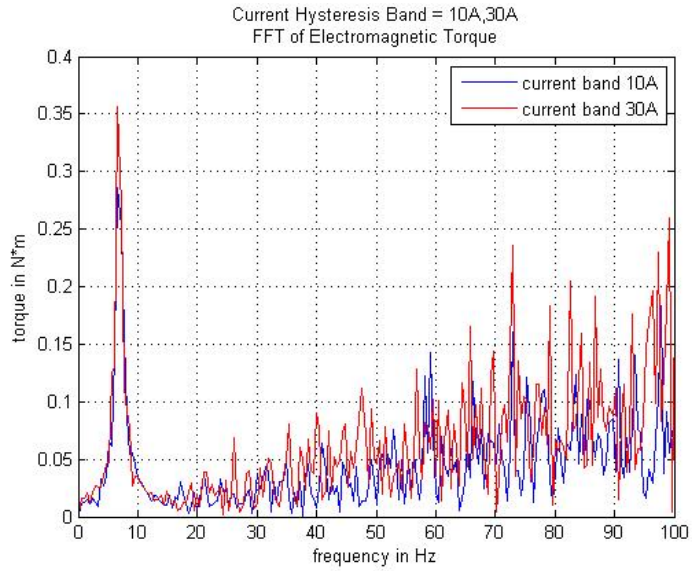

(b) Frequency Domain

Fig. 112. Motor-Gearbox-Compressor Train with FOC; Electromagnetic Torque – Motor Target Speed 1750 rpm; Current Hysteresis Band = 10 A and 30 A

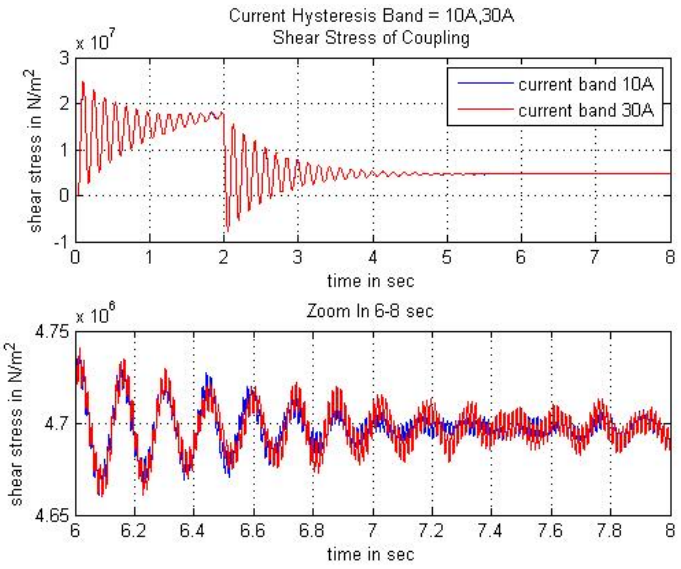

Fig. 113. Motor-Gearbox-Compressor Train with FOC; Shear Stress of Coupling#1 – Motor Target Speed 1750 rpm; Current Hysteresis Band = 10 A and 30 A

b. Maximum Switching Frequency

Simulations are performed for maximum switching frequency of 5000 Hz and 20000 Hz. The results are shown in Fig. 114 to Fig. 117. It is obvious that for PWM the higher the switching frequency, the fewer harmonic the output contains. From the waveforms of relative angular velocity and shear stress, the oscillation for maximum switching frequency 5000 Hz is bigger than 20000 Hz case.

The simulation results of oscillation are compared in Table XIX.

Table XIX. Comparison of Oscillation for Motor-Compressor Train with Closed-Loop FOC; Maximum Switching Frequency = 5000 Hz and 20000 Hz

Maximum Switching Frequency	Relative Angular Dispalcement between Motor and Gear#1 (Peak-Peak, Steady State)	Shear Stress of Coupling (Peak-Peak, Steady State)
5000 Hz	0.0001585 rad	3.6865e4 N/m^2
20000 Hz	0.0000654 rad	1.6023e4 N/m^2

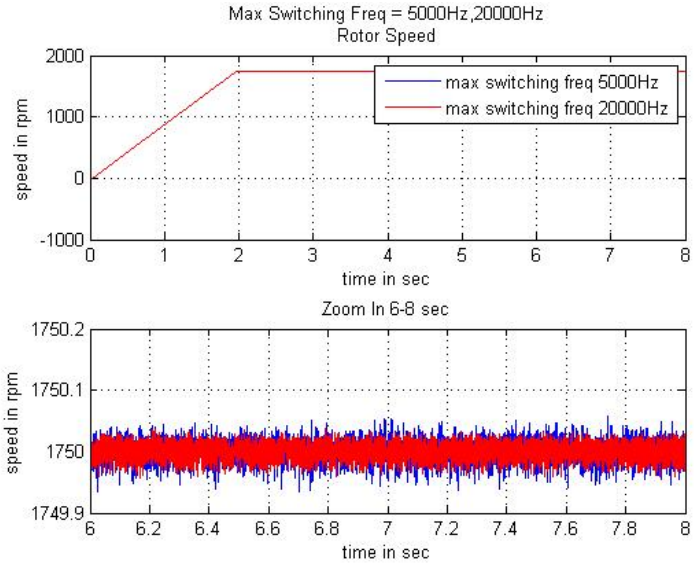

Fig. 114. Motor-Gearbox-Compressor Train with FOC; Rotor Speed – Motor Target Speed 1750 rpm; Maximum Switching Frequency = 5000 Hz and 20000 Hz

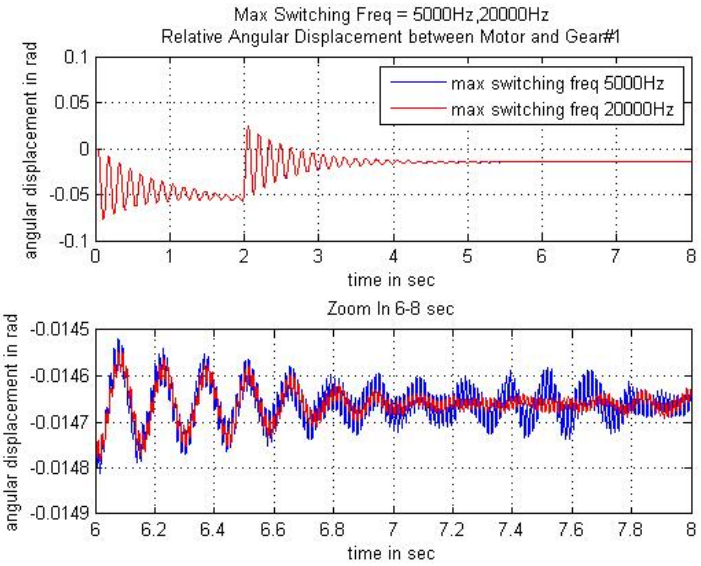

(a) Time Domain

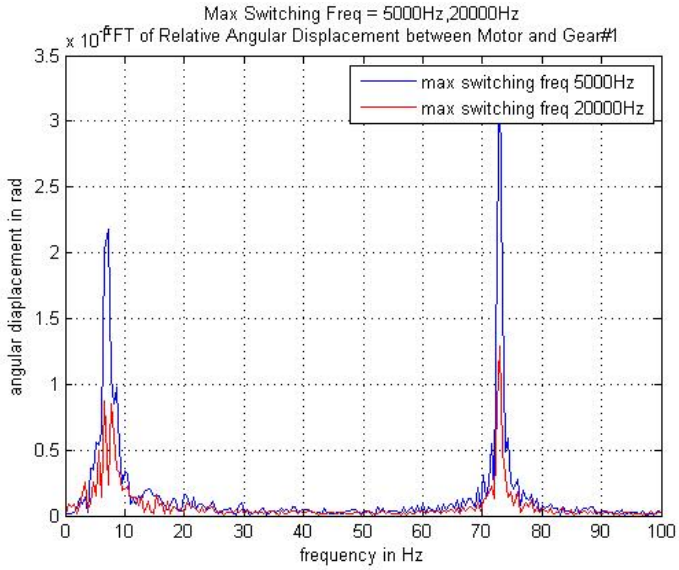

(b) Frequency Domain

Fig. 115. Motor-Gearbox-Compressor Train with FOC; Relative Angular Displacement between Motor and Gear#1 – Motor Target Speed 1750 rpm; Maximum Switching Frequency = 5000 Hz and 20000 Hz

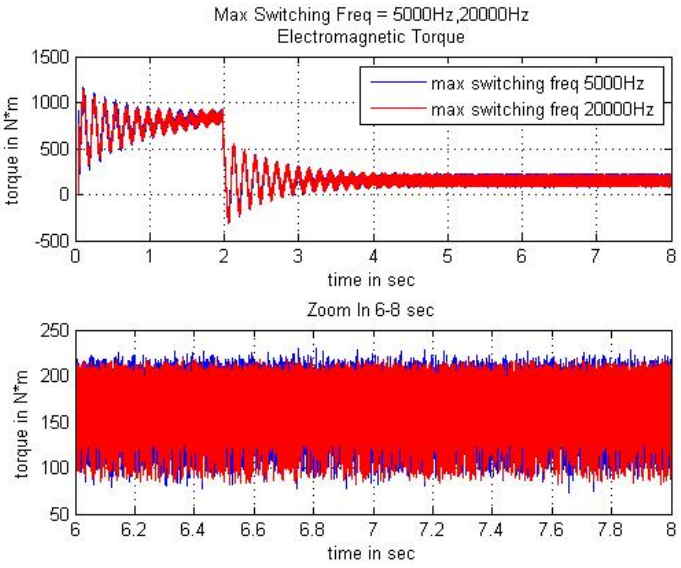

(a) Time Domain

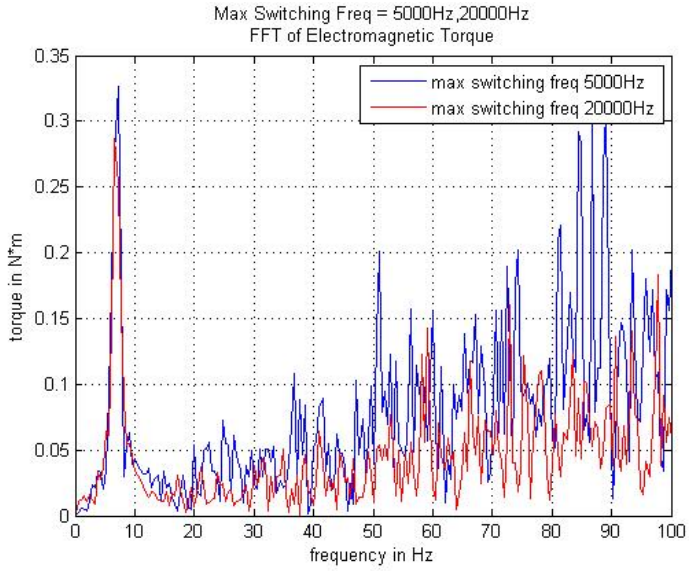

(b) Frequency Domain

Fig. 116. Motor-Gearbox-Compressor Train with FOC; Electromagnetic Torque – Motor Target Speed 1750 rpm; Maximum Switching Frequency = 5000 Hz and 20000 Hz

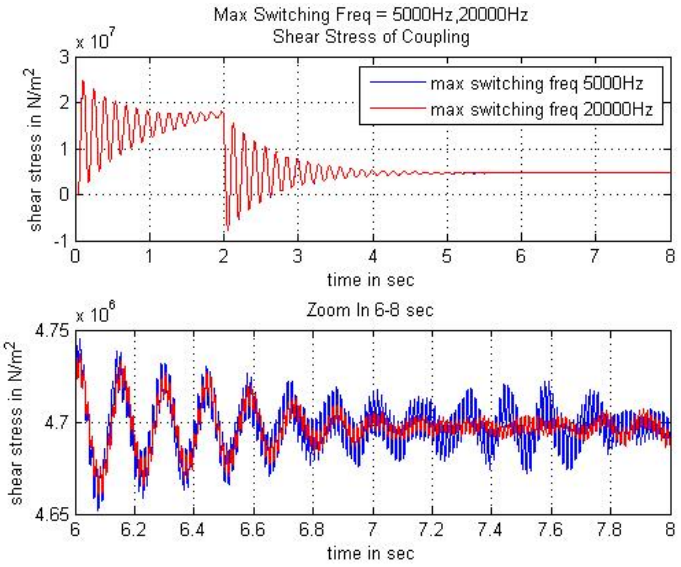

Fig. 117. Motor-Gearbox-Compressor Train with FOC; Shear Stress of Coupling#1 – Motor Target Speed 1750 rpm; Maximum Switching Frequency = 5000 Hz and 20000 Hz

CHAPTER VI

SUMMARY

A. Modeling for Machinery Train System with VFD

In Chapter III, a modeling method for coupling electrical system and mechanical system for mechanical train driven by VFD system is presented. Two softwares extending Simulink in Matlab are introduced – SimPowerSystems for electrical system modeling and SimMechanics for mechanical modeling. Two interface methods of combining SimPowerSystems and SimMechanics are discussed – one is "extended rotor with zero-inertia", and the other one is "two-rotor-model". A test case is modeled to verify the validation of these interface methods.

B. Study of Open-Loop Volts/Hertz Control

The open-loop Volts/Hertz control method is studied in Chapter IV. The findings are summarized as following.

- Effect of Volts/Hertz Control Method

  With carrier-based PWM, harmonic frequency of electromagnetic torque is in the form of $c \times f_{PWM} \pm d \times f_e$, where $c + d$ is an even integer. When the harmonic frequency of electromagnetic torque coincides with the torsional natural frequency, a resonance may occur.

- Effect of Non-ideal Power Switches

  The effect of non-ideal characteristics of IGBT/Diodes is quite small. It does not influences the system torsional response much. But the power switchese

consume a little energy.

- Effect of DC Bus Hamonics

  A DC bus ripple can influence the oscillation response. The DC bus harmonic induces a harmoinc in electromagnetic torque with a frequency lower than the DC bus harmonic frequency. The mechanical system is subject to a forced vibration at this frequency. DC bus harmonics of system characteristic frequencies – motor operation frequency or mechanical torsional natural frequency tend to increase the system torsoinal oscillation at steady state, when the harmonic amplitude increases. For the motor-compressor train discussed in Chapter IV, when the DC bus harmonic frequency is the motor operation frequency (50 Hz) and harmonic amplitude is 10% of the DC bus voltage, the system vibration amplitude is about 13 times that of ideal DC bus case. The vibration amplitude is about 3 times when DC bus frequency equals to the torsional natural frequency (20 Hz).

  However, these harmonics of characteristic frequencies do not induce resonance. For the motor-compressor train discussed in Chapter IV, a DC bus harmonic of 120 Hz causes the mechanical torsional resonance. When the DC bus harmoic amplitude is just 2.5% of the DC bus voltage, the torsional vibration amplitude is 17.25 times the ideal DC bus case.

C. Study of Closed-Loop FOC Control

The closed-loop FOC control system is studied in Chapter V. The following shows the findings.

- Effect of FOC Control Method

This closed-loop control only generates small oscillations at high frequencies. But with the inside PI controller, there is a frequency switch phenomena on the mechanical oscillation frequency. For the studied machinery train, the lower oscillating frequency is around 7 Hz while the first torsional natural frequency is 10.73 Hz. The upper oscillating frequency is just the same as the second torsional natural frequency.

- Complete VFD System of FOC A complete VFD system with rectifier, DC bus filter and inverter does not induce bigger vibrations. Instead, the simulation results show that the steady state oscillation of a complete VFD system is smaller than the drive system with ideal DC bus voltage and ideal switchse in inverter. The shear stress if 1.6023e4 N/m^2 compared with 3.6405e4 N/m^2.

- Effects of FOC Control Parameter Settings

  Even with closed-loop control, an inappropriate setting of FOC controller can induce relatively big steady state torsional oscillations.

  – *Speed PI Controller*

    For the speed PI controller, both speed P controller and speed I controller influence the system vibration, while the influence of speed P controller is much bigger. Speed I controller influences the steady state speed error.

    The speed P controller has a effect as damping. It can switch the system oscillation frequency away from the natural frequency. In the motor-gearbox-compressor train discussed in Chapter V, the first vibration frequency is 7 Hz which is switched from the first torsional natural frequency 10.73 Hz.

  – *Speed Ramp*

    The speed ramp is not only related to the acceleration, but also influ-

ences the steady state vibration. For the motor-gearbox-compressor, a high speed ramp shows relative big oscillation.

– *Torque Limit*

The torque limit does not affect the steady state responses when it is set big enough. Since the required torque at steady state is always much smaller than the maximum torque.

– *Flux PI Controller*

Both flux P and I controllers affect the system torsional response. However, the flux PI controller does not have as much influence as the speed PI controller. And the flux P controller has more influence on the mechanical oscillation than the flux I controller.

– *Flx Output Limit*

A smaller flux output limit gives a smaller oscillation. For the studied machinery train, the oscillation magnitude is obviously bigger with a smaller flux output limit.

– *Current Hysteresis Band*

A small current hysteresis band results in an obviously smaller oscillation. This is because the current hysteresis band is the allowable error of the actual current with respect to the reference.

– *Maximum Switching Frequency*

Increase the maximum switching frequency can reduce the mechanical oscillation magnitude. It is obvious that for PWM the higher the switching frequency, the fewer harmonic the output contains.

D. Future Work

This thesis analyzes the two control method of VFDs with voltage source rectifier for squirrel-cage induction motor, based on the simulation results from SimPowerSystems and SimMechanics. Some future works are listed below, which help deeply investigate the VFD related torsional vibration problems.

- Introduce edge filters and sensors model to the existing VFD model
- Introduce detailed mathematical model for mechanical components, i.e. back-slash for gears.
- Perform simulations for fault conditions
- Investigate the approximate mathematical model for the entire system

REFERENCES

[1] Feese, T., and Maxfield, R., 2008, "Torsional Vibration Problem with Motor/ID Fan System due to PWM Variable Frequency Drive," Proceedings of 37th Turbomachinery Symposium, Houston, TX, pp. 45-56.

[2] Kocur, J. A. Jr., and Corcoran, J. P., 2008, "VFD Induced Coupling Failure", 37th Turbomachinery Symposium Case History, Houston, TX.

[3] Kerkman, R. J., Theisen, J., and Shah, K., 2008, "PWM Inverters Producing Torsional Components in AC Motors," Proceedings of 55th Annual IEEE Petroleum and Chemical Industry Technical Conference, Cincinnati, OH, pp. 1-9.

[4] Wachel, J. C., and Szenasi, F. R., 1993, "Analysis of Torsional Vibrations in Rotating Machinery," Proceedings of 22nd Turbomachinery Symposium, Houston, TX, pp.127-151.

[5] Mayer, C. B., 1981, "Torsional Vibration Problems and Analyses of Cement Industry Drives," IEEE Transactions on Industry Applications, **17**(1), pp. 81-89.

[6] Sheppard, D. J., 1988, "Torsional Vibration Resulting from Adjustable-Frequency AC Drives," IEEE Transactions on Industry Applications, **24**(5), pp. 812-817.

[7] Tripp, H., Kim, D., and Whitney, R., 1993, "A Comprehensive Cause Analysis of a Coupling Failure Induced by Torsional Oscillations in a Variable Speed Motor," Proceedings of 22nd Turbomachinery Symposium, Houston, TX, pp.17-23.

[8] Lee, K., Jahns, T. M., Berkopec, W. E., and Lipo, T. A., 2004, "Closed-Form Analysis of Adjustable Speed Drive Performance Under Input Voltage Unbalance and Sag Conditons," Proceedings of 35th Annual IEEE Power Electronics Specialists Conference, Aachen, Germany, pp. 469-475 Vol.1.

[9] Lee, K., Jahns, T. M., Novotny, D. W., Lipo, T. A., Berkopec, W. E., and Blasko, V., 2006, "Impact of Inductor Placement on the Performance of Adjustable-Speed Drives Under Input Voltage Unbalance and Sag Conditions," IEEE Transactions on Industry Applications, **42**(5), pp. 1230-1240 .

[10] Globalshiksha, 2010, Induction Motors, Globalshiksha.com, Bangalore, India. Available;
http://www.globalshiksha.com/Induction-Motors/ugc/202394320383038

[11] Finney, D., 1988, *Variable Frequency AC Motor Drive Systems*, Peter Peregrinus Ltd. on behalf of The Institution of Engineering and Technology, London, U.K..

[12] Amin, B., 2001, *Induction Motors: Analysis and Torque Control*, Springer, New York.

[13] Lipo, T. A., 2008, *Analysis of Synchronous Machines*, Wisconsin Power Electronics Research Center, University of Wisconsin, Madison, WI.

[14] Fitzgerald, A. E., Kingsley, C. Jr., and Umans, S. D., 2002, *Electric Machinery*, 6th Edition, McGraw-Hill, New York.

[15] Sen, P. C., 1997, *Principles of Electric Machines and Power Electronics*, 2nd Edition, John Wiley & Sons, Inc., New York.

[16] Bose, B., 2006, *Power Electronics and Motor Drives: Advances and Trends*, Academic Press, Boston, MA.

[17] Novotny, D. W., and Lipo, T. A., 1996, *Vector Control and Dynamics of AC Drives*, Oxford University Press, New York.

[18] Vas, P., 1998, *Sensorless Vector and Direct Torque Control*, Oxford University Press, New York.

[19] Trzynadlowski, A. M., 2000, *Control of Induction Motors*, Academic Press, San Diego, CA.

[20] Toliyat, H.A., 2009, Class Notes, Course ECEN632 Motor Dynamics, Texas A&M University, College Station, TX.

[21] MathWorks, September 2010, SimPowerSystems Documentation, The MathWorks, Inc., Natick, MA. Available;
http://www.mathworks.com/help/toolbox/physmod/powersys/

[22] MathWorks, September 2010, SimMechanics Documentation, The MathWorks, Inc., Natick, MA. Available;
http://www.mathworks.com/help/toolbox/physmod/mech/

APPENDIX A

VECTOR TRANSFORM

A. Transform between Three-Dimensional and Two-Dimensional Vectors

Fig. 118 shows a stationary three-dimensional frame a-b-c and a rotating two-dimensional frame Q-D. The rotating velocity of the Q-D frame is ω. The angular displacement between the two frame is $\theta = \omega t$, which is the angle between a-axis and D-axis.

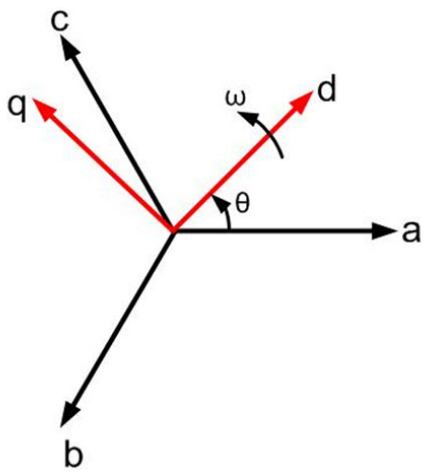

Fig. 118. Three-Dimensional Frame a-b-c and Two-Dimensional Frame Q-D

The transform from a-b-c frame to a Q-D frame with arbitrary rotating velocity ω is as Eq. (A.1).

$$\begin{bmatrix} i_d \\ i_q \end{bmatrix} = \sqrt{\frac{2}{3}} \begin{bmatrix} cos\theta & cos(\theta - \frac{2}{3}\pi) & cos(\theta + \frac{2}{3}\pi) \\ sin\theta & sin(\theta - \frac{2}{3}\pi) & sin(\theta + \frac{2}{3}\pi) \end{bmatrix} \begin{bmatrix} i_a \\ i_b \\ i_c \end{bmatrix} \tag{A.1}$$

The transform from Q-D frame to a-b-c frame is given by Eqn A.2.

$$\begin{bmatrix} i_a \\ i_b \\ i_c \end{bmatrix} = \sqrt{\frac{2}{3}} \begin{bmatrix} cos\theta & sin\theta \\ cos(\theta - \frac{2}{3}\pi) & sin(\theta - \frac{2}{3}\pi) \\ cos(\theta + \frac{2}{3}\pi) & sin(\theta + \frac{2}{3}\pi) \end{bmatrix} \begin{bmatrix} i_d \\ i_q \end{bmatrix} \tag{A.2}$$

B. Park Transform

Park transform means the transform from a-b-c frame to a stationary Q-D frame, which means the rotating velocity ω of Q-D frame is zero as shown in Fig. 119. The transform is given in Eq. (A.3), where the superscript s indicates the stationary Q-D frame.

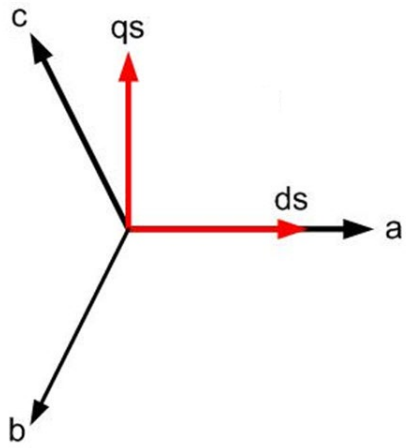

Fig. 119. a-b-c Frame and Stationary Q-D Frame

$$\begin{bmatrix} i_d^s \\ i_q^s \end{bmatrix} = \sqrt{\frac{2}{3}} \begin{bmatrix} 1 & -\frac{1}{2} & -\frac{1}{2} \\ 0 & -\frac{\sqrt{3}}{2} & \frac{\sqrt{3}}{2} \end{bmatrix} \begin{bmatrix} i_a \\ i_b \\ i_c \end{bmatrix} \tag{A.3}$$

C. Clarke Transform

Clarke transform means the transform from the stationary Q-D frame to a rotating Q-D frame with the motor's synchronous speed ω_e. This rotating Q-D frame is called synchronous frame. The transform is given in Eq. (A.4), where the superscript e indicates the synchronous q-d frame. θ is the angle between the two frames as shown in Fig. 120.

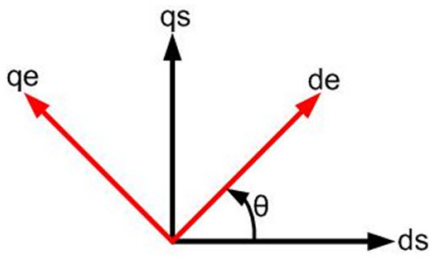

Fig. 120. Stationary Q-D Frame and Synchronous Q-D Frame

$$\begin{bmatrix} i_d^e \\ i_q^e \end{bmatrix} = \begin{bmatrix} cos\theta & sin\theta \\ -sin\theta & cos\theta \end{bmatrix} \begin{bmatrix} i_d^s \\ i_q^s \end{bmatrix} \tag{A.4}$$

APPENDIX B

PARAMETERS FOR SIMULATED SYSTEMS

A. Verification Case in Chapter III

1. 3 HP Motor

The parameters for the 3 HP motor are listed in Table XX.

2. IGBT/Diode

The parameters for IGBT/Diode bridge are listed in Table XXI.

3. PWM Generator

The settings for PWM generator are listed in Table XXII.

B. Motor-Compressor Train in Chapter IV

1. 150 HP Motor Parameters

The parameters for the 150 HP motor are listed in Table XXIII.

2. IGBT/Diode Parameters

The parameters for IGBT/Diode bridge are listed in Table XXIV.

3. PWM Generator

The settings for PWM generator are listed in Table XXV.

Table XX. 3 HP Motor Parameters

Nominal Power	3 HP
Nominal Voltage (line-line, peak-peak)	220 V
Nominal Frequency	60 Hz
Stator Resistance	1.115 Ohm
Stator Inductance	0.005974 H
Rotor Resistance	1.083 Ohm
Rotor Inductance	0.005974 H
Mutual Inductance	0.2037 H
Rotor Inertia	0.02 kg·m^2
Shaft Friction	0.005752 N·m/(rad/s)
Pole Pairs	2

Table XXI. IGBT/Diode Bridge Parameters for 3 HP Motor Train

Switch Type	IGBT/Diodes
Number of Arms	3
Snubber Resistance	1e5 Ohm
Snubber Capacitance	Inf
On-State Resistance	1e-3 Ohm
IGBT Forward Voltage	0 V
Diode Forward Voltage	0 V
IGBT Fall Time	1e-6 sec
IGBT Tail Time	2e-6 sec

Table XXII. PWM Generator Settings for 3 HP Motor Train

Converter Type	2-level
Mode of Operation	Un-Synchronized
Carrier Frequency	18×60 Hz
Modulation Index	0.9
Output Voltage Frequency	60 Hz
Output Voltage Phase	0 deg
Sample Time	10e-6 sec

Table XXIII. 150 HP Motor Parameters

Nominal Power	150 HP
Nominal Voltage (line-line, peak-peak)	400 V
Nominal Frequency	50 Hz
Stator Resistance	0.02155 Ohm
Stator Inductance	0.000226 H
Rotor Resistance	0.01231 Ohm
Rotor Inductance	0.000226 H
Mutual Inductance	0.01038 H
Rotor Inertia	2.3 $kg \cdot m^2$
Shaft Friction	0.05421 N·m/(rad/s)
Pole Pairs	2

Table XXIV. IGBT/Diode Bridge Parameters for 150 HP Motor Train

Switch Type	IGBT/Diodes
Number of Arms	3
Snubber Resistance	5e3 Ohm
Snubber Capacitance	Inf
On-State Resistance	1e-3 Ohm
IGBT Forward Voltage	0.8 V
Diode Forward Voltage	0.8 V
IGBT Fall Time	1e-6 sec
IGBT Tail Time	2e-6 sec

Table XXV. PWM Generator Settings for 150 HP Motor Train

Converter Type	2-level
Mode of Operation	Un-Synchronized
Carrier Frequency	950 Hz
Modulation Index	0.8165
Output Voltage Frequency	50 Hz
Output Voltage Phase	0 deg

C. Motor-Gearbox-Compressor Train in Chapter V

1. 200HP Motor Parameters

The parameters for the 200 HP motor are listed in Table XXVI.

Table XXVI. 200 HP Motor Parameters

Nominal Power	200 HP
Nominal Voltage (line-line, peak-peak)	460 V
Nominal Frequency	60 Hz
Stator Resistance	14.85e-3 Ohm
Stator Inductance	0.3027e-3 H
Rotor Resistance	9.295e-3 Ohm
Rotor Inductance	0.3027e-3 H
Mutual Inductance	10.46e-3 H
Rotor Inertia	3.1 kg·m^2
Shaft Friction	0.08 N·m/(rad/s)
Pole Pairs	2

2. Converters and DC Bus

The parameters of rectifier, DC bus, dynamic braking chopper and inverter are listed in Table XXVII.

Table XXVII. Converters and DC Bus

Rectifier	
Snubber Resistance	10e3 Ohm
Snubber Capacitance	20e-9 F
Diode On-State Resistance	1e-3 Ohm
Diode Forward Voltage	1.3 V
DC Bus	
Capacitance	7500e-6 F
Dynamic Braking Chopper	
Resistance	8 Ohm
Chopper Frequency	4000 Hz
Activation Voltage	700 V
Shutdown Voltage	660 V
Inverter	
IGBT On-State Resistance	1e-3 Ohm
IGBT Device Forward Voltage	0.8 V
Diode Forward Voltage	0.8 V
IGBT Fall Time	1e-6 sec
IGBT Tail Time	2e-6 sec
Snubber Resistance	5e3 Ohm
Snubber Capacitance	inf

VITA

Xu Han received her Bachelor of Science degree in electrical engineering from Zhejiang University in Hangzhou, China, June 2008. She entered the Power Electronics and Electric Power group in the Department of Electrical Engineering at Texas A&M University in September 2008. After one year, she switched to the Department of Mechanical Engineering and received her M.S. in December 2010. Her research interests include electric motors, motor controls, control theory, linear and non-linear vibration, chaos, and finite elements.

Xu Han may be reached at Room 018, Wisenbaker Engineering Research Center, Texas A&M University, College Station, TX 77843 - 3123. Her email is hanxu_zju@tamu.edu.

The typist for this thesis was Xu Han.